

~~CONFIDENTIAL~~

NACA RM L53D13

7419

TECH LIBRARY KAFB, NM  
014409  
NACA

## RESEARCH MEMORANDUM

EFFECTS OF TRAILING-EDGE BLUNTNES ON  
THE LIFT, DRAG, AND PITCHING-MOMENT CHARACTERISTICS  
OF UNSWEPT, 45° SWEPT, AND 45° DELTA WINGS AT MACH  
NUMBERS OF 1.41, 1.62, AND 1.96

By Kenneth L. Goin and Gertrude C. Westrick

Langley Aeronautical Laboratory  
Langley Field, Va.

CLASSIFIED DOCUMENT

This material contains information affecting the National Defense of the United States within the meaning of the espionage laws, Title 18, U.S.C., Secs. 793 and 794, the transmission or revelation of which in any manner to an unauthorized person is prohibited by law.

NATIONAL ADVISORY COMMITTEE  
FOR AERONAUTICS

WASHINGTON

June 10, 1953

~~CONFIDENTIAL~~RECEIPT SIGNATURE  
REQUIRED

319.98/13



## NATIONAL ADVISORY COMMITTEE FOR AERONAUTICS

## RESEARCH MEMORANDUM

EFFECTS OF TRAILING-EDGE BLUNTNESS ON  
THE LIFT, DRAG, AND PITCHING-MOMENT CHARACTERISTICS  
OF UNSWEPT, 45° SWEPT, AND 45° DELTA WINGS AT MACH  
NUMBERS OF 1.41, 1.62, AND 1.96

By Kenneth L. Goin and Gertrude C. Westrick

## SUMMARY

An investigation of systematic series of sharp- and blunt-trailing-edge wings has been made to determine the effects of thickening the trailing edges on the lift, drag, and pitching-moment characteristics at Mach numbers of 1.41, 1.62, and 1.96. The wings tested consisted of 0° and 45° sweptback untapered wings of aspect ratio 2.7 and 45° delta wings. The wings had hexagonal sections with thickness ratios ranging from 0.030 to 0.100 and were tested with fixed transition at Reynolds numbers of  $1.1 \times 10^6$  to  $2.2 \times 10^6$ .

Results of the investigation indicate that no appreciable zero-lift drag reductions may be obtained by thickening the trailing edges at Mach numbers of 1.41 to 1.96, but that trailing edges can be thickened appreciably with no increases in zero-lift drag. Reductions in the drag at lift coefficients of 0.2 and above were obtained by thickening the trailing edges of the 45° swept wings by various amounts. The ratio of trailing-edge thickness to maximum thickness  $h/t$  for minimum drag of wings with this plan form increased with increases in airfoil-section thickness ratio, operating lift coefficient, and Mach number.

Moderate thickening of the trailing edges caused no appreciable reductions in maximum lift-drag ratios  $(L/D)_{\max}$  for any of the wings, and for some of the swept wings caused slight increases in  $(L/D)_{\max}$ .

Lift-curve slopes of the wings, in general, tended to increase with increases in  $h/t$ . Center-of-pressure locations for the unswept wings were relatively independent of  $h/t$ , but for the 45° swept wings they moved rearward somewhat with increases in  $h/t$ .

~~CONFIDENTIAL~~

## INTRODUCTION

Previous experimental investigations have shown that wings with blunt trailing edges will, in some cases, have higher lift-curve slopes, higher maximum ratios of lift to drag, and lower minimum drag at supersonic speeds than similar wings with sharp trailing edges (ref. 1). Similar increases in lift-curve slopes and maximum ratios of lift to drag due to thickening the trailing edges have also been shown at transonic speeds with no increases in minimum drag (ref. 2). In consideration of these improved aerodynamic characteristics, together with obvious structural advantages, wings with blunt trailing edges appear promising for use at supersonic speeds.

Experimental information available on blunt-trailing-edge wings at supersonic speeds consists of fairly comprehensive base-pressure data (refs. 2 to 6) but relatively few data on other aerodynamic characteristics (refs. 1 and 2). Considerably more experimental information is needed to predict reliably the effects of thickening the trailing edges on the aerodynamic characteristics of wings.

In order to provide additional information on the effects of thickened trailing edges, an investigation has been made of the lift, drag, and pitching-moment characteristics of systematic series of wings with blunt and sharp trailing edges at Mach numbers of 1.41, 1.62, and 1.96. This investigation is the second phase of a general investigation of blunt-trailing-edge wings (the first phase was a base-pressure investigation, ref. 3) and includes detailed effects of wing section and representative effects of wing plan form.

## SYMBOLS

M	Mach number
R	Reynolds number based on mean aerodynamic chord
q	free-stream dynamic pressure
c	wing chord
$\bar{c}$	mean aerodynamic chord
t	maximum section thickness
h	trailing-edge thickness

CONFIDENTIAL

$l$  length of trailing-edge bevel (see fig. 1(a))  
 $A$  wing aspect ratio  
 $\lambda$  wing taper ratio  
 $\Lambda$  sweepback of wing leading edge  
 $S$  total area of semispan wing  
 $L$  lift  
 $D$  drag  
 $m$  pitching moment about  $0.25\bar{c}$

$$C_L = \frac{L}{qS}$$

$$C_D = \frac{D}{qS}$$

$$C_m = \frac{m}{qS\bar{c}}$$

$$C_{L_\alpha} = \frac{dC_L}{d\alpha}$$

#### DESCRIPTION OF MODELS

The wing models tested consisted of a  $45^\circ$  delta plan form and two untapered plan forms of aspect ratio 2.7, the first being unswept and the second having  $45^\circ$  of leading-edge sweepback. Systematic variations of airfoil section thickness ratio and trailing-edge thickness ratio were obtained with each plan form.

The geometric details of the semispan wing models tested are given in figure 1(a) and the various wing sections are illustrated in figure 1(b). Each of the wings had symmetrical straight-sided sections, polished surfaces, and a slightly rounded leading edge with a radius of approximately 0.002 inch. Details of the half-body on which the wings were mounted are given in figure 2.

## TUNNEL

The tests were conducted in the Langley 9- by 12-inch supersonic blowdown tunnel which utilizes the compressed air of the Langley 19-foot pressure tunnel. The compressed air is conditioned to insure condensation-free flow in the test section by being passed through a silica-gel drier and through banks of finned electrical heaters. Turbulence-damping screens are located in the tunnel settling chamber. The absolute stagnation pressure of the air entering the test section is about 2 atmospheres. The three test-section Mach numbers are provided by use of interchangeable nozzle blocks.

Deviations of the flow conditions in the test section, as determined from extensive calibration tests and reported in reference 7, are presented in the following table:

Average Mach number . . . . .	1.41	1.62	1.96
Maximum deviation in Mach number . . . . .	$\pm 0.02$	$\pm 0.01$	$\pm 0.02$
Maximum deviation in stream angle, deg . . . . .	$\pm 0.25$	$\pm 0.20$	$\pm 0.20$

## TEST TECHNIQUE

Details of the model test arrangement are shown in figure 2. Each semispan wing and attached half-body was cantilevered from a five-component strain-gage balance which is mounted flush with the tunnel wall and rotates through the angle-of-attack range with the model. The half-body consisted of a half-body of revolution and a quarter-inch shim. The shim was used to raise the body of revolution so as to minimize the effects of the tunnel-wall boundary layer on the flow over its surface (ref. 8). A clearance gap of about 0.007 to 0.015 inch was maintained between the fuselage shim and the tunnel wall under a no-load condition.

Base-pressure measurements of reference 3 indicated an effect on base pressures of the wall-reflected disturbance originating at the nose of the body when the wings were located aft on the body. In the present tests, the wings were located at the positions indicated in figure 2 and shown by the photographs of figure 3, which were far enough forward on the body to avoid this effect.

All wings were tested with transition fixed by means of bands of roughness (carborundum grains having maximum dimensions of about 0.004 inch) cemented to the upper and lower surfaces and extending over the complete exposed semispan. The bands of roughness were of about 5-percent-chord width and were located approximately between the 10- and 15-percent-chord stations. The ability of such bands to fix transition is illustrated by results of liquid-film-flow studies presented in reference 3.

The wings were tested with fixed transition because the type of boundary layer has been found to have important effects on base pressures (ref. 4), and turbulent-boundary-layer data should have a greater range of practical application. The data of reference 4 indicate that wing base pressures obtained at Reynolds numbers of about  $1 \times 10^6$  to  $2 \times 10^6$  with fixed transition are approximately equal to those obtained at higher Reynolds numbers (up to about  $4 \times 10^6$ ) with natural transition and that the data of this report, as affected by base pressures, should therefore be representative of higher Reynolds number results. Data of reference 4 also indicate that the method of fixing transition at Reynolds numbers of  $1 \times 10^6$  to  $2 \times 10^6$  has no important effect on wing base pressures. It should be pointed out, however, that, for bodies of revolution, the data of reference 9 show that base pressures at low Reynolds numbers with fixed transition are not representative of data at higher Reynolds numbers with natural transition; also that the thickness of transition strip has an important effect on base pressures.

Data were also obtained for the sharp-trailing-edge wings with smooth surfaces for purposes of comparison with data for wings with fixed transition.

The Reynolds numbers varied during tests of each wing and also between tests for the different wings because of varying reservoir stagnation pressures. The average Reynolds numbers of the tests, based on mean aerodynamic chord, are shown in the following table:

Mach number	Average R (untapered wings)	Average R (delta wings)
1.41	$1.5 \times 10^6$	$2.0 \times 10^6$
1.62	1.4	1.8
1.96	1.3	1.7

Maximum deviations from these average values during the course of the investigations were about  $\pm 0.2 \times 10^6$ .

#### ACCURACY

From general considerations of accuracy of balance calibration and repeatability of data, the accuracy of lift and drag measurements in terms of coefficients is believed to be about as indicated below:

$C_L$  . . . . .  $\pm 0.005$   
 $C_D$  when  $C_L = 0$  . . . . .  $\pm 0.001$

Possible errors in  $C_D$  increase somewhat with increase in  $C_L$ .

The relative accuracy of the pitching-moment measurements (the accuracy of each data point with respect to each other point at the same value of lift) is believed to be about  $\pm 0.002$  in terms of  $C_m$ . The absolute accuracy of the measurements is not known, however, because subsequent to the measurements the balance was modified and since the modification the pitching moments of this report cannot be repeated. There is a consistent unexplained discrepancy between data obtained before and after the modification which amounts to an indicated difference in aerodynamic-center location of approximately 0.05 inch (0.027 for the untapered wings).

Angle-of-attack measurements, relative to the tunnel axis, are accurate to about  $\pm 0.05^\circ$ .

## RESULTS AND DISCUSSION

In reducing the data of the present tests, values of the lift, drag, and pitching-moment coefficients of the body alone were subtracted from similar values for the wing-plus-body combinations. The lift, drag, and pitching-moment data presented for the wings therefore include wing-body interference effects. The absolute magnitudes of these data should be used with caution because the interference effects included are peculiar to the wing-body combinations tested. The trends indicated by the variations of the coefficients with wing section would, however, not be expected to be significantly affected by the interference.

Figure 4 contains body-alone data which were used as tares in reducing the data of the present investigation. The tares were obtained from tests of two bodies manufactured to the same specifications, one of which was used in tests of the swept wings and one of which was used in tests of the unswept and the  $45^\circ$  delta wings. Different tare coefficients for the different wings result from different model constants and from slight differences in the geometry of the two bodies.

An index to the figures containing wing-plus-interference data is included in table I. The basic wing-plus-interference lift, drag, and pitching-moment characteristics are presented in figures 5 to 10 for the unswept wings, in figures 11 to 16 for the swept wings, and in figures 17 to 22 for the delta wings. Summaries and comparisons of the basic data are included in figures 23 to 34.

### Drag at Zero Lift

Variations with trailing-edge thickness.— The variations of wing-plus-interference drag coefficient at zero lift with trailing-edge thickness are summarized in figure 23 for all wings having the trailing 20 percent of their chords beveled.



Data for the unswept wings show that the drag remains essentially constant as the trailing edges are thickened from 0 to about  $1/3$  of the maximum wing thickness and then increases appreciably with further increases in trailing-edge thickness.

Data for the swept wings show that the drag remains essentially constant as  $h/t$  is increased from 0 to about  $1/3$  at a Mach number of 1.41 and from 0 to about  $2/3$  at a Mach number of 1.62. At a Mach number of 1.96, slight decreases in drag with increasing  $h/t$  are shown for the 3.0-, 4.5-, and 6.0-percent-thick wings and minimum drag values are indicated at values of  $h/t$  of about  $3/4$ .

Since data for the  $45^\circ$  delta wings having small values of  $h/t$  were not obtained, detailed effects of blunting the trailing edges cannot be established. One interesting result indicated by the  $45^\circ$  delta-wing data, however, is that the trailing-edge thickness of a 4.5-percent-thick wing can be increased from  $\frac{h}{t} = \frac{2}{3}$  to  $\frac{h}{t} = 1$  with no appreciable increase in drag at a Mach number of 1.96.

In general, the data of figure 23 indicate that no appreciable decrease in drag at zero lift may be obtained by blunting the trailing edges. Of significance, however, is the indication that trailing edges can be thickened appreciably, resulting in improved structural properties and increased volume, with no increases in drag.

Although comparisons of drag data for wings of a fixed section and different plan forms probably do not have direct practical application because of structural and aerodynamic considerations, it is of interest to compare the magnitudes of the drags for the various plan forms. Such comparisons in general indicate that values of  $C_D$  are appreciably higher for the unswept wings than for corresponding  $45^\circ$  sweptback wings at values of  $h/t$  from about  $1/2$  to 1. At low values of  $h/t$  the values of  $C_D$  for the unswept and  $45^\circ$  swept wings are about the same except in the case of the 10.0-percent-thick wings, where the drags of the unswept wings are somewhat higher, especially at the lower Mach numbers. Comparisons of data for the  $45^\circ$  delta wings with data for the  $45^\circ$  swept wings of similar sections, in general, indicate slightly lower drags for the delta wings at a Mach number of 1.41 and slightly higher drags for the delta wings at a Mach number of 1.96.

Comparison of experimental and calculated values.— In figure 24, experimental and calculated drag coefficients for the 3.0- and 6.0-percent-thick unswept wings are compared and are shown to be in good general agreement. Illustrations of the breakdown of the calculated drag into various components are included. The friction drags are turbulent-boundary-layer values calculated for a flat plate by use of reference 10.

~~CONFIDENTIAL~~



The nose and boattail drags were obtained by use of second-order two-dimensional theory and the base drags were obtained by use of experimental base pressures from reference 2.

Effects of boattail angle.- From the drag breakdowns of figure 24, it can be seen that the variations of total drag with trailing-edge thickness are determined by the sum of the boattail and base drags. Experiments of reference 3 have indicated that base pressures and, therefore, base drags, are relatively unaffected by changes in boattail angle when values of  $h/t$  are fixed. Consequently, the variation of total drag with trailing-edge thickness for a wing with a fixed thickness ratio ( $t/c$ ) and leading wedge can be changed only by changing the boattail drag. It can be seen from figure 24 that a decrease in boattail drag, with the other drag components remaining fixed, would result in a lower drag at  $\frac{h}{t} = 0$  and in a more pronounced increase in drag with increases in trailing-edge thickness. (Such a decrease in boattail drag could be accomplished by increasing the length of trailing-edge bevel and thereby decreasing the boattail angle.) This fact indicates that drag increases due to thickening of the trailing edges would be expected to increase with increasing  $l/c$  and that the data of the present tests for wings having fixed lengths of trailing-edge bevel are therefore not completely representative. It should be noted, however, that the boattail drag diminishes with decreasing wing thickness and consequently would be expected to have little effect on drag variations with  $h/t$  for the thinner wings.

In order to obtain indications of its effect on drag, the length of the trailing-edge bevel was varied on the 10.0-percent-thick wings with  $\frac{h}{t} = 0.375$  and on the 6.0-percent-thick wings with  $\frac{h}{t} = 0.250$ . Figure 25 presents the variations of drag of these wings with  $l/c$ . It can be seen in figure 25 that the decreases in drag due to increasing the lengths of trailing-edge bevel are appreciable for the 10.0-percent-thick wings but are somewhat less for the 6.0-percent-thick wings. As previously mentioned, these smaller effects for the thinner wings would be expected because of their lower boattail drags.

#### Drag at Various Lift Coefficients

The drag at zero lift, to which the previous discussion has been limited, is of significance mainly because it is an important part of the drag at finite lift coefficients at which the wings will be operating. The drag coefficients of the wings at various lift coefficients, which are probably of more direct interest, are summarized in figure 26 for the unswept wings, in figure 27 for the  $45^\circ$  swept wings, and in figure 28 for

the  $45^\circ$  delta wings. Values of  $C_D$  presented in figures 26 to 28 are averages of values at positive and negative lift coefficients of the symmetrical wings.

Unswep wings.- Data for the unswept 10.0-percent-thick wings in figure 26 show that, at Mach numbers of 1.41 and 1.62, the increases in drag with increasing  $h/t$  become smaller as the lift coefficient becomes larger. At the highest lift coefficients a slight decrease in drag due to thickening the trailing edges is shown. Data for the 10.0-percent-thick wings at a Mach number of 1.96 and for the 3.0-, 4.5-, and 6.0-percent-thick wings at all Mach numbers show variations of drag with  $h/t$  at various lift coefficients which are very similar to those at zero lift coefficient. In general, the increases in  $C_D$  with  $h/t$  are about the same at all lift coefficients. This fact is significant in that percentage increases in drag at zero lift due to thickening of the trailing edges might be sufficient to outweigh the advantages of increases in wing strength, stiffness, and volume, whereas at moderate to high lift coefficients, the percentage increases in drag would be small by comparison.

Swept wings.- Data for the  $45^\circ$  swept wings show that, at lift coefficients of 0.2 and above, the drag coefficients generally decrease with increases in  $h/t$  from values near zero, as was shown for the 10.0-percent-thick unswept wings at the lower Mach numbers and high lift coefficients. The data also show that values of  $h/t$  for minimum drag usually increase with increases in wing thickness, operating lift coefficient, and Mach number. For wings operating at values of  $C_L$  between 0.2 and 0.4, the data indicate that a drag reduction could be obtained by thickening the trailing edges to about half the maximum wing thickness. For wings operating at higher values of  $C_L$ , the data indicate that  $C_D$  could be decreased by thickening the trailing edges even more.

$45^\circ$  delta wings.- The data for the  $45^\circ$  delta wings in figure 28 are similar to the data for the 3.0- to 6.0-percent-thick unswept wings in that variations of  $C_D$  with  $h/t$  for the wings tested are about the same at all values of  $C_L$ . As mentioned for the zero-lift case, it is interesting to note that the drag of the 4.5-percent-thick wing at various lift coefficients shows no appreciable increase with increase in  $h/t$  from  $2/3$  to 1.0 at a Mach number of 1.96.

#### Maximum Lift-Drag Ratio

The maximum lift-drag ratios and values of  $C_L$  at  $(L/D)_{\max}$  are presented in figure 29 for the unswept wings, in figure 30 for the  $45^\circ$  swept wings, and in figure 31 for the  $45^\circ$  delta wings. Values of

$(L/D)_{\max}$  and  $C_L$  presented are averages of values obtained at positive and negative angles of attack for the symmetrical wings.

Unswept wings.- Values of  $(L/D)_{\max}$  for the unswept wings (fig. 29) vary with  $h/t$  in the general manner which would be predicted from consideration of the variations of drag at zero lift. That is, the highest values of  $(L/D)_{\max}$  occur near values of  $h/t$  for which the drag at zero lift was a minimum; also, decreasing values of  $(L/D)_{\max}$  with  $h/t$  generally correspond to increasing values of  $C_D$  at zero lift. Values of  $C_L$  at  $(L/D)_{\max}$  increase with increasing airfoil-section thickness ratio and with increasing trailing-edge thickness, as would be expected from the corresponding increases in drag at zero lift.

45° swept wings.- As shown in figure 30, the highest values of  $(L/D)_{\max}$  for the 45° swept wings occur for 3.0-percent-thick wings having  $\frac{h}{t} = 0$  and for 4.5- and 6.0-percent-thick wings having values of  $h/t$  between 1/2 and 3/4. Variations of  $(L/D)_{\max}$  with  $h/t$  are somewhat different from what would be expected from consideration of the variations of drag at zero lift. Whereas the drag at zero lift in general remains about constant with increase in  $h/t$  from 0 to about 1/2, the values of  $(L/D)_{\max}$  for the 3.0-percent-thick wings decrease and values of  $(L/D)_{\max}$  for the 4.5- and 6.0-percent-thick wings increase. Values of  $C_L$  at  $(L/D)_{\max}$  increase with increases in airfoil-section thickness ratio and with increases in trailing-edge thickness in much the same manner as in the case of the unswept wings.

45° delta wings.- The data of figure 31 show that the values of  $(L/D)_{\max}$  for the 6.0-percent-thick 45° delta wings decrease slightly with increases in  $h/t$  and that these decreases are about the same at all Mach numbers. This type of variation is similar to that shown for the unswept wings in the same  $h/t$  range. The plots of  $(L/D)_{\max}$  for the 4.5-percent-thick 45° delta wings, however, indicate that effects of  $h/t$  decrease with increasing Mach number and are insignificant at a Mach number of 1.96. This effect of Mach number on  $(L/D)_{\max}$  variations with  $h/t$  corresponds to the effects on  $C_D$  at zero lift shown in figure 23. The variations of  $C_L$  at  $(L/D)_{\max}$  shown in figure 31 would be expected from consideration of the variations of drag at zero lift.

#### Lift-Curve Slopes

The lift-curve slopes of the wings at zero angle of attack are summarized in figure 32. The data indicate increases in  $C_{L\alpha}$  with

increasing  $h/t$ , as would be predicted from two-dimensional theory. The increases for the  $45^\circ$  swept wings are somewhat larger than those for the unswept wings.

The data for the unswept and  $45^\circ$  delta wings indicate no appreciable effect of wing section thickness ratio on lift-curve slope. Data for the  $45^\circ$  swept wings show that values of  $C_{L_\alpha}$  for 4.5- and 6.0-percent-thick wings are about equal but are consistently higher than values for the 3.0-percent-thick wings. The lower values of  $C_{L_\alpha}$  for the 3.0-percent-thick wings can probably be attributed to the elasticity of the thin sweptback wings. Data also show that values of  $C_{L_\alpha}$  for the 10.0-percent-thick  $45^\circ$  swept wings are about equal to those for the 4.5- and 6.0-percent-thick wings at  $\frac{h}{t} = 1.0$  but are somewhat lower at lower values of  $h/t$ . These lower values of  $C_{L_\alpha}$  at low values of  $h/t$  probably result from losses in loading over the boattail section of the 10.0-percent-thick wing as a result of the large trailing-edge angle.

#### Pitching-Moment Parameter $\partial C_m / \partial C_L$

Values at zero lift of the pitching-moment parameter  $\partial C_m / \partial C_L$ , which gives an indication of center-of-pressure location for the symmetrical wings, are summarized in figure 33 for the unswept, the  $45^\circ$  swept, and the  $45^\circ$  delta wings. It will be noted in figure 33 that the general level of values of  $\partial C_m / \partial C_L$  is somewhat more negative (centers of pressure are farther aft) than would be expected, particularly at the higher Mach numbers, probably because of the effect of wing interference on body loading. The rearward movement of the center-of-pressure location with increases in Mach number, which is particularly pronounced for the unswept wings, can probably also be attributed in part to interference effects. Comparisons of the pitching-moment data to determine effects of section are necessarily based on the premise that the interference effects are not appreciably influenced by airfoil section.

The data of figure 33, in general, show that centers of pressure for the unswept wings are not influenced to a great extent by variations in trailing-edge thickness, although two-dimensional theory indicates appreciable rearward movements with increases in  $h/t$  from 0 to 1.0 (approximately 0.05c for 10.0-percent-thick wings and 0.015c for 3.0-percent-thick wings).

For the  $45^\circ$  swept wings, the data indicate a tendency toward a rearward movement of the center of pressure with increases in  $h/t$ , the movement being fairly rapid at low values of  $h/t$  and decreasing with

increasing  $h/t$ . For the 6.0-percent-thick wings at Mach numbers of 1.41 and 1.62, the rate of rearward movement is much greater than for the 3.0- and 4.5-percent-thick wings at low values of  $h/t$  but about the same at high values of  $h/t$ . It is believed that this type of variation for the 6.0-percent-thick wings is due to a loss in loading over the boattail portion of the wing, resulting from a thickened or separated boundary layer, which is alleviated by decreases in trailing-edge angle (increases in  $h/t$ ).

The variations of the center-of-pressure location with  $h/t$  for the  $45^\circ$  delta wings are similar to those for the  $45^\circ$  swept wings in the  $h/t$  range between 0.5 and 1.0; that is, there is a tendency toward a slight rearward movement of the center of pressure with increases in  $h/t$ .

Data for the unswept wings indicate forward movements of the center-of-pressure location with increases in section thickness ratio, as predicted by theory. The theoretical effects of  $t/c$  are, however, somewhat inconsistent with experiment in that theory indicates that the effects of  $t/c$  decrease considerably with increases in  $h/t$ , whereas figure 33 shows no appreciable variation with  $h/t$  of the effects of  $t/c$ . Also, the theoretical movements of the center of pressure due to increases in  $t/c$  are considerably less than shown by the data of figure 33. Data for the  $45^\circ$  delta wings show no effects of  $t/c$ , and data for the  $45^\circ$  swept wings, in general, indicate small effects except, as previously mentioned, at the low values of  $h/t$ .

#### Effects of Fixed Transition

In order to provide some indication of the effects of fixed transition on the data of the present tests, lift, drag, and pitching-moment parameters for the sharp-trailing-edge wings are compared in figure 34 with similar parameters obtained from the tests in which the model surfaces were smooth.

Data for the unswept wing in figure 34 show, as would be expected, that the drags of the models tested with fixed transition were higher than those for the smooth-surfaced models by amounts which are relatively independent of wing thickness. It is of interest to note that the increments in drag resulting from fixing transition are approximately equal to the differences between calculated flat-plate drag with turbulent boundary layer and with laminar boundary layer (calculated increments are 0.0042 at a Mach number of 1.41, 0.0039 at a Mach number of 1.62, and 0.0036 at a Mach number of 1.96).

The plots of  $C_{L\alpha}$  indicate that fixing transition has no measurable effects on the lift-curve slopes of the unswept wings. The plots of  $\partial C_m / \partial C_L$  indicate that the centers of pressure of the wings with fixed transition were slightly aft of the centers of pressure of the wings with smooth surfaces.

Data for the  $45^\circ$  swept wings show the drags of the wings with fixed transition to be higher than the drags of the wings with smooth surfaces. The drag increments due to fixing the transition are, however, somewhat less than calculated. As in the case of the unswept wings, the lift-curve slopes show no effects of fixing transition. Plots of  $\partial C_m / \partial C_L$  indicate that fixing transition has small but somewhat inconsistent effects on this parameter.

#### CONCLUDING REMARKS

Results of an investigation of systematic series of  $0^\circ$  and  $45^\circ$  swept-back untapered wings and  $45^\circ$  delta wings with blunt trailing edges at Mach numbers of 1.41, 1.62, and 1.96 are as follow:

In general, no appreciable drag reductions at zero lift due to thickening of the wing trailing edges are indicated. However, data show that trailing edges can be thickened appreciably, resulting in improved structural properties and increased volume, with no increase in drag. Values of zero-lift drag for representative unswept wings, calculated by use of experimental base pressures and existing theoretical methods, were found to be in good agreement with experimental values.

Variations of drag of the 3.0-, 4.5-, and 6.0-percent-thick unswept wings with trailing-edge thickness, at various lift coefficients, were very similar to those at zero lift; that is, the drag remained essentially constant with increases in trailing-edge thickness up to about  $1/3$  of the maximum wing thickness and then increased fairly rapidly. Data for the  $45^\circ$  swept wings operating at lift coefficients 0.2 or above, however, showed drag reductions due to thickening the trailing edges by various amounts. The trailing-edge thickness for minimum drag increased with increases in airfoil-section thickness ratio, operating lift coefficient, and Mach number. Data for the  $45^\circ$  delta wings with sharp trailing edges were not obtained and detailed effects of blunting their trailing edges were not determined.

Values of the maximum lift-drag ratio  $(L/D)_{\max}$  for the 3.0-, 4.5-, and 6.0-percent-thick unswept wings remained essentially constant

with increases in trailing-edge thickness to about  $1/4$  or  $1/3$  of the maximum wing thickness and then decreased fairly rapidly. Highest values of  $(L/D)_{\max}$  for the  $45^\circ$  swept wings occurred for 3.0-percent-thick wings having sharp trailing edges and for the 4.5- and 6.0-percent-thick wings having ratios of trailing edge to maximum thickness from about  $1/2$  to  $3/4$ .

Lift-curve slopes of the wings, in general, tended to increase slightly with increases in trailing-edge thickness and were essentially unaffected by variations in airfoil-section thickness ratio.

Center-of-pressure locations for the unswept wings were relatively independent of trailing-edge thickness ratio  $h/t$ . For the  $45^\circ$  swept wings, the centers of pressure moved rearward with increases in  $h/t$ , the movement being fairly rapid at small values of  $h/t$  and decreasing with increases in  $h/t$ . For the  $45^\circ$  delta wings, there was a slight rearward movement of the center of pressure with increases in  $h/t$  from 0.5 to 1.0.

Langley Aeronautical Laboratory,  
National Advisory Committee for Aeronautics,  
Langley Field, Va.



## REFERENCES

1. Chapman, Dean R.: Reduction of Profile Drag at Supersonic Velocities by the Use of Airfoil Sections Having a Blunt Trailing Edge. NACA RM A9H11, 1949.
2. Cleary, Joseph W., and Stevens, George L.: The Effects at Transonic Speeds of Thickening the Trailing Edge of a Wing With a 4-Percent-Thick Circular-Arc Airfoil. NACA RM A51J11, 1951.
3. Goin, Kenneth L.: Effects of Plan Form, Airfoil Section, and Angle of Attack on the Pressures Along the Base of Blunt-Trailing-Edge Wings at Mach Numbers of 1.41, 1.62, and 1.96. NACA RM L52D21, 1952.
4. Chapman, Dean R., Wimbrow, William R., and Kester, Robert H.: Experimental Investigation of Base Pressure on Blunt-Trailing-Edge Wings at Supersonic Velocities. NACA TN 2611, 1952.
5. Morrow, John D., and Katz, Ellis: Flight Investigation at Mach Numbers From 0.6 to 1.7 To Determine Drag and Base Pressures on a Blunt-Trailing-Edge Airfoil and Drag of Diamond and Circular-Arc Airfoils at Zero Lift. NACA RM L50E19a, 1950.
6. Sawyer, Richard H., and Daum, Fred L.: Measurement Through the Speed of Sound of Static Pressures on the Rear of Unswept and Sweptback Circular Cylinders and on the Rear and Sides of a Wedge by the NACA Wing-Flow Method. NACA RM L8B13, 1948.
7. May, Ellery B., Jr.: Investigation of the Effects of Leading-Edge Chord-Extensions on the Aerodynamic and Control Characteristics of Two Sweptback Wings at Mach Numbers of 1.41, 1.62, and 1.96. NACA RM L50L06a, 1951.
8. Conner, D. William: Aerodynamic Characteristics of Two All-Movable Wings Tested in the Presence of a Fuselage at a Mach Number of 1.9. NACA RM L8H04, 1948.
9. Bogdonoff, Seymour M.: A Preliminary Study of Reynolds Number Effects on Base Pressure at  $M = 2.95$ . Jour. Aero. Sci., vol. 19, no. 3, Mar. 1952, pp. 201-206.
10. Wilson, Robert E.: Turbulent Boundary-Layer Flow on a Smooth Flat Plate at Supersonic Speeds. NAVORD Rep. 1651, Proceedings of the Bureau of Ordnance Symposium on Aeroballistics, Nov. 16-17, 1950, pp. 245-278.

CONFIDENTIAL

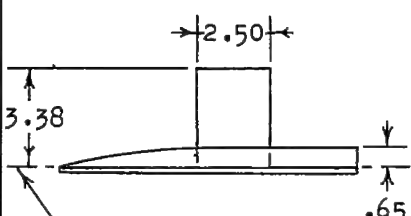
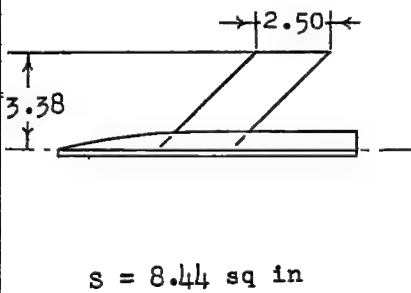
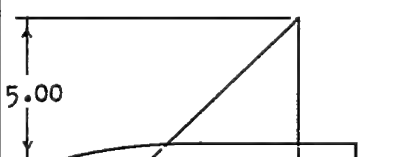
TABLE I.- INDEX TO FIGURES

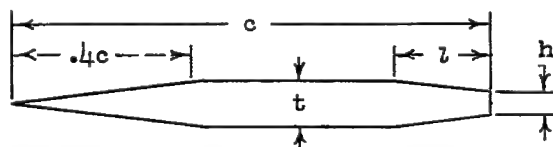
Basic data				
Figure for variation of -		M	t/c	Wings
$C_L$ with $\alpha$ $C_L$ with $C_D$	$C_m$ with $C_L$			
5	8	1.41	0.100 .060 .045 .030	Unswept
6	9	1.62	.100 .060 .045 .030	
7	10	1.96	.100 .060 .045 .030	
11	14	1.41	.100 .060 .045 .030	45° sweptback
12	15	1.62	.100 .060 .045 .030	
13	16	1.96	.100 .060 .045 .030	
17	20	1.41	.060 .045	45° delta
18	21	1.62	.060 .045	
19	22	1.96	.060 .045	

Fig. Summaries and Cross Plots

23. Summary of  $C_D$  at  $C_L = 0$   
 24. Comparison of experimental and calculated values of  $C_D$  at  $C_L = 0$   
 25. Variations of  $C_D$  with length of trailing-edge bevel of untapered wings at  $C_L = 0$   
 26. Summary of  $C_D$  at various values of  $C_L$  for unswept wings  
 27. Summary of  $C_D$  at various values of  $C_L$  for 45° sweptback wings  
 28. Summary of  $C_D$  at various values of  $C_L$  for 45° delta wings  
 29. Summary of  $(L/D)_{max}$  and  $C_L$  at  $(L/D)_{max}$  for unswept wings  
 30. Summary of  $(L/D)_{max}$  and  $C_L$  at  $(L/D)_{max}$  for 45° sweptback wings  
 31. Summary of  $(L/D)_{max}$  and  $C_L$  at  $(L/D)_{max}$  for 45° delta wings  
 32. Summary of  $C_{L\alpha}$  at  $C_L = 0$  for unswept, 45° sweptback, and 45° delta wings  
 33. Summary of  $\partial C_m / \partial C_L$  at  $C_L = 0$  for unswept, 45° sweptback, and 45° delta wings  
 34. Effects of fixed transition on  $C_D$ ,  $C_{L\alpha}$ , and  $\partial C_m / \partial C_L$  for untapered sharp trailing-edge wings

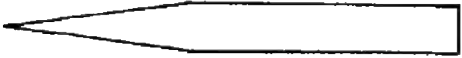
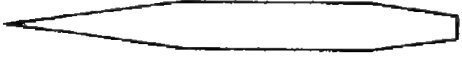
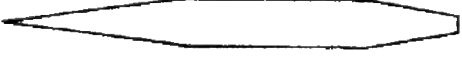


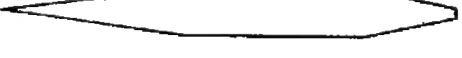



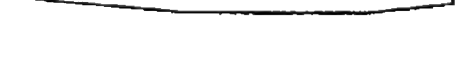
CONFIDENTIAL


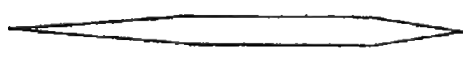
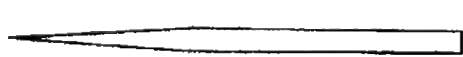
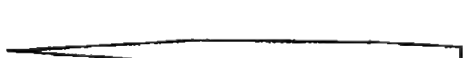





Plan form				Section		
	A	$\lambda$	$\Lambda$	t/c	h/t	l/c
 <p>Fuselage center line</p> <p><math>s = 8.44 \text{ sq in}</math></p>	2.7	1.0	$0^\circ$	0.100	1.000 .500 .375 .375 .375 .200	0 .20 .20 .35 .50 .20
				.060	1.000 .500 .250 .250 0	0 .20 .20 .35 .20
				.045	1.000 .667 .333 0	0 .20 .20 .20
				.030	1.000 .500 0	0 .20 .20
 <p><math>s = 8.44 \text{ sq in}</math></p>	2.7	1.0	$45^\circ$	.100	1.000 .375 .375 .200	0 .20 .35 .20
				.060	1.000 .500 .250 .250 0	0 .20 .20 .35 .20
				.045	1.000 .667 .333 0	0 .20 .20 .20
				.030	1.000 .500 0	0 .20 .20
 <p><math>s = 12.50 \text{ sq in}</math></p>	4.0	0	$45^\circ$	.060	1.000 .750 .500	0 .20 .20
				.045	1.000 .667	0 .20



(a) Geometric details of models (all dimensions in inches).

Figure 1.- Plan-form and section characteristics of wing models investigated.

	$t/c$	$h/t$	$l/c$
	0.100	1.000	0
	.100	.500	.20
	.100	.375	.20
	.100	.375	.35
	.100	.375	.50
	.100	.200	.20
	.060	1.000	0
	.060	.750	.20
	.060	.500	.20
	.060	.250	.20

	$t/c$	$h/t$	$l/c$
	0.060	0.250	0.35
	.060	0	.20
	.045	1.000	0
	.045	.667	.20
	.045	.333	.20
	.045	0	.20
	.030	1.000	0
	.030	.500	.20
	.030	0	.20



(b) Illustration of wing sections.

Figure 1.- Concluded.

Wing	distance from fuselage nose to mean quarter chord of wing
Unswapt	5.191 inches
45° swapt	5.571 inches
45° delta	5.571 inches

Fuselage ordinates  
(inches)

x	r
0	0
.522	.125
1.305	.295
1.957	.410
2.609	.510
3.261	.588
3.914	.634
4.566	.652
10.000	.652

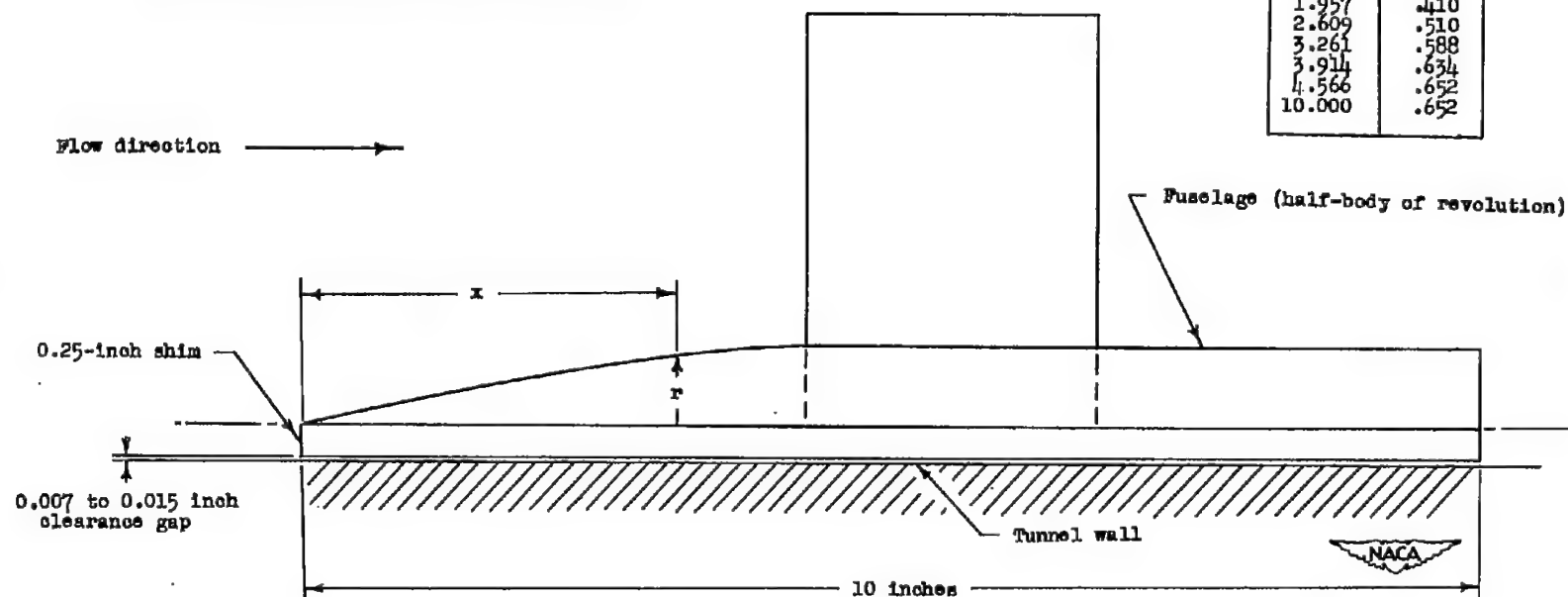
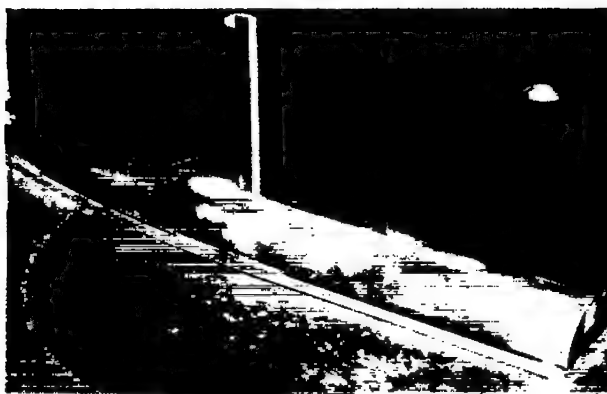
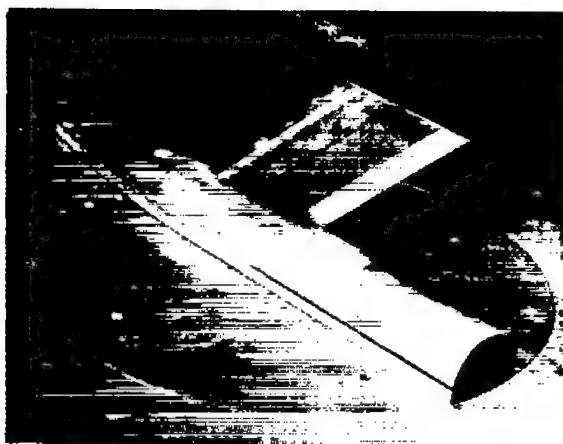
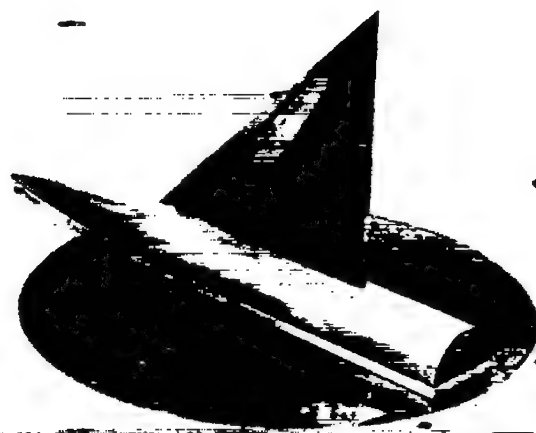


Figure 2.- Details of model mounting arrangement.



unswept wing

 $45^\circ$  swept wing $45^\circ$  delta wing

NACA  
L-79244

Figure 3.- Photographs of model arrangements for the three wing plan forms investigated.

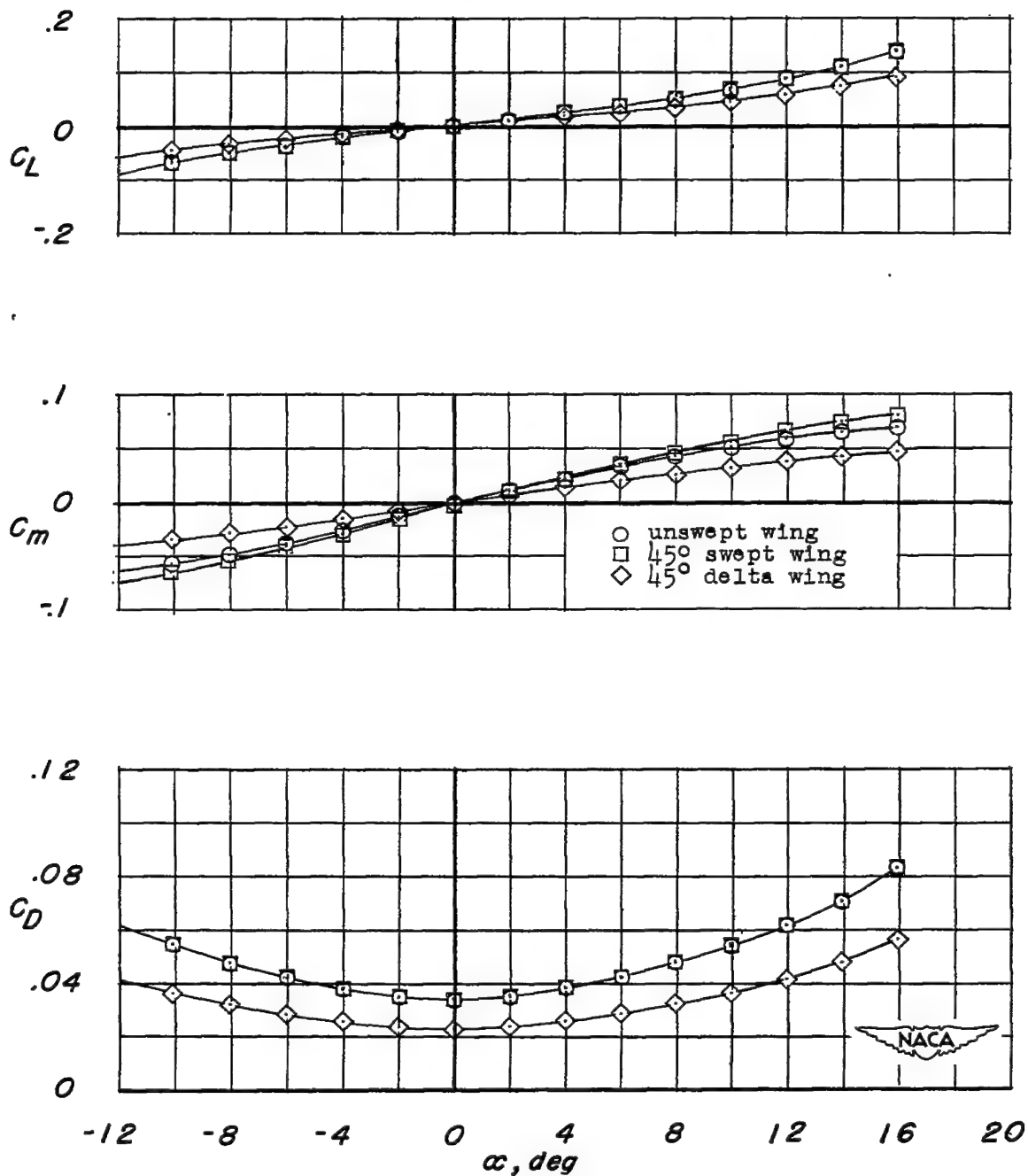
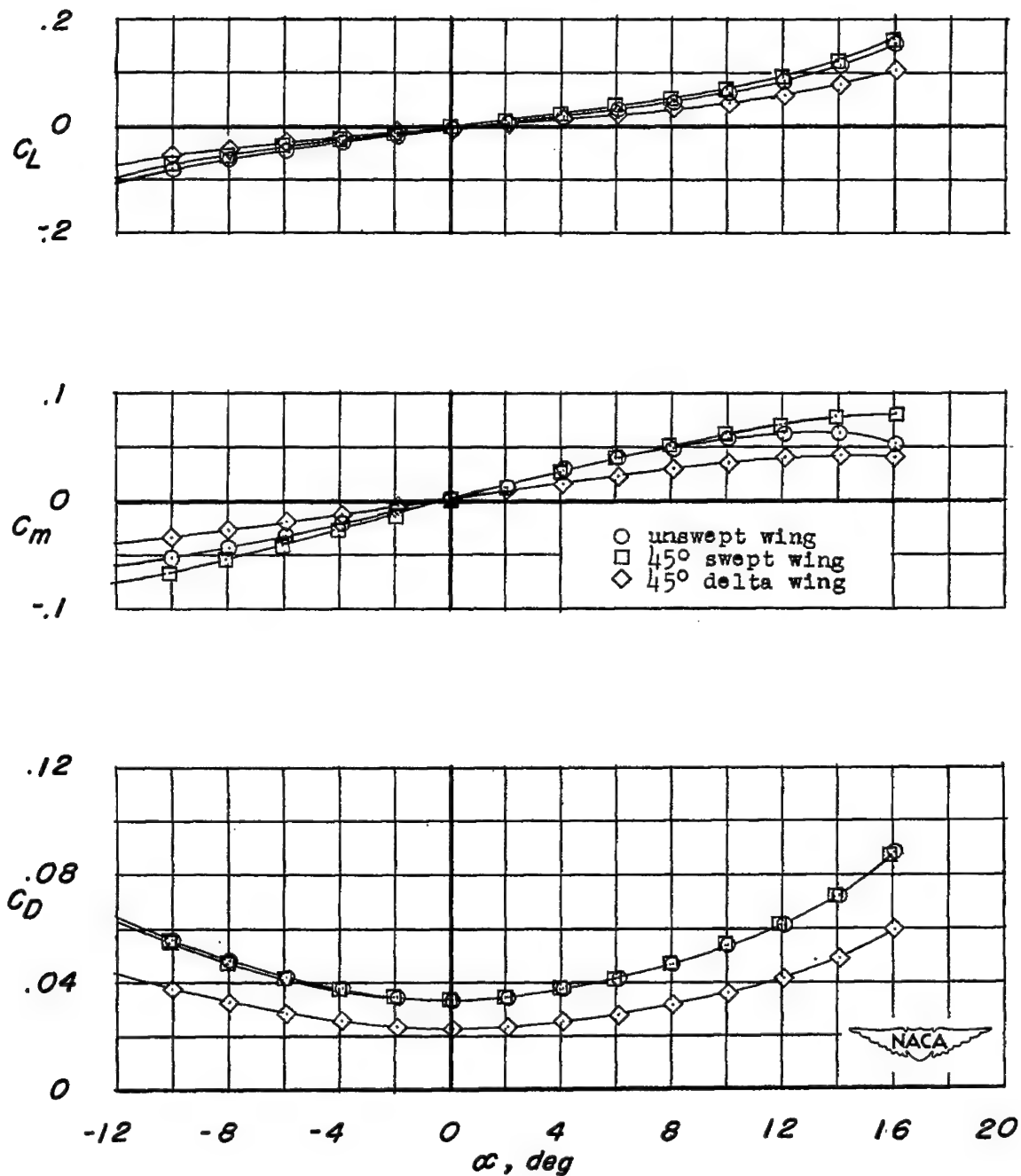
(a)  $M = 1.41$ .

Figure 4.- Test-body lift, drag and pitching-moment tares applied to data for the wing-body combinations.





(b)  $M = 1.62$ .

Figure 4.- Continued.

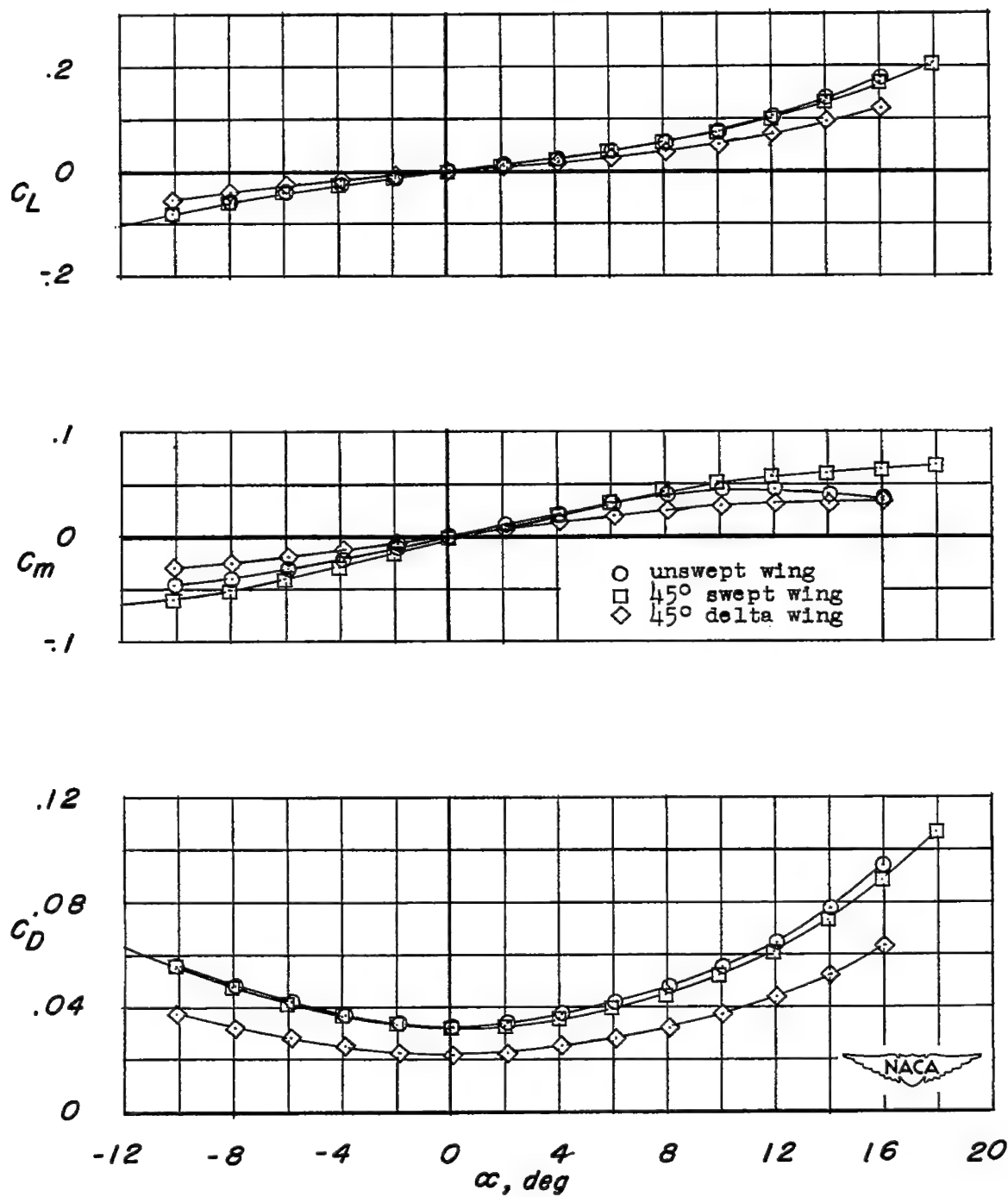
(c)  $M = 1.96$ .

Figure 4.- Concluded.

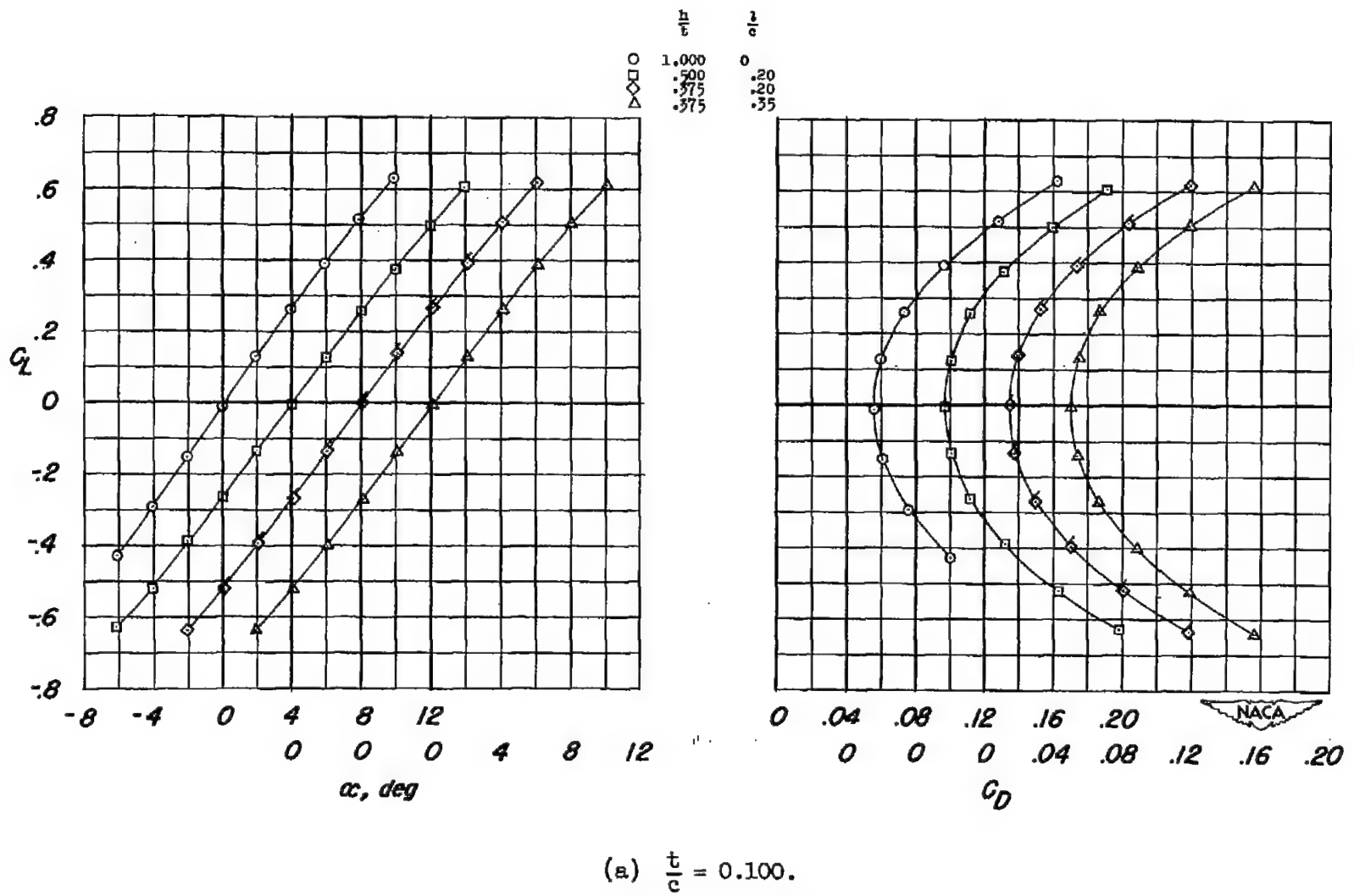
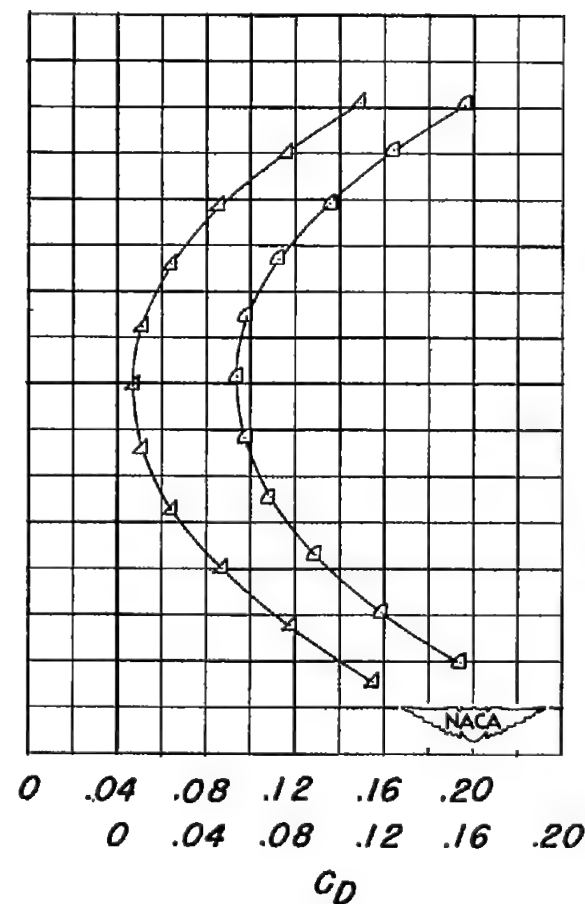
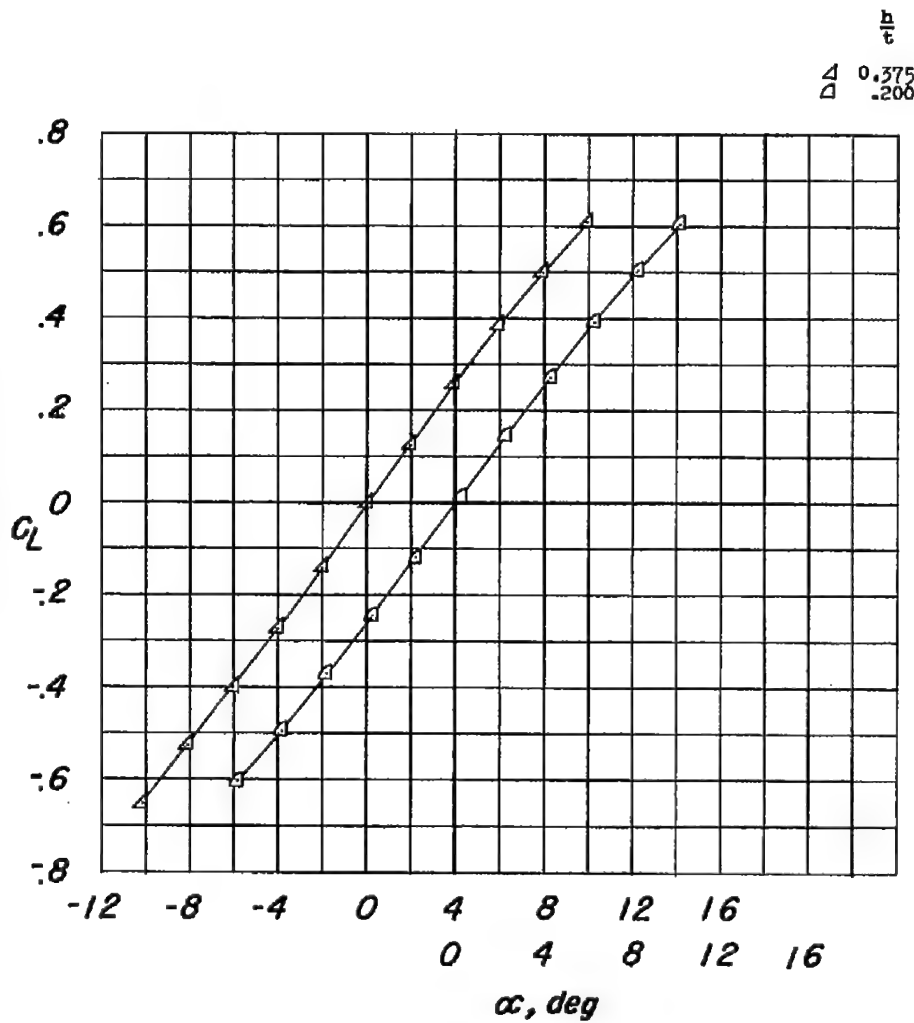
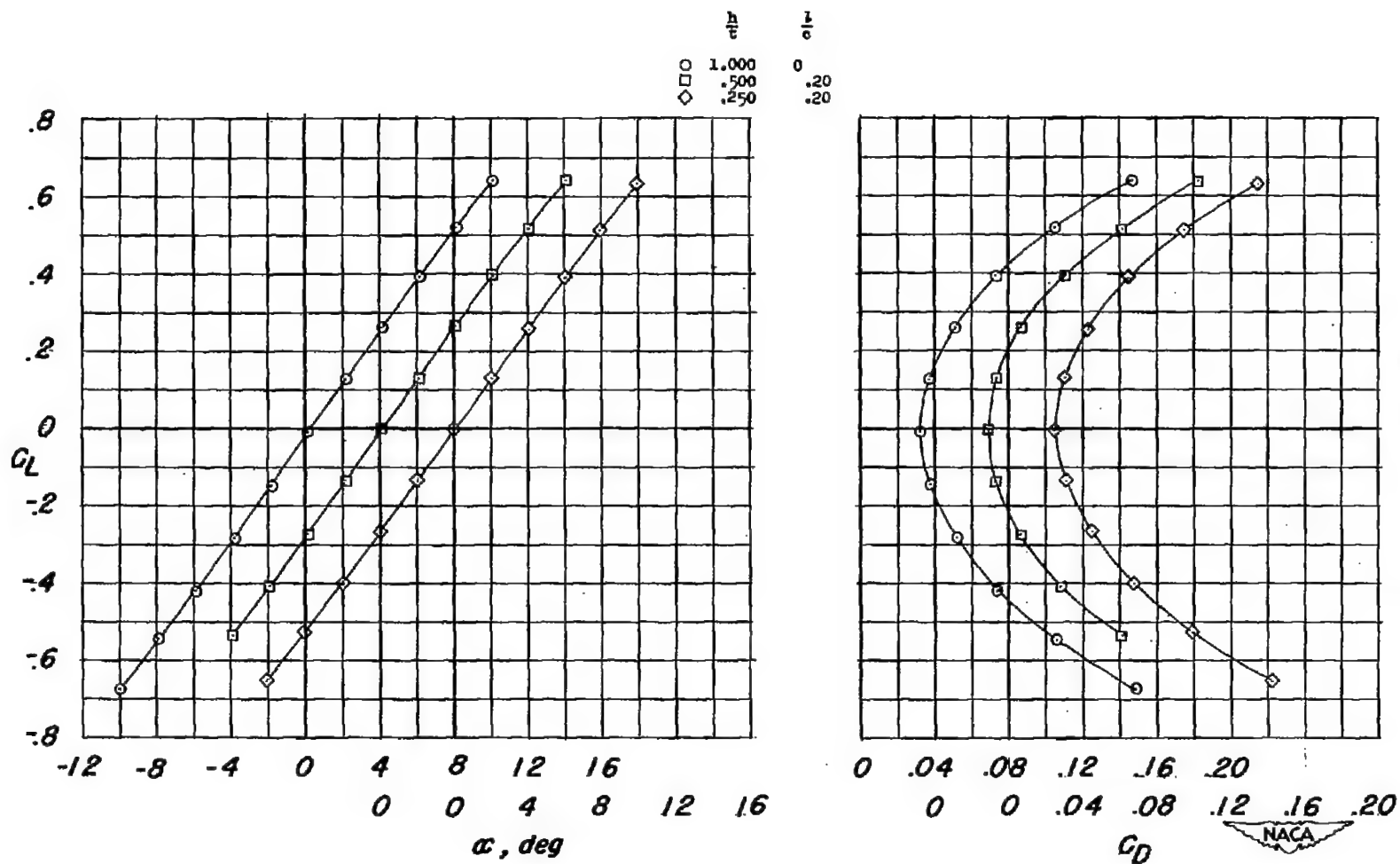


Figure 5.- Wing-plus-interference lift and drag characteristics of unswept wings at a Mach number of 1.41.



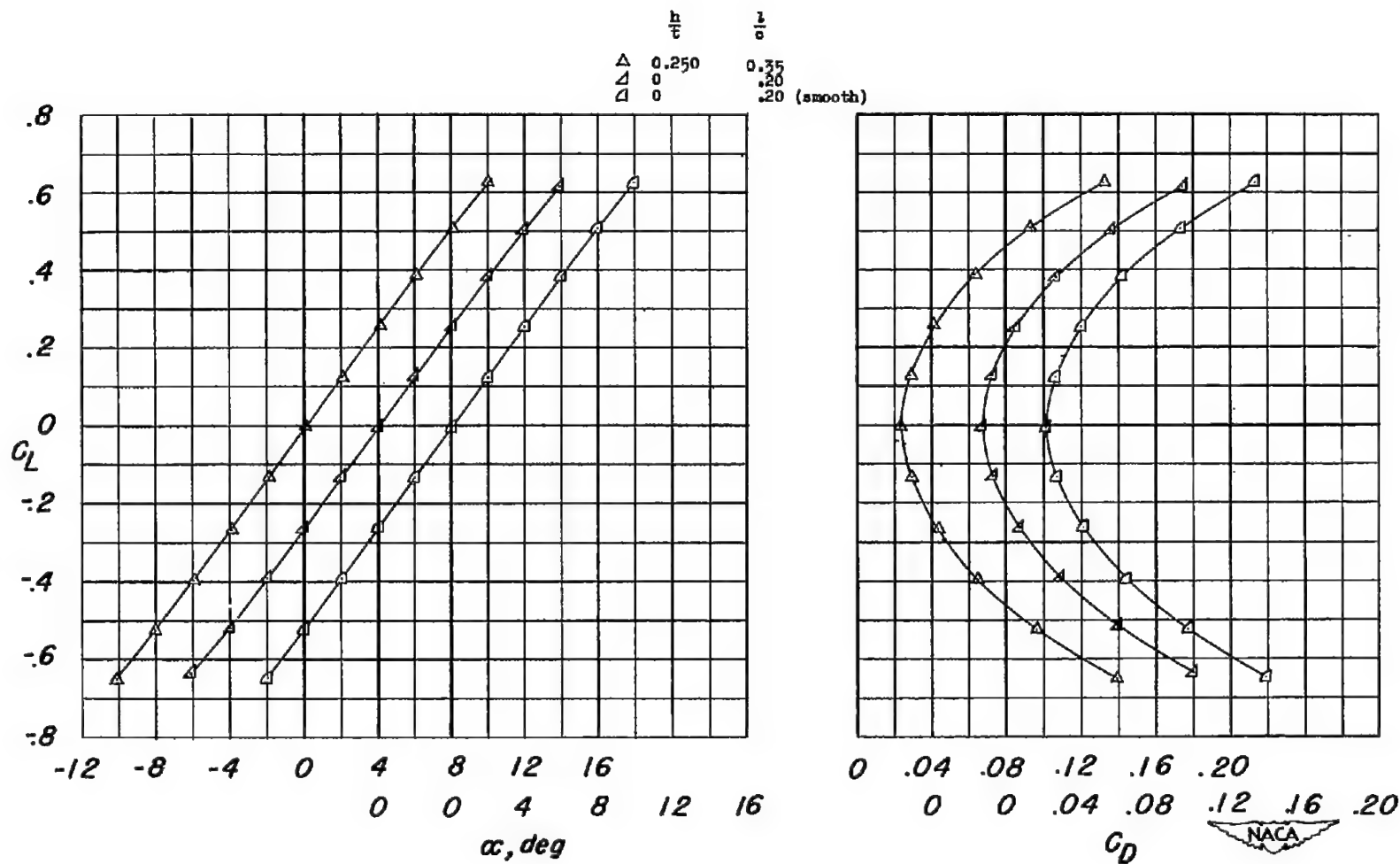
(a) Concluded.

Figure 5.- Continued.



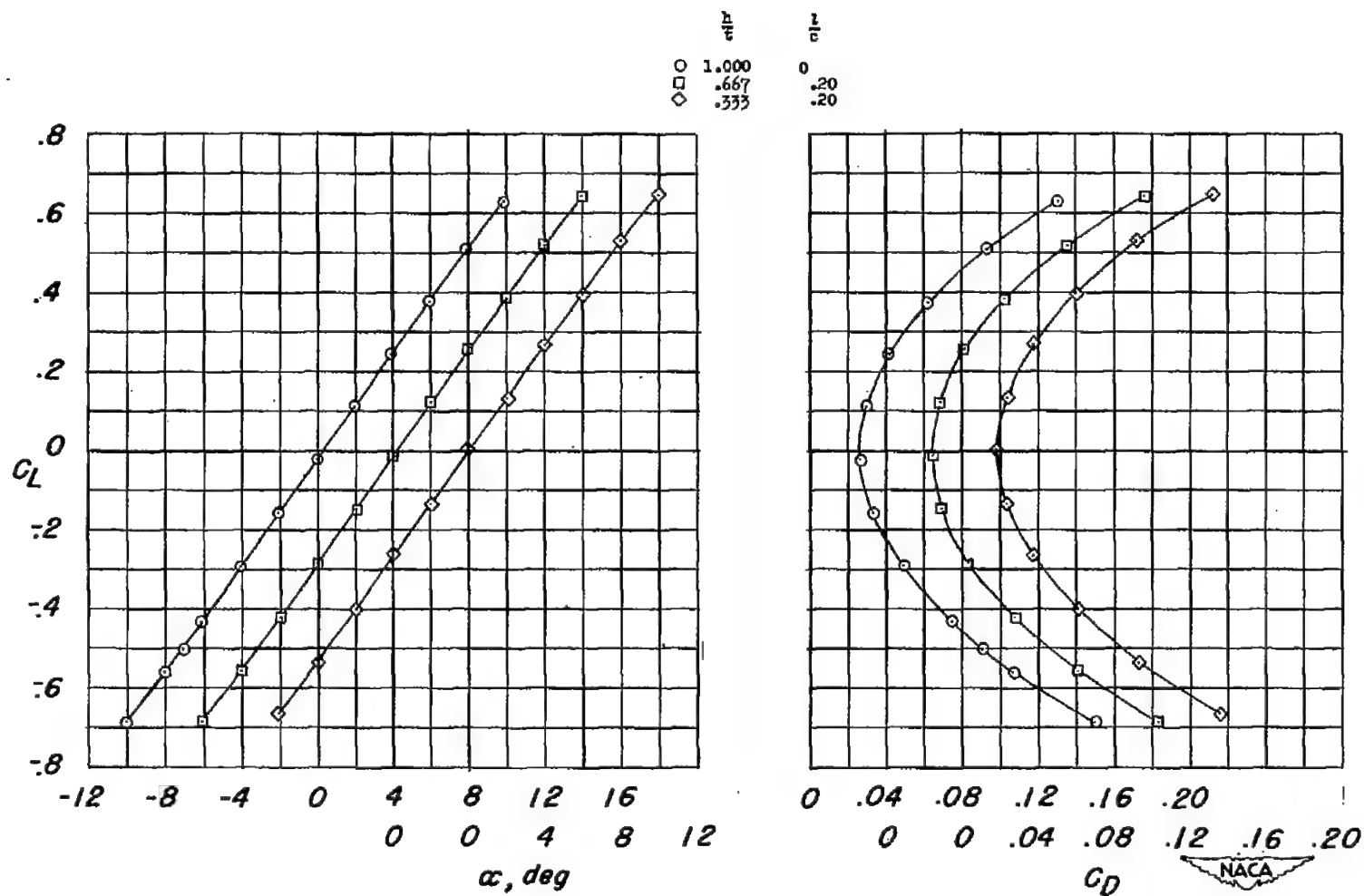
(b)  $\frac{t}{c} = 0.060$ .

Figure 5.- Continued.



(b) Concluded.

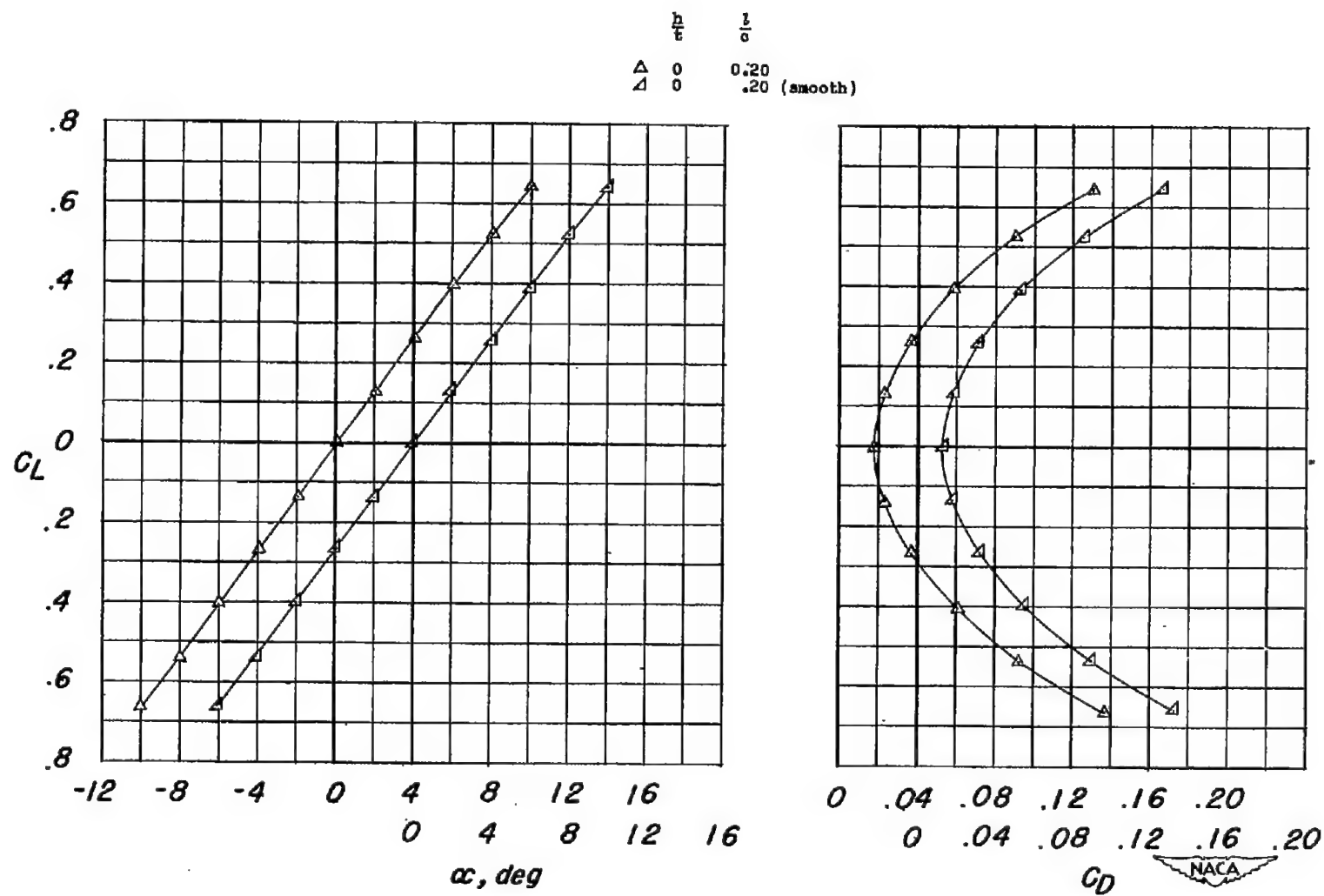
Figure 5.- Continued.



(c)  $\frac{t}{c} = 0.045$ .

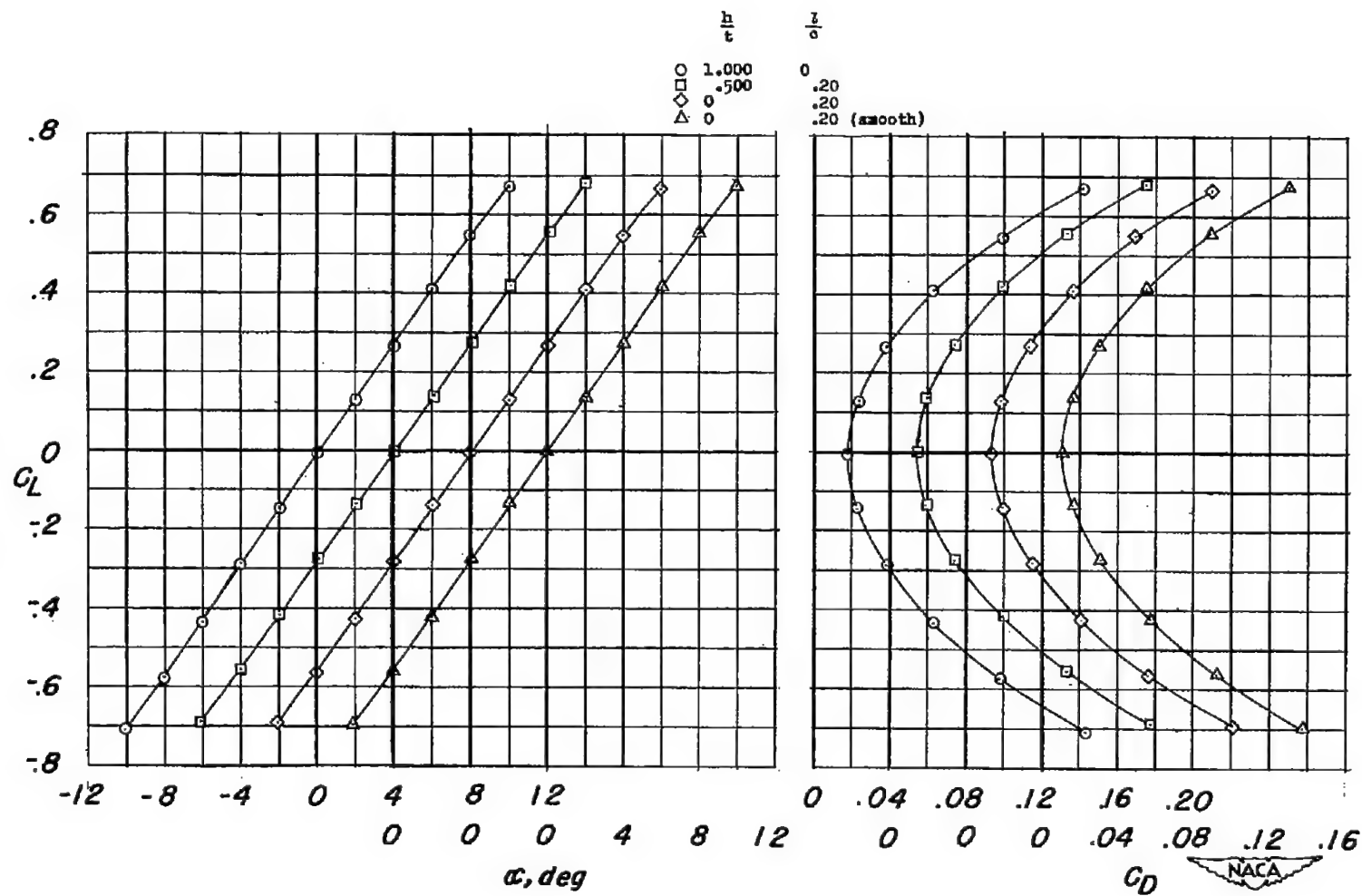
Figure 5.- Continued.





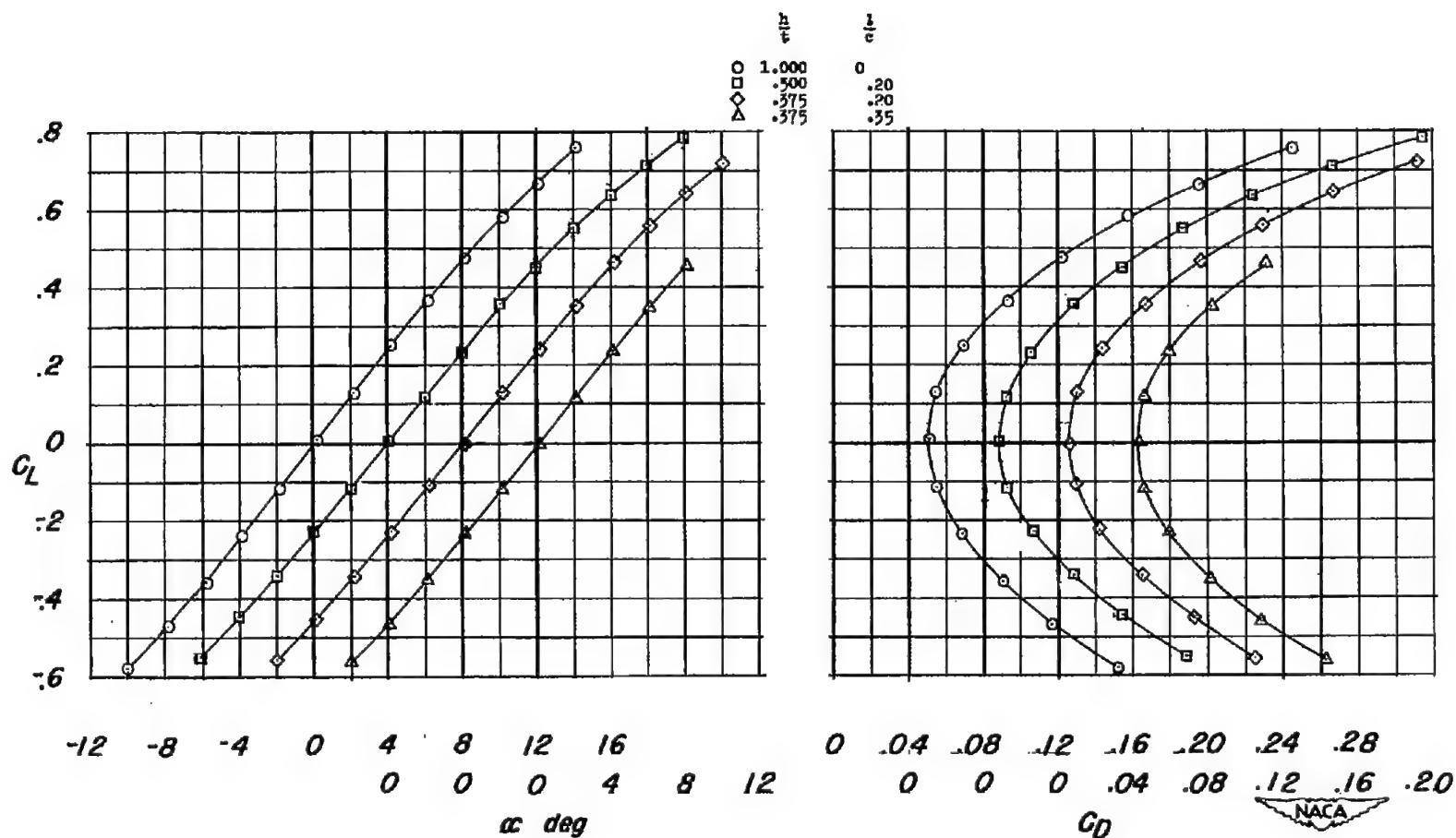
(c) Concluded.

Figure 5.- Continued.



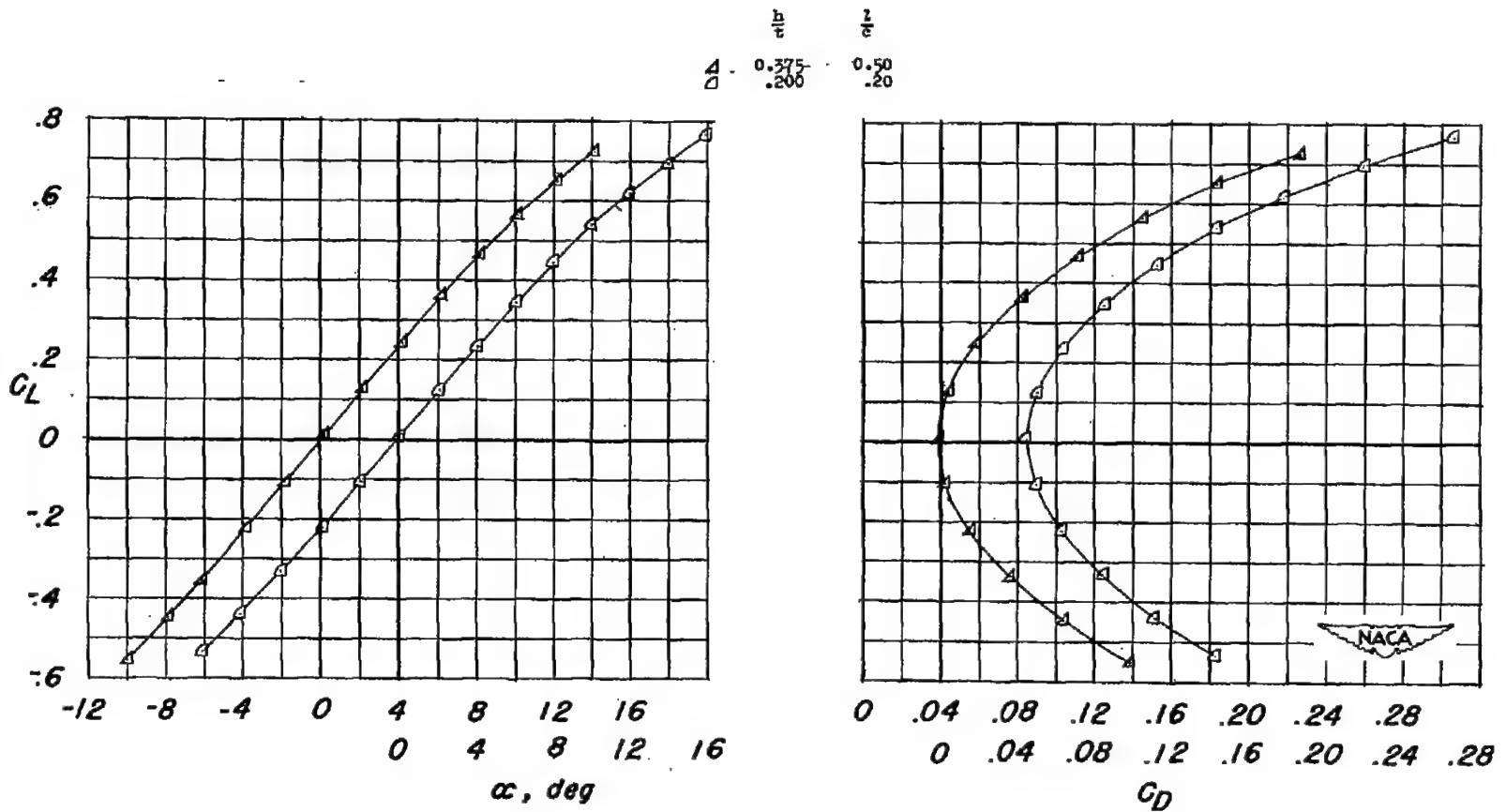
(a)  $\frac{t}{c} = 0.030$ .

Figure 5.- Concluded.



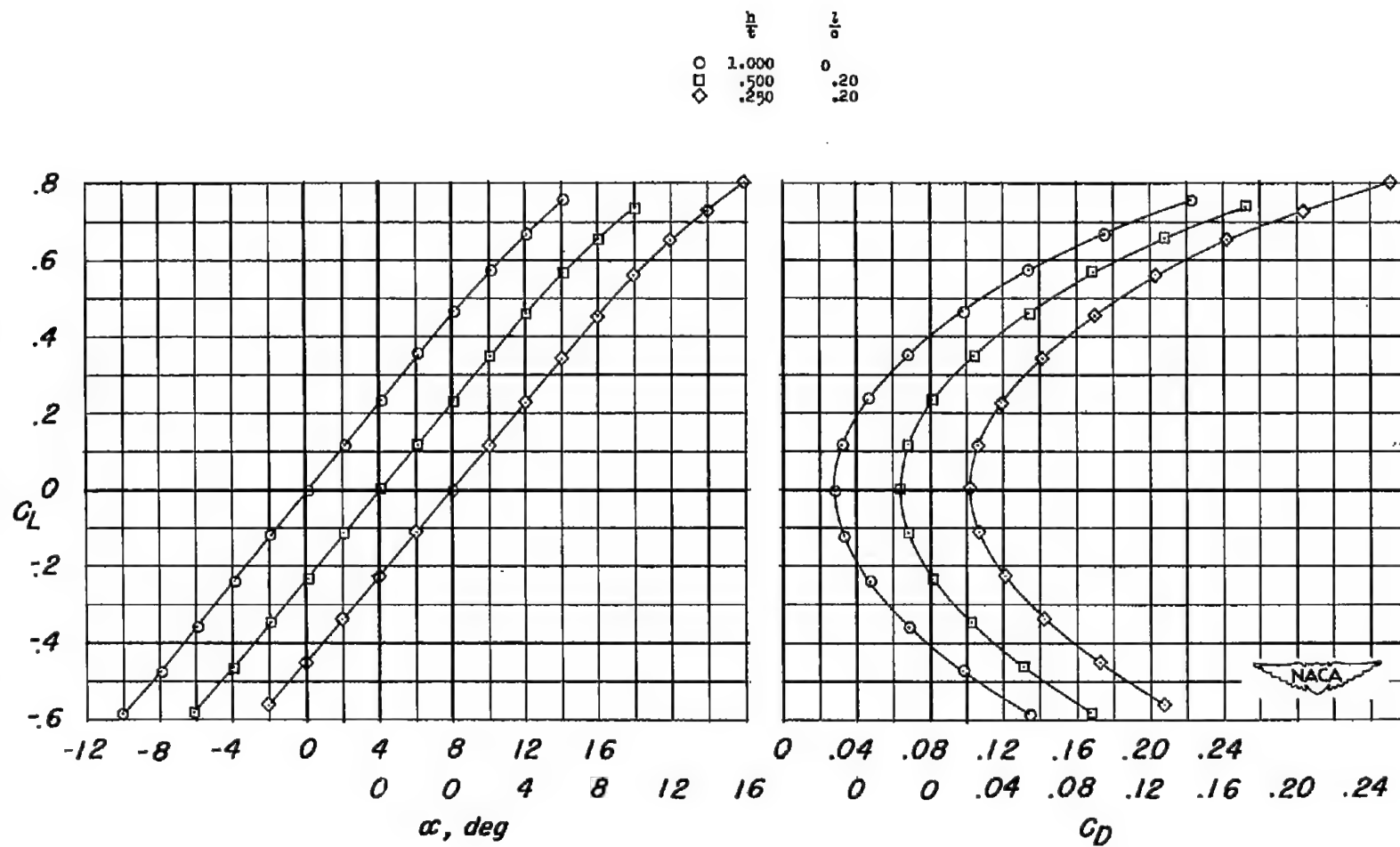
(a)  $\frac{t}{c} = 0.100$ .

Figure 6.- Wing-plus-interference lift and drag characteristics of unswept wings at a Mach number of 1.62.



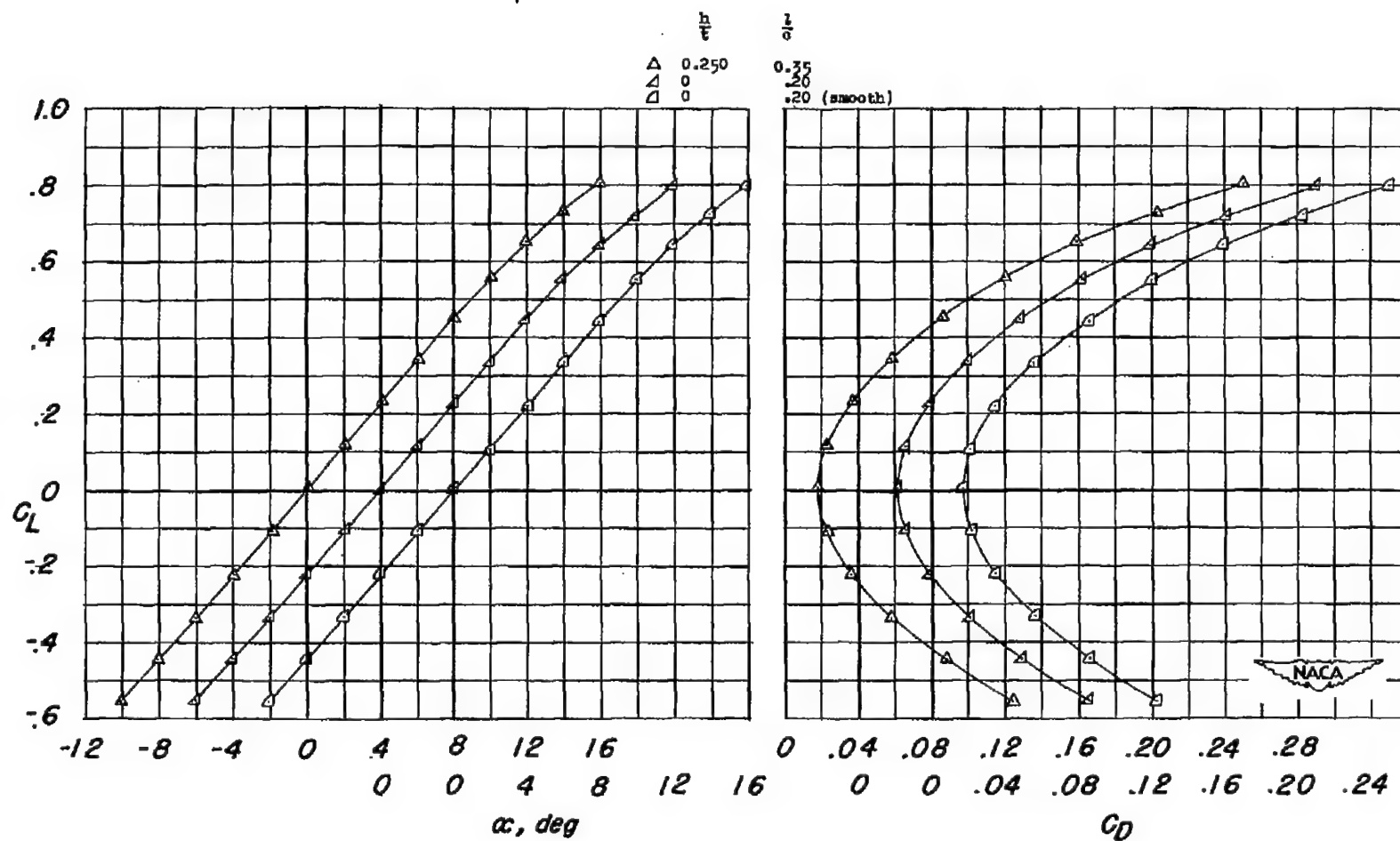
(a) Concluded.

Figure 6.- Continued.



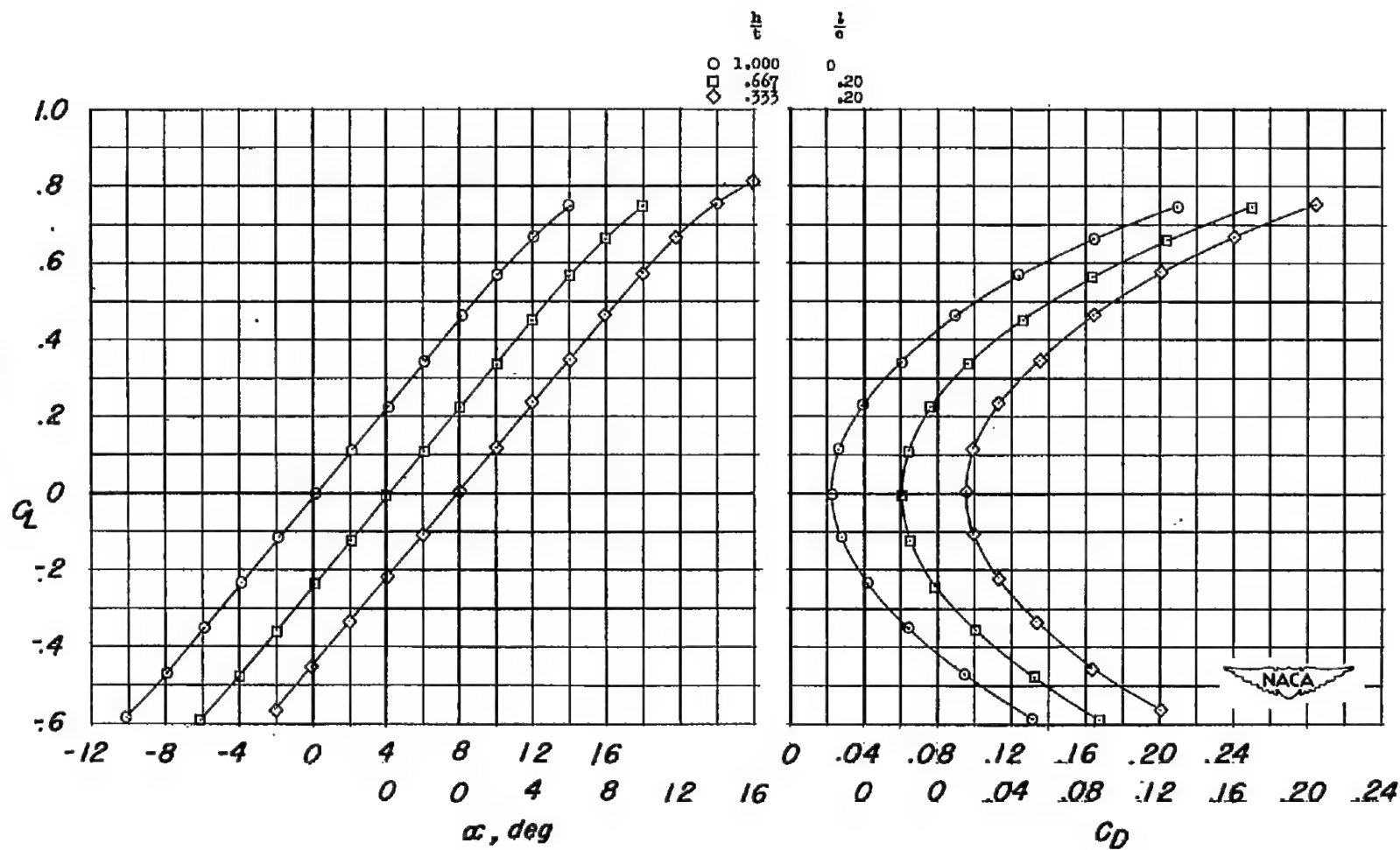
(b)  $\frac{t}{c} = 0.060$ .

Figure 6.- Continued.



(b) Concluded.

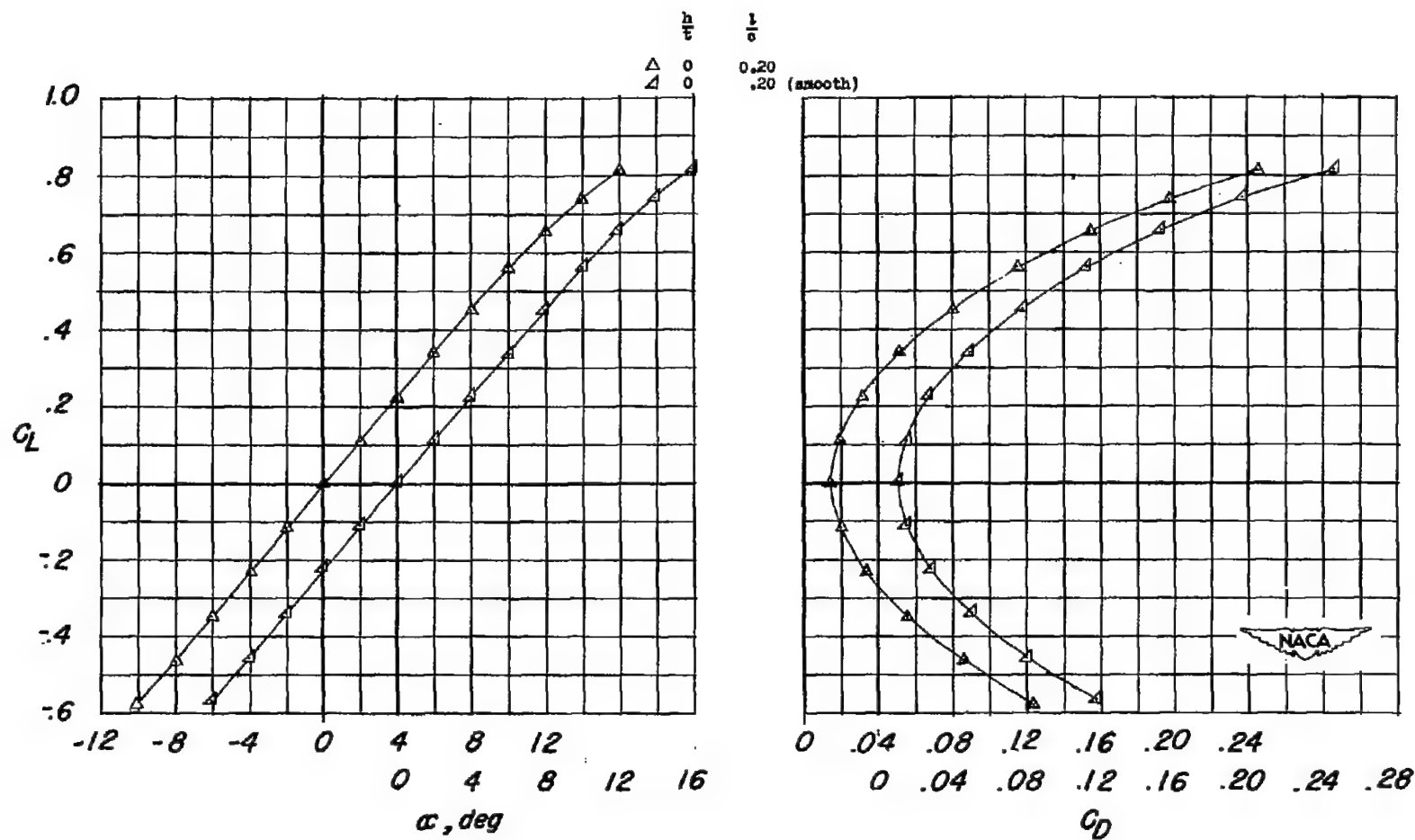
Figure 6.- Continued.



(c)  $\frac{t}{c} = 0.045$ .

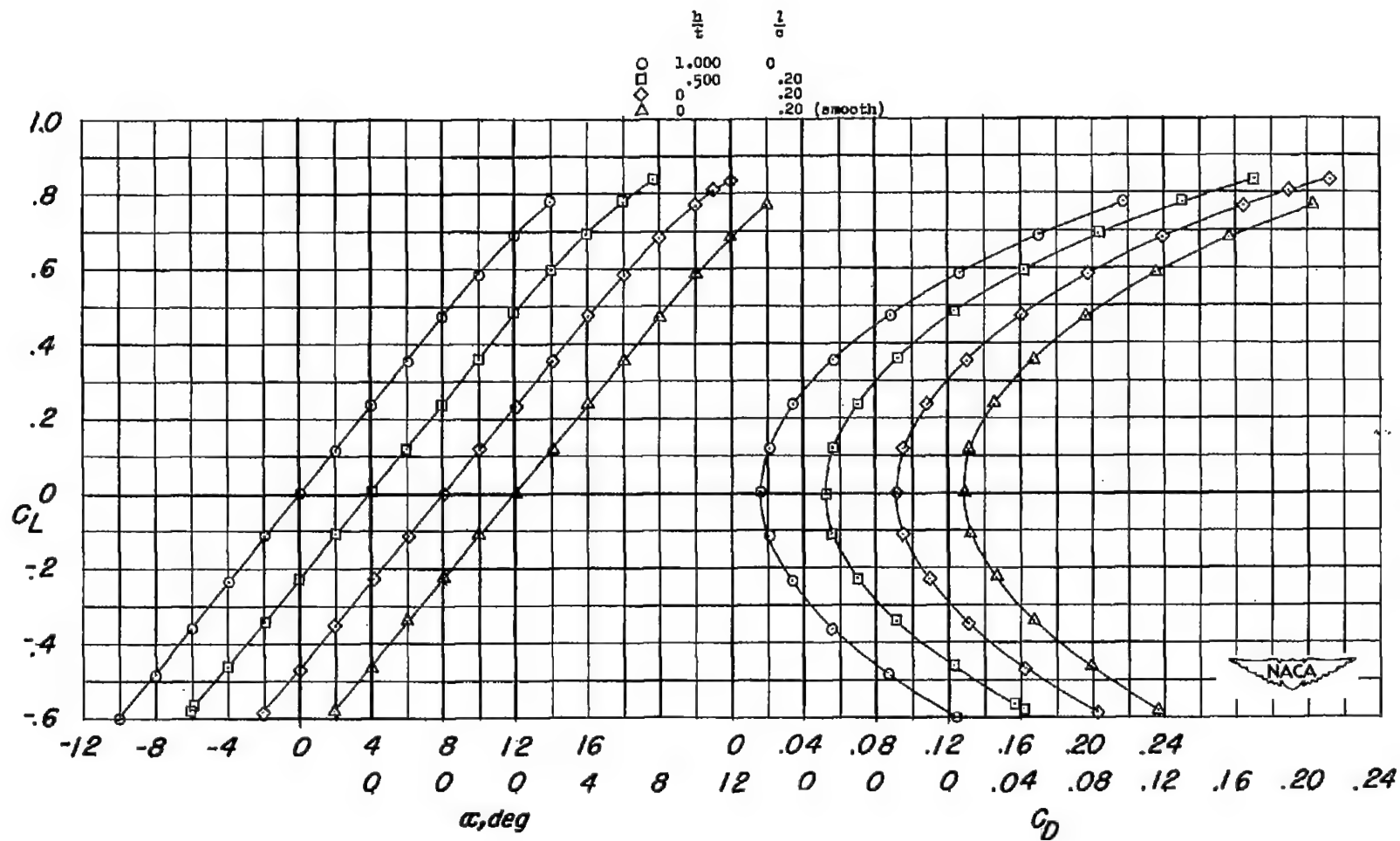
Figure 6.- Continued.





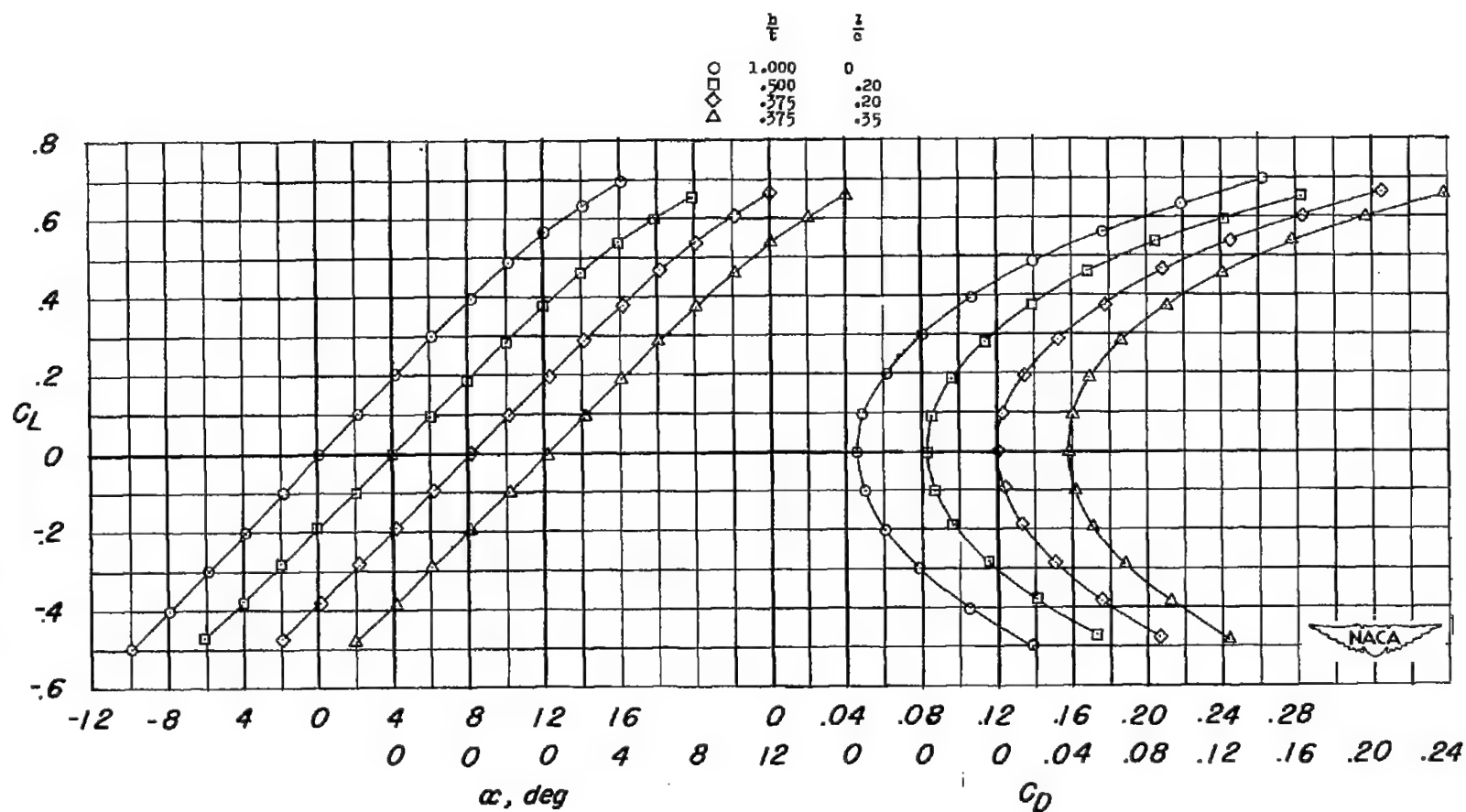
(c) Concluded.

Figure 6.- Continued.



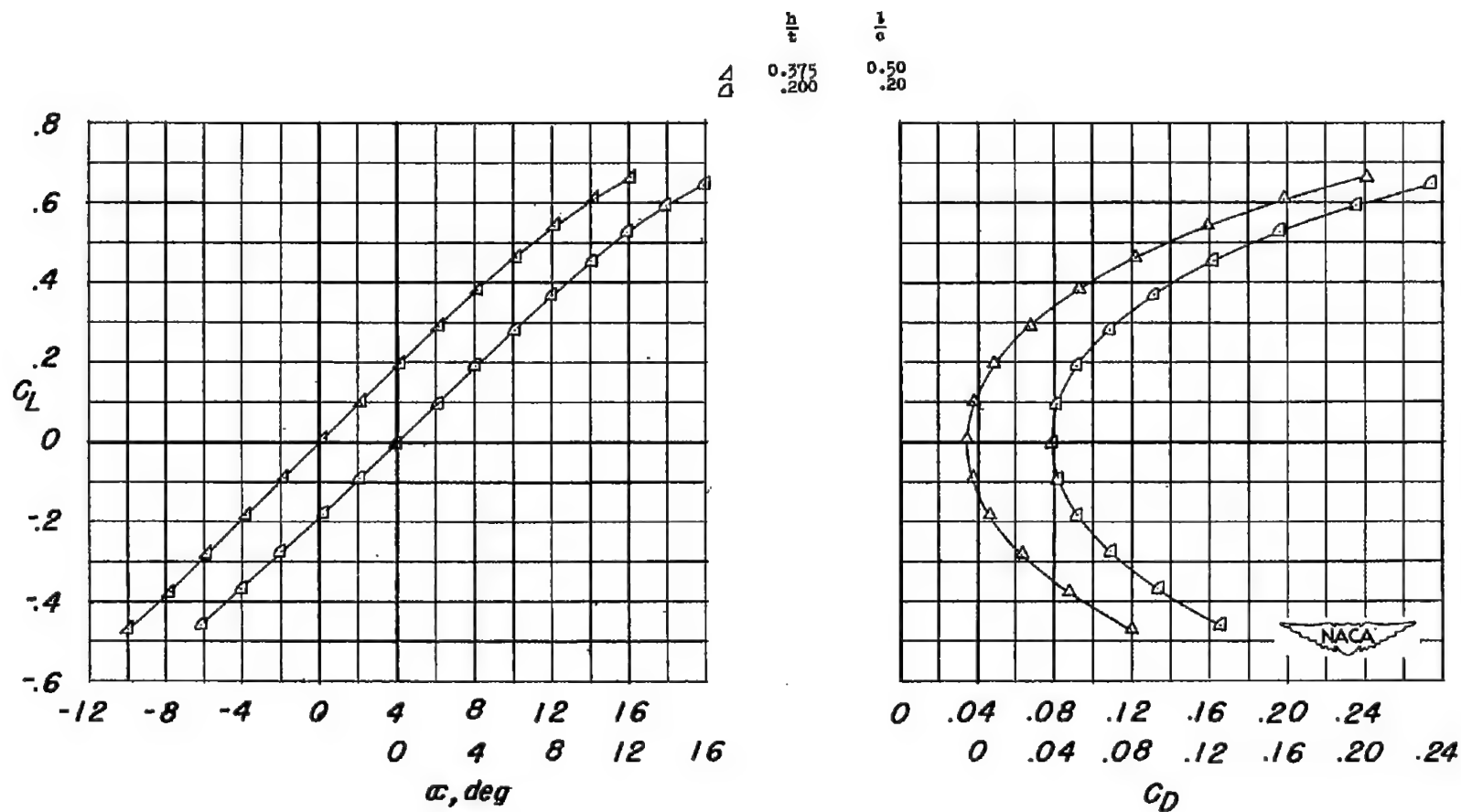
(d)  $\frac{t}{c} = 0.030$ .

Figure 6.- Concluded.



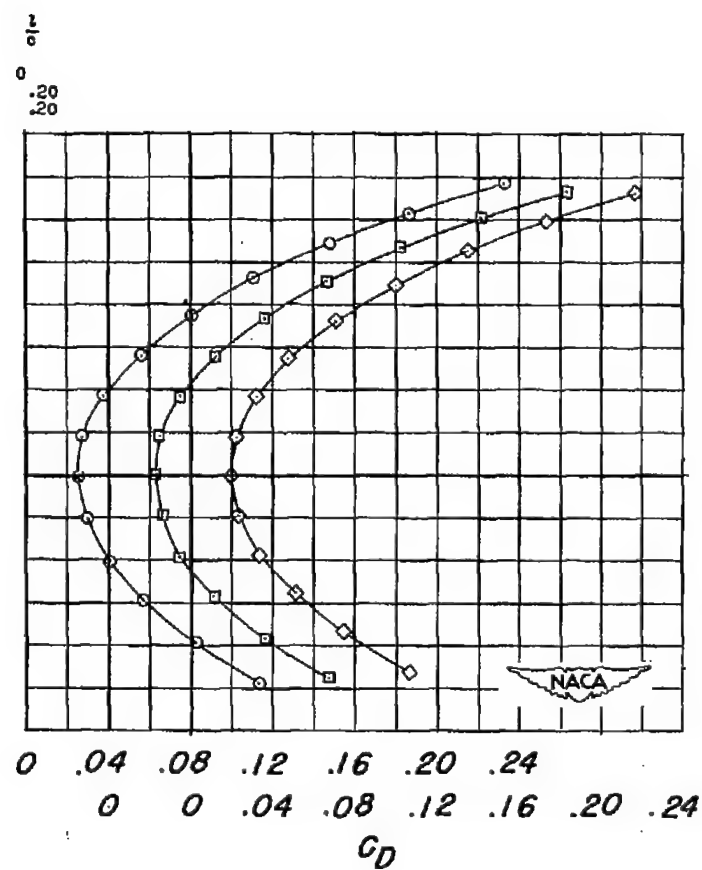
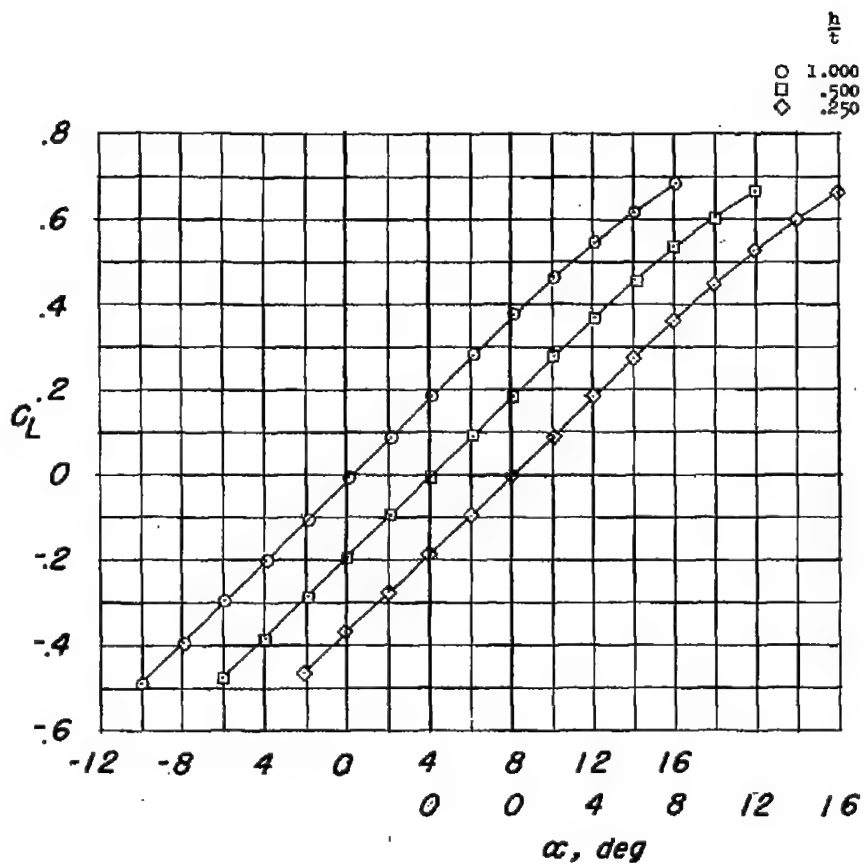
(a)  $\frac{t}{c} = 0.100$ .

Figure 7.- Wing-plus-interference lift and drag characteristics of unswept wings at a Mach number of 1.96.



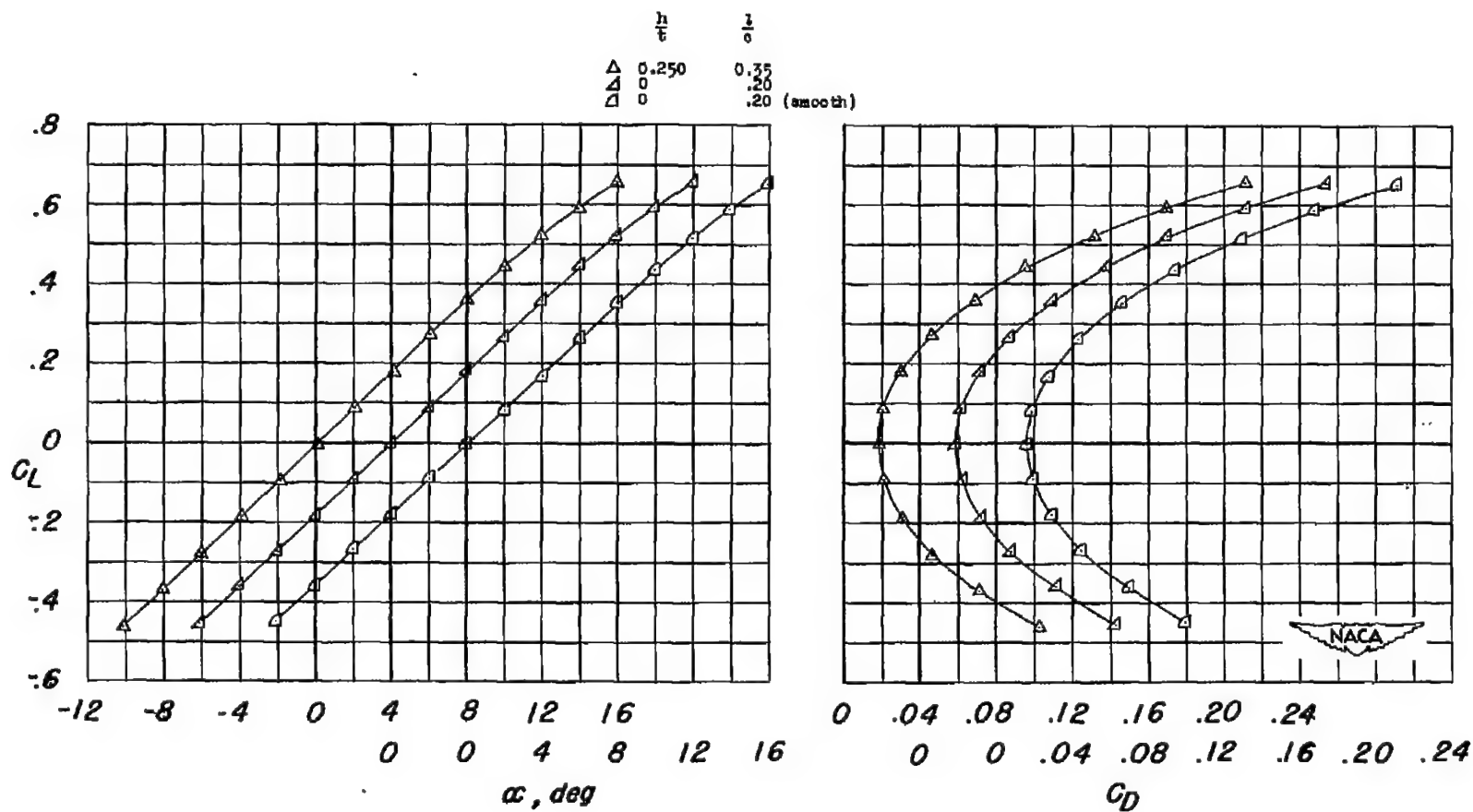
(a) Concluded.

Figure 7.- Continued.



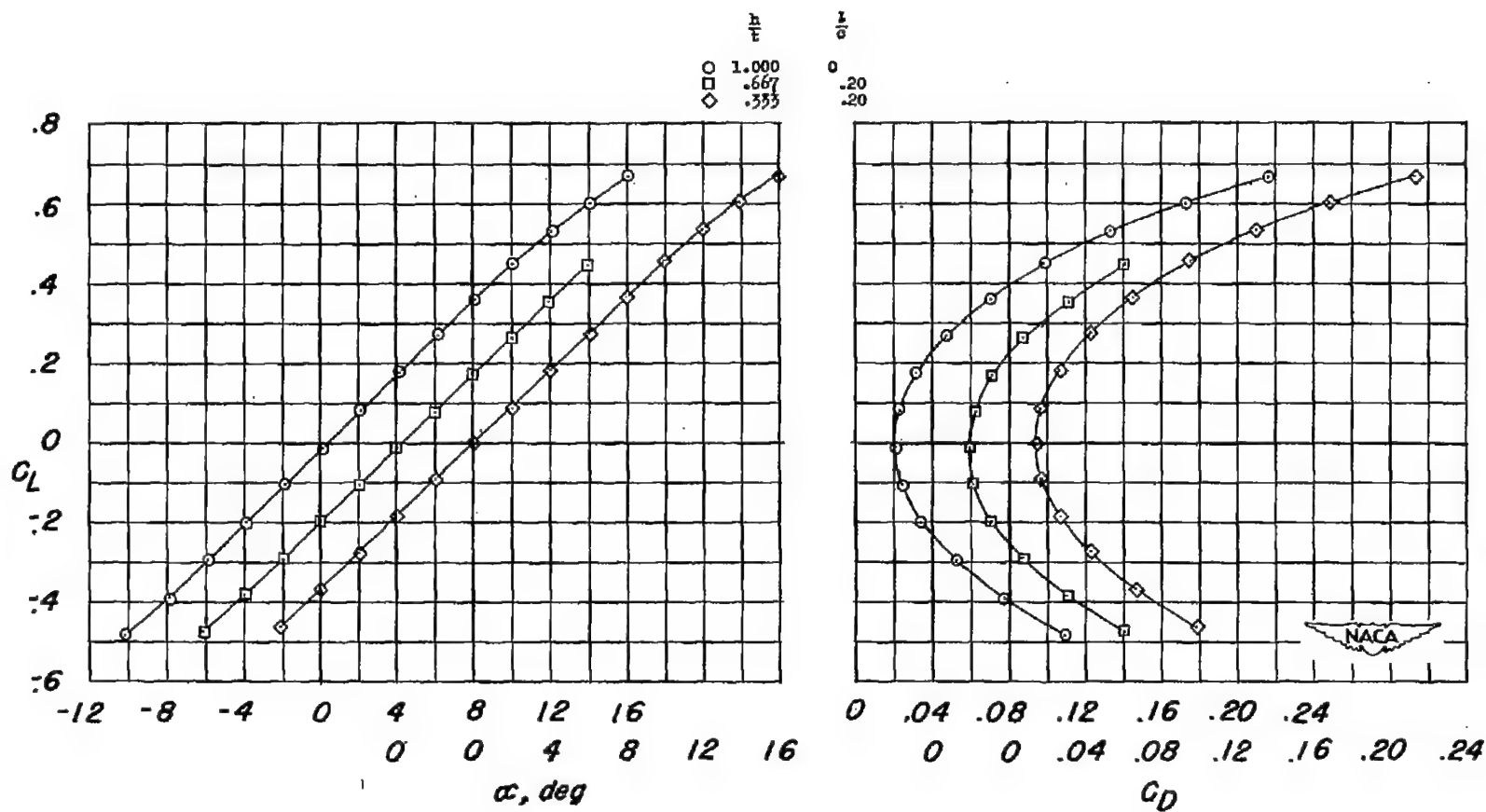
(b)  $\frac{t}{c} = 0.060$ .

Figure 7.- Continued.



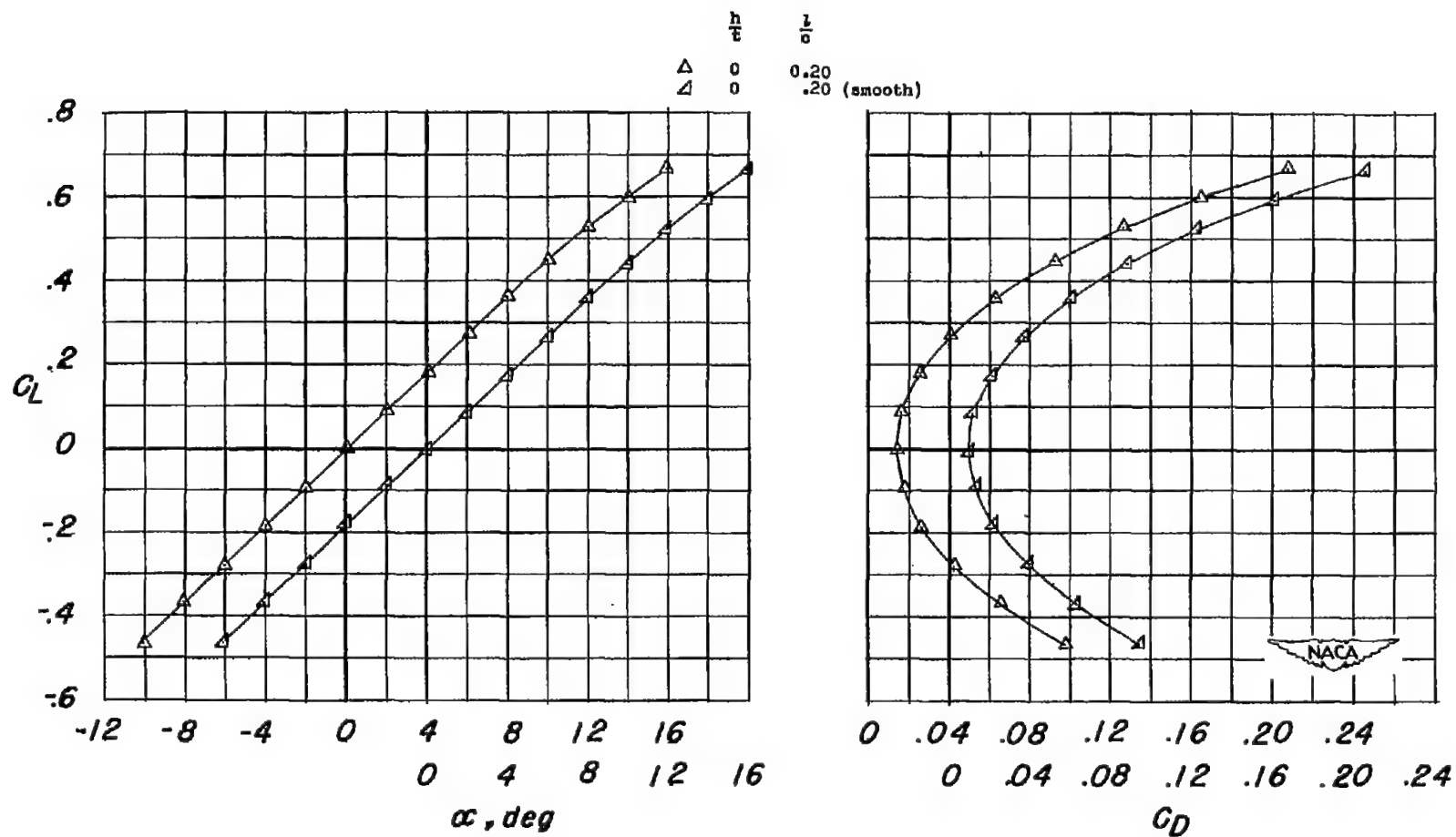
(b) Concluded.

Figure 7.- Continued.



(c)  $\frac{t}{c} = 0.045$ .

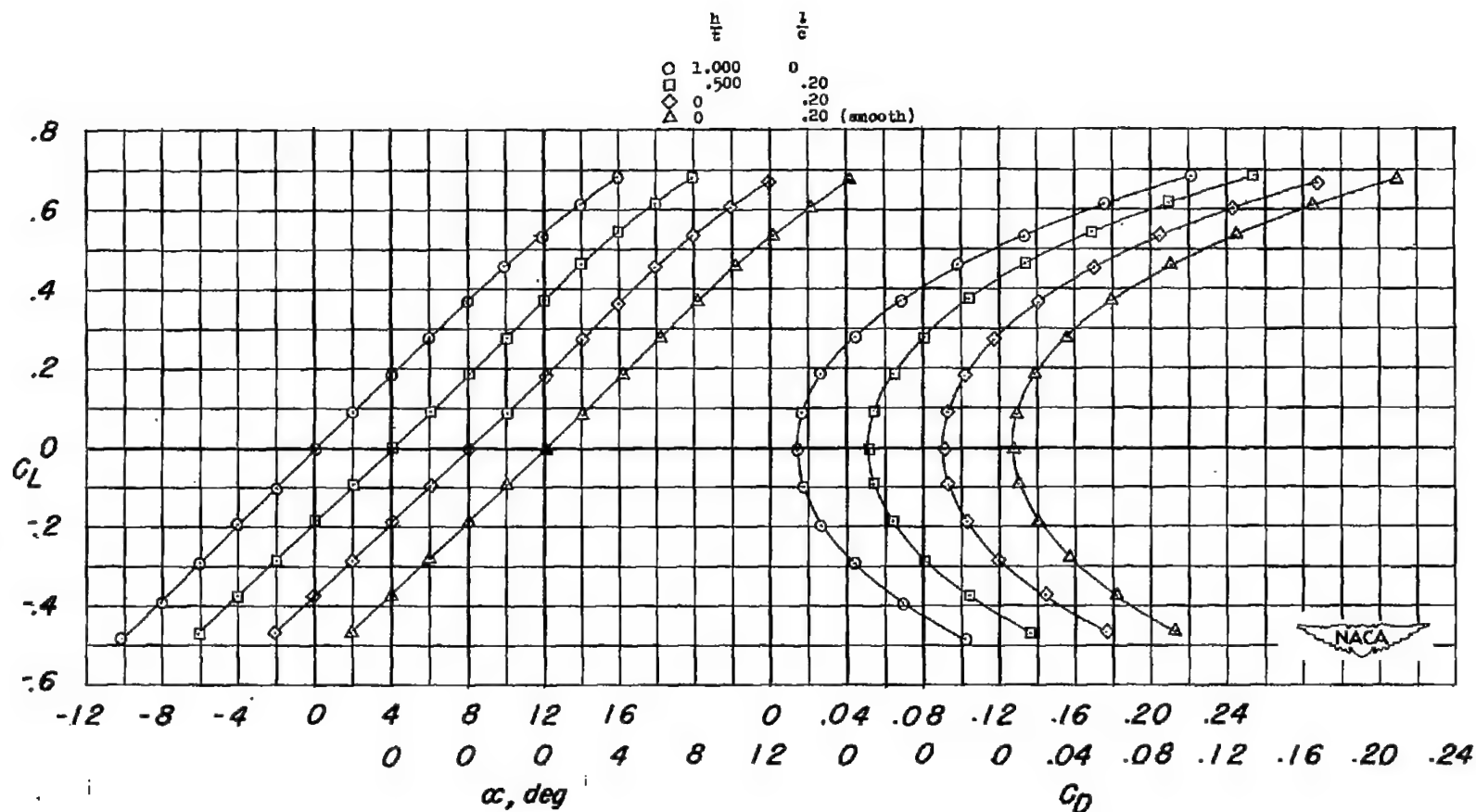
Figure 7.- Continued.



(c) Concluded.

Figure 7.- Continued.





(d)  $\frac{t}{c} = 0.030$ .

Figure 7.- Concluded.

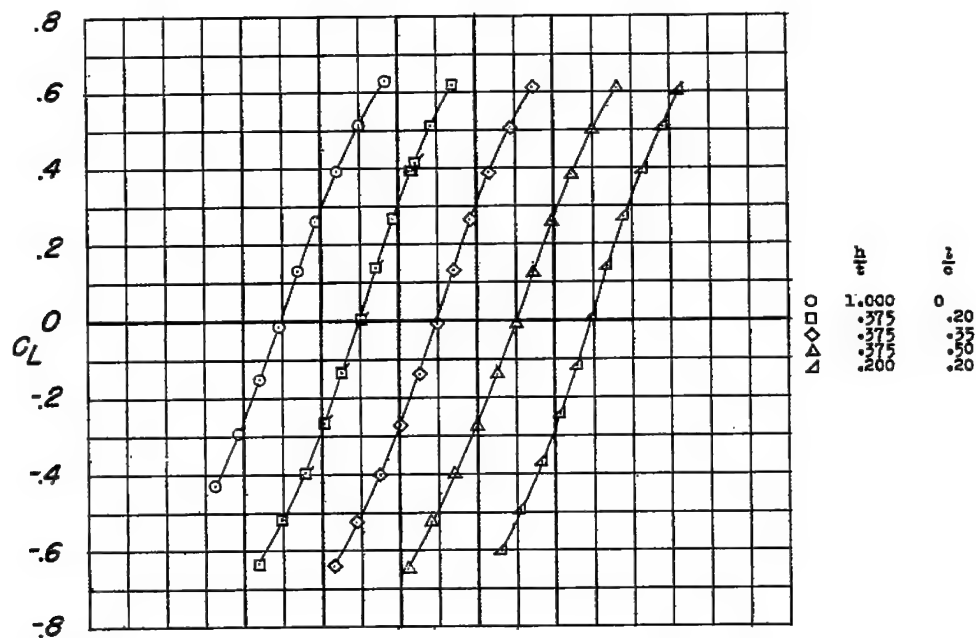
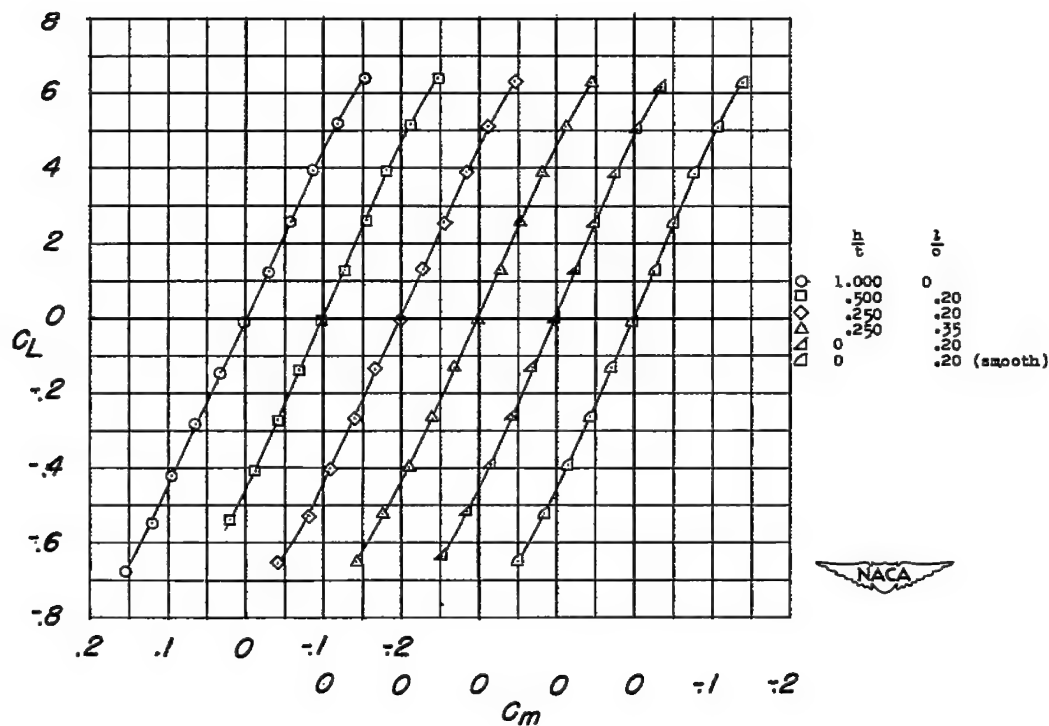
(a)  $\frac{t}{c} = 0.100$ .(b)  $\frac{t}{c} = 0.060$ .

Figure 8.- Wing-plus-interference pitching-moment characteristics of unswept wings at a Mach number of 1.41.

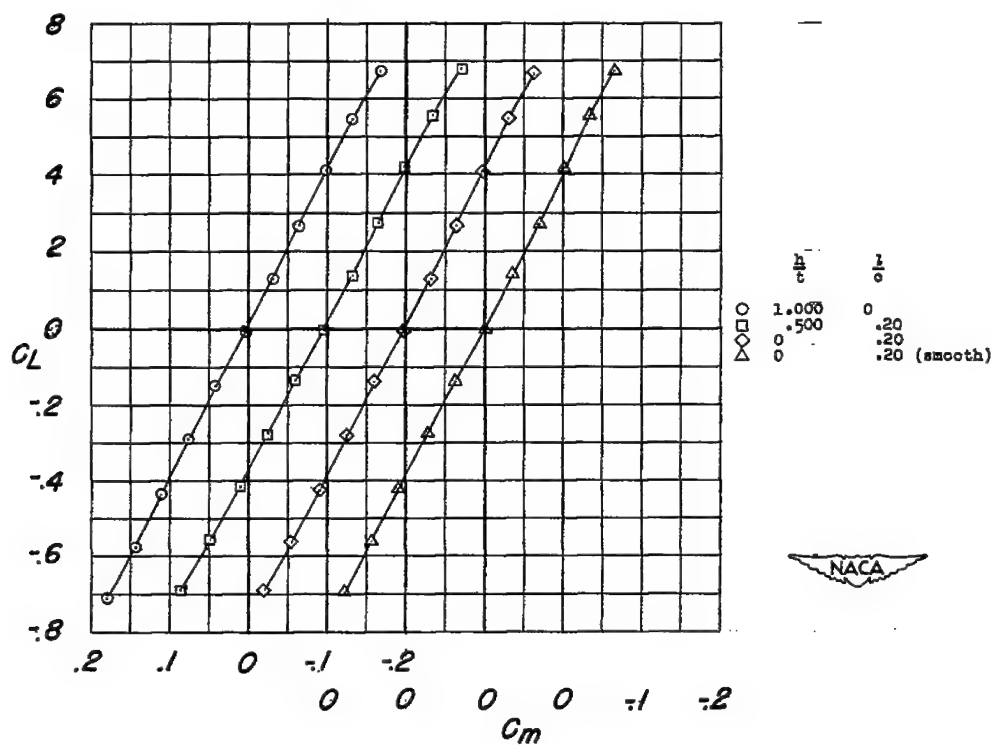
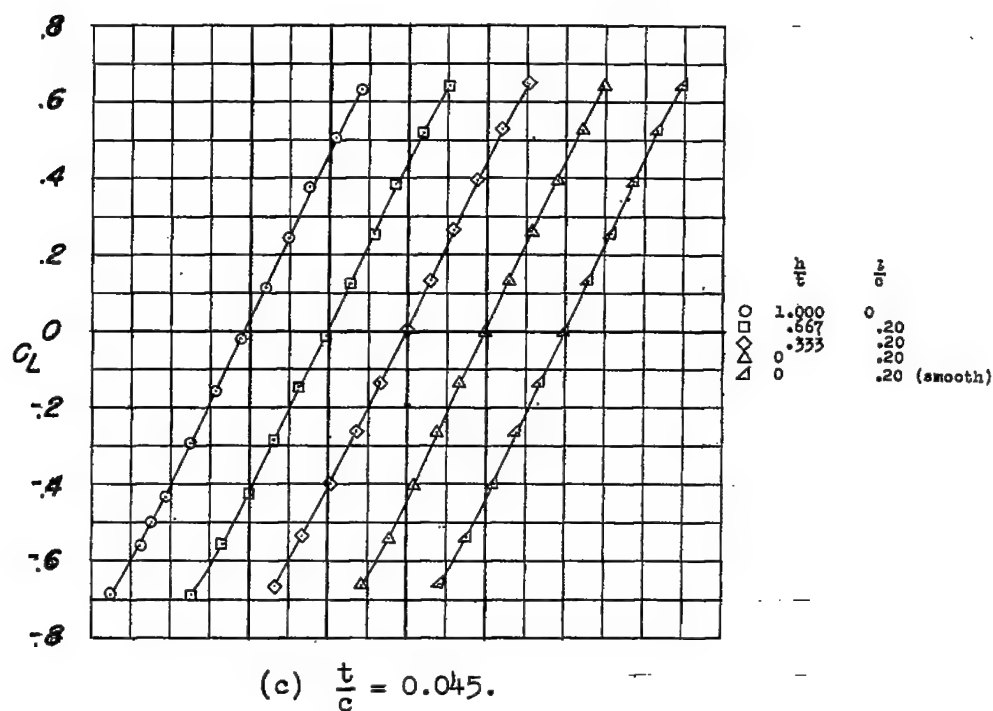


Figure 8.- Concluded.

~~CONFIDENTIAL~~

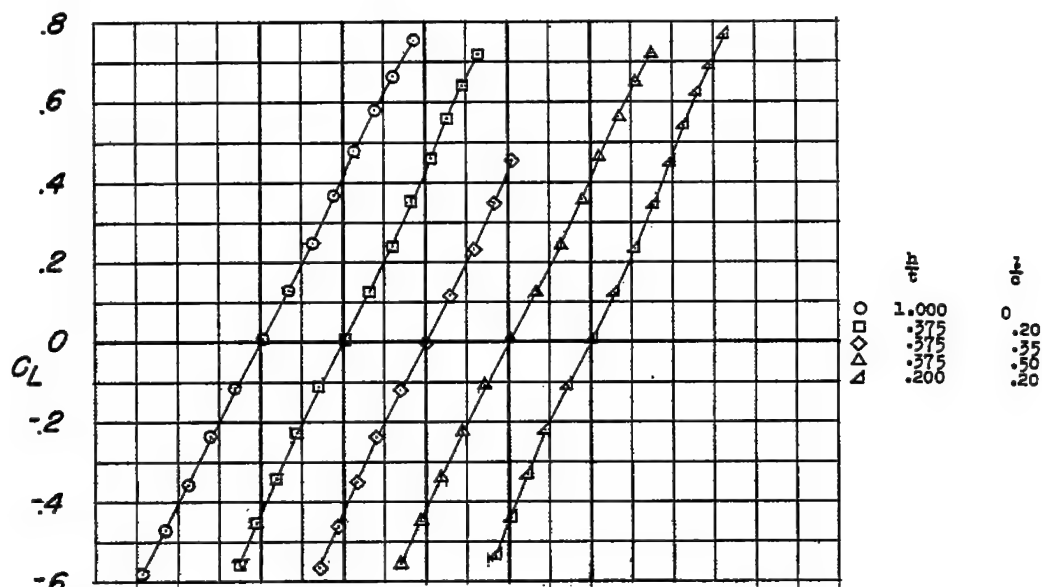
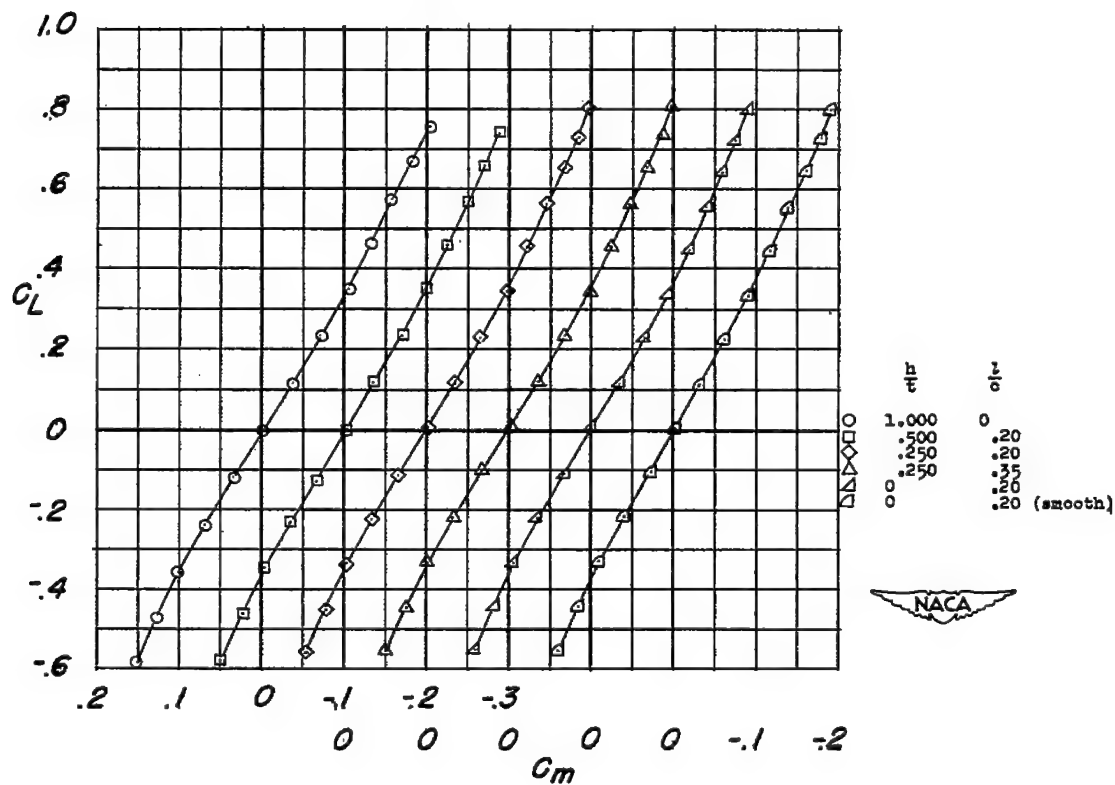
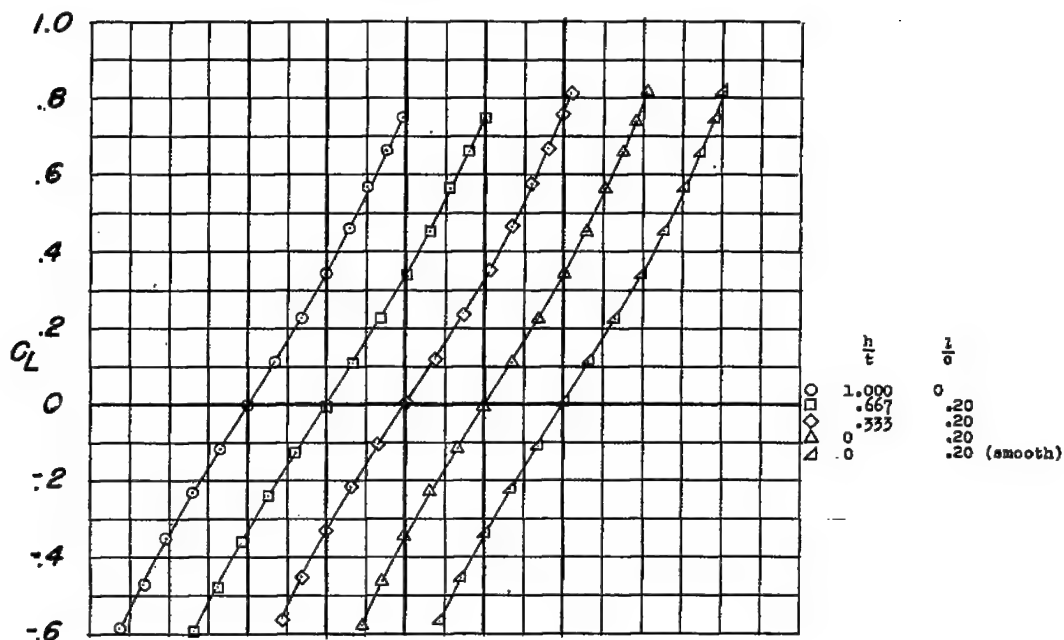
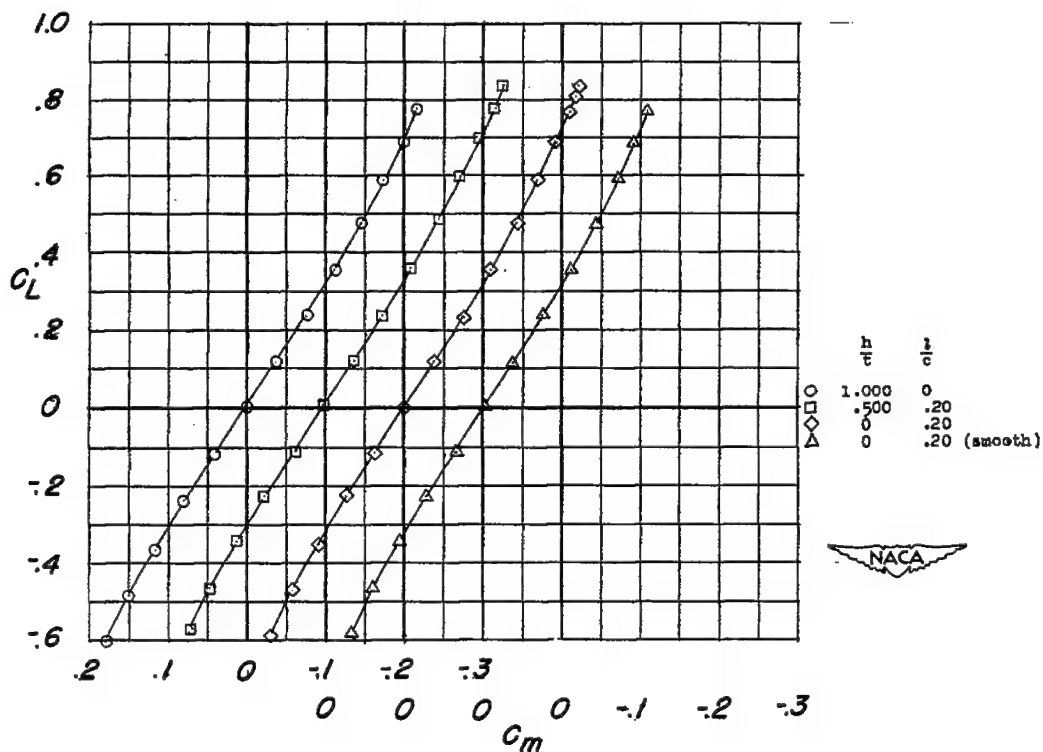
(a)  $\frac{t}{c} = 0.100$ .(b)  $\frac{t}{c} = 0.060$ .

Figure 9.- Wing-plus-interference pitching-moment characteristics of unswept wings at a Mach number of 1.62.

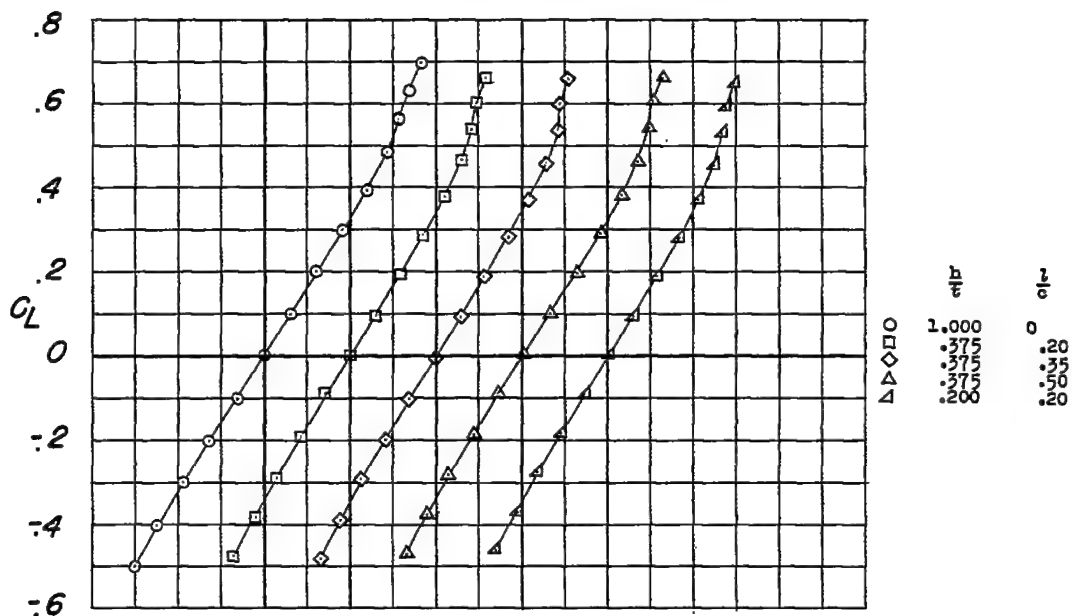


(c)  $\frac{t}{c} = 0.045$ .

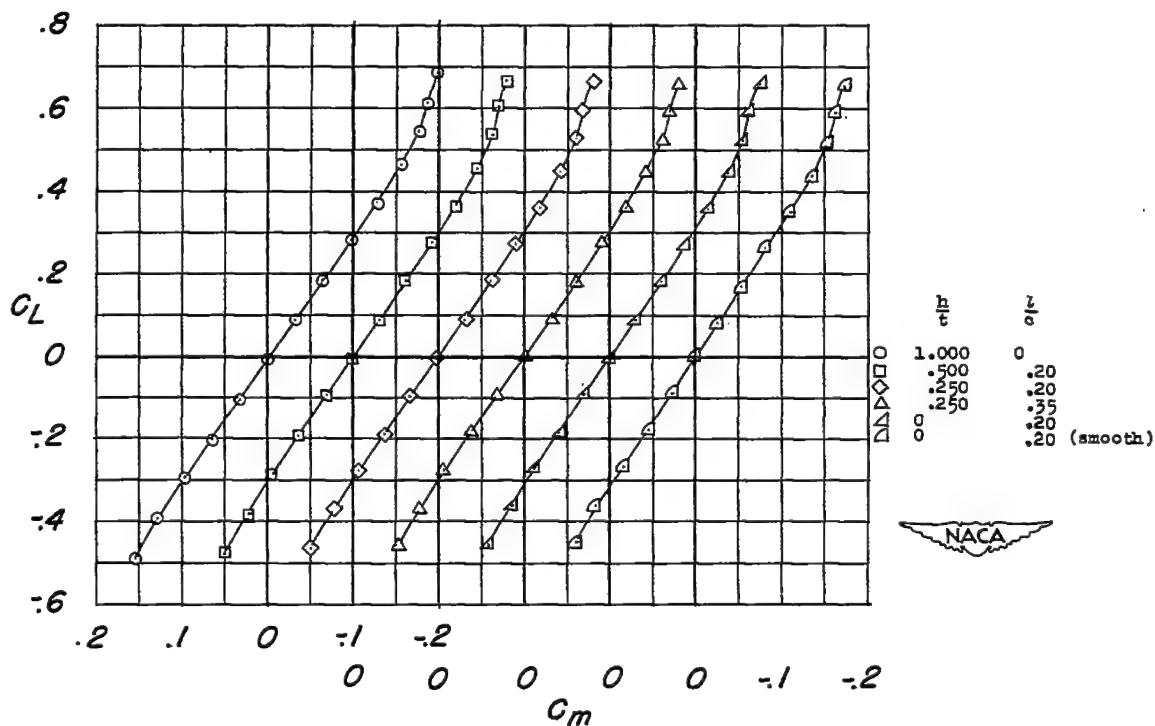


(d)  $\frac{t}{c} = 0.030$ .

Figure 9.- Concluded.

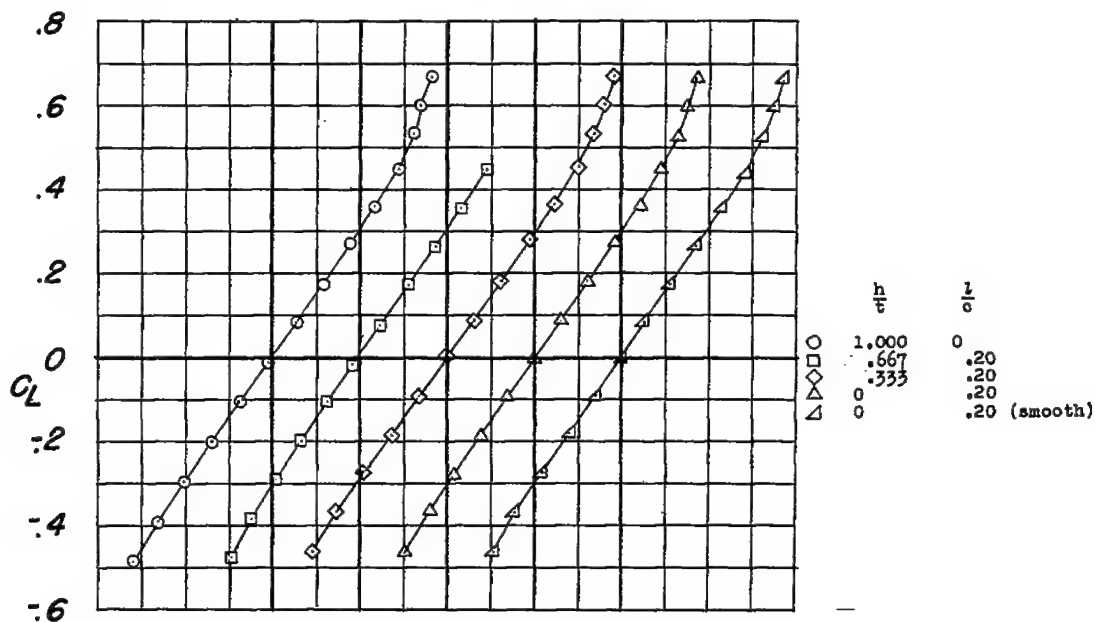


(a)  $\frac{t}{c} = 0.100$ .

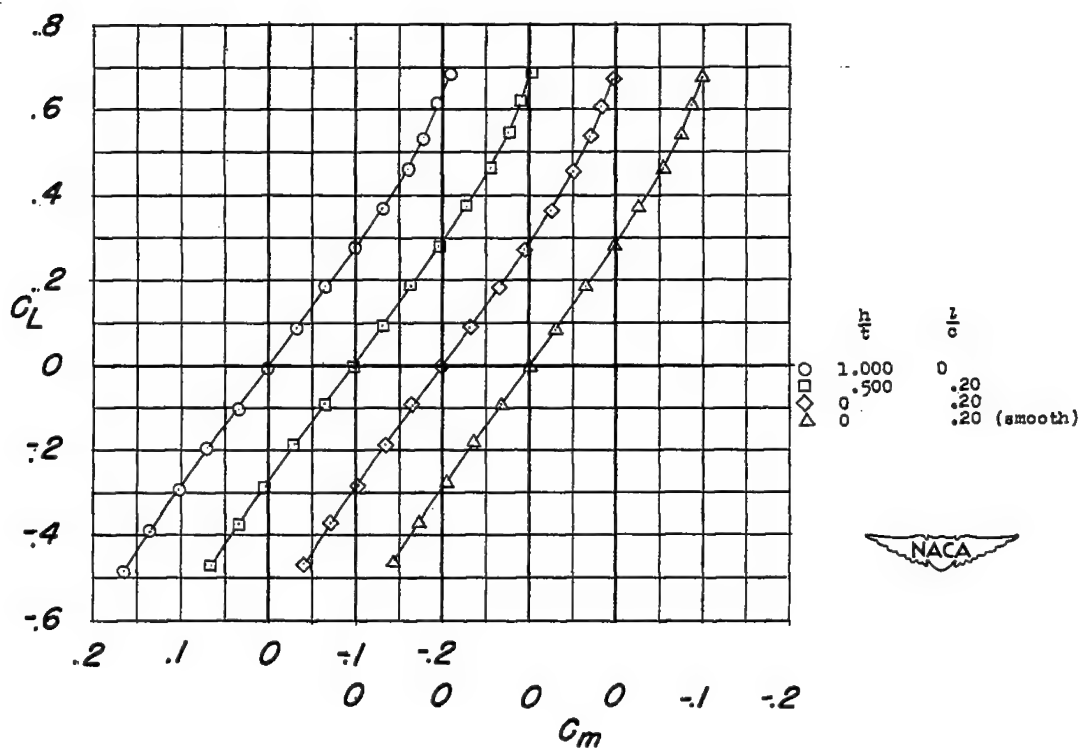


(b)  $\frac{t}{c} = 0.060$ .

Figure 10.- Wing-plus-interference pitching-moment characteristics of unswept wings at a Mach number of 1.96.

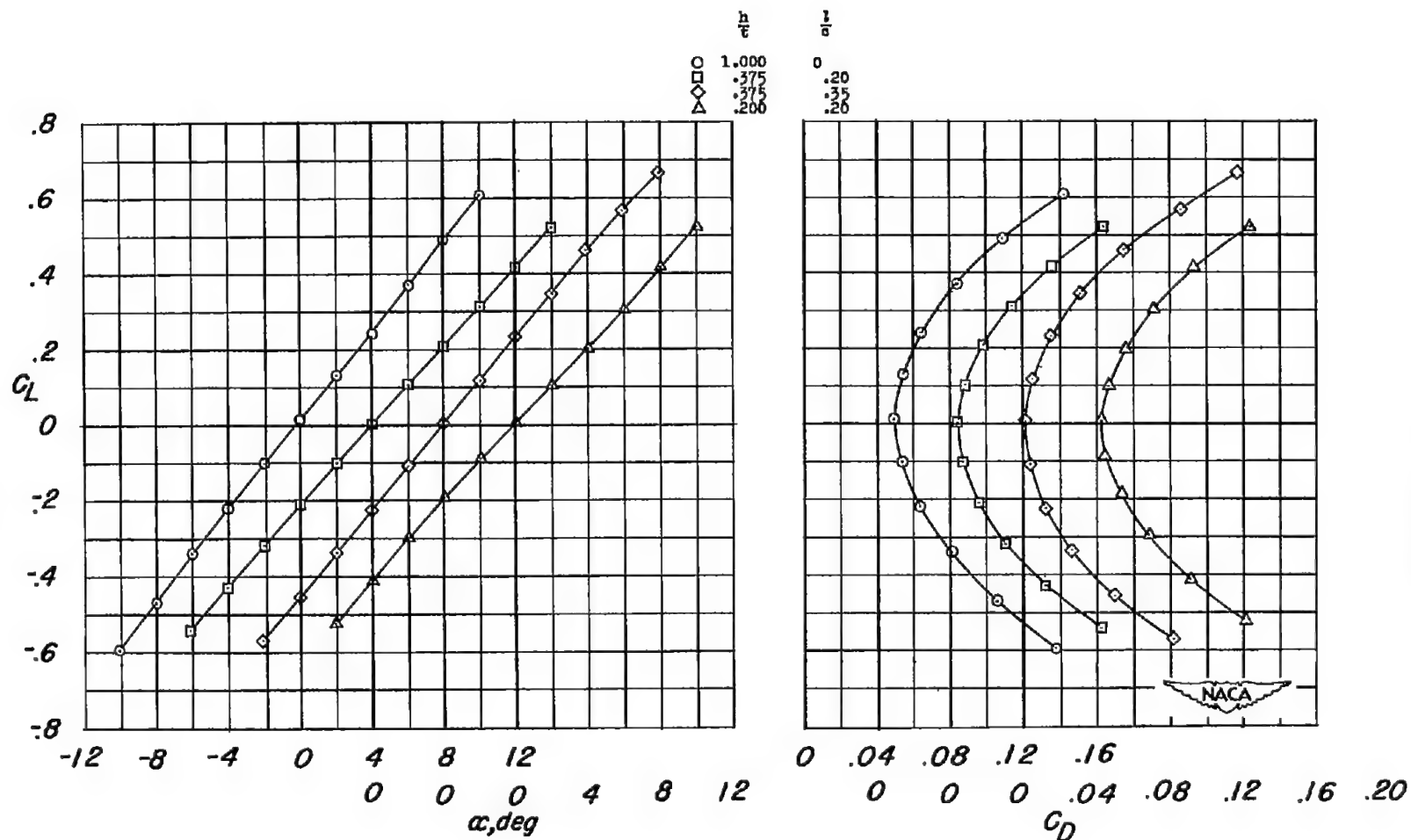


(c)  $\frac{t}{c} = 0.045$ .



(d)  $\frac{t}{c} = 0.030$ .

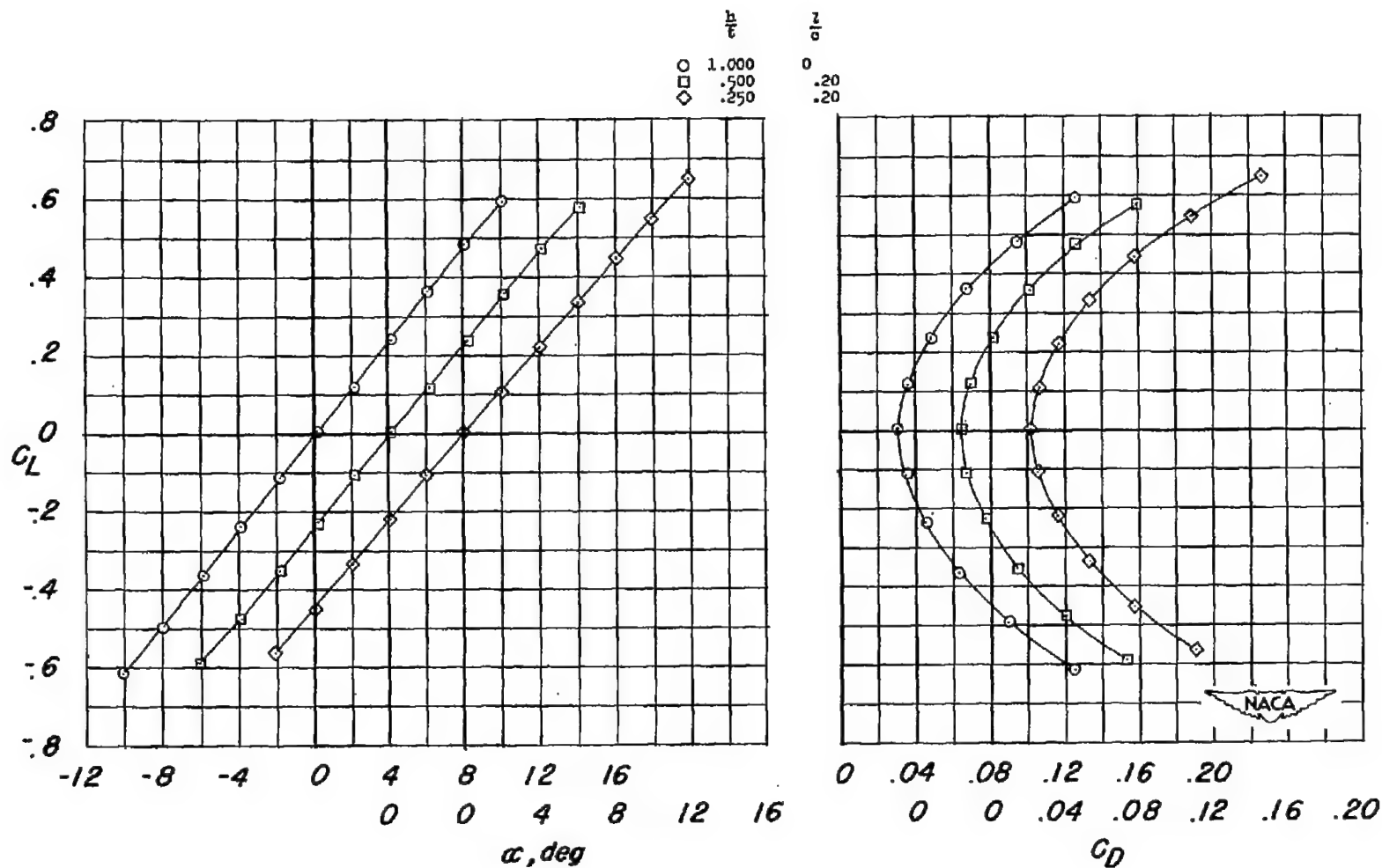
Figure 10.- Concluded.



(a)  $\frac{t}{c} = 0.100$ .

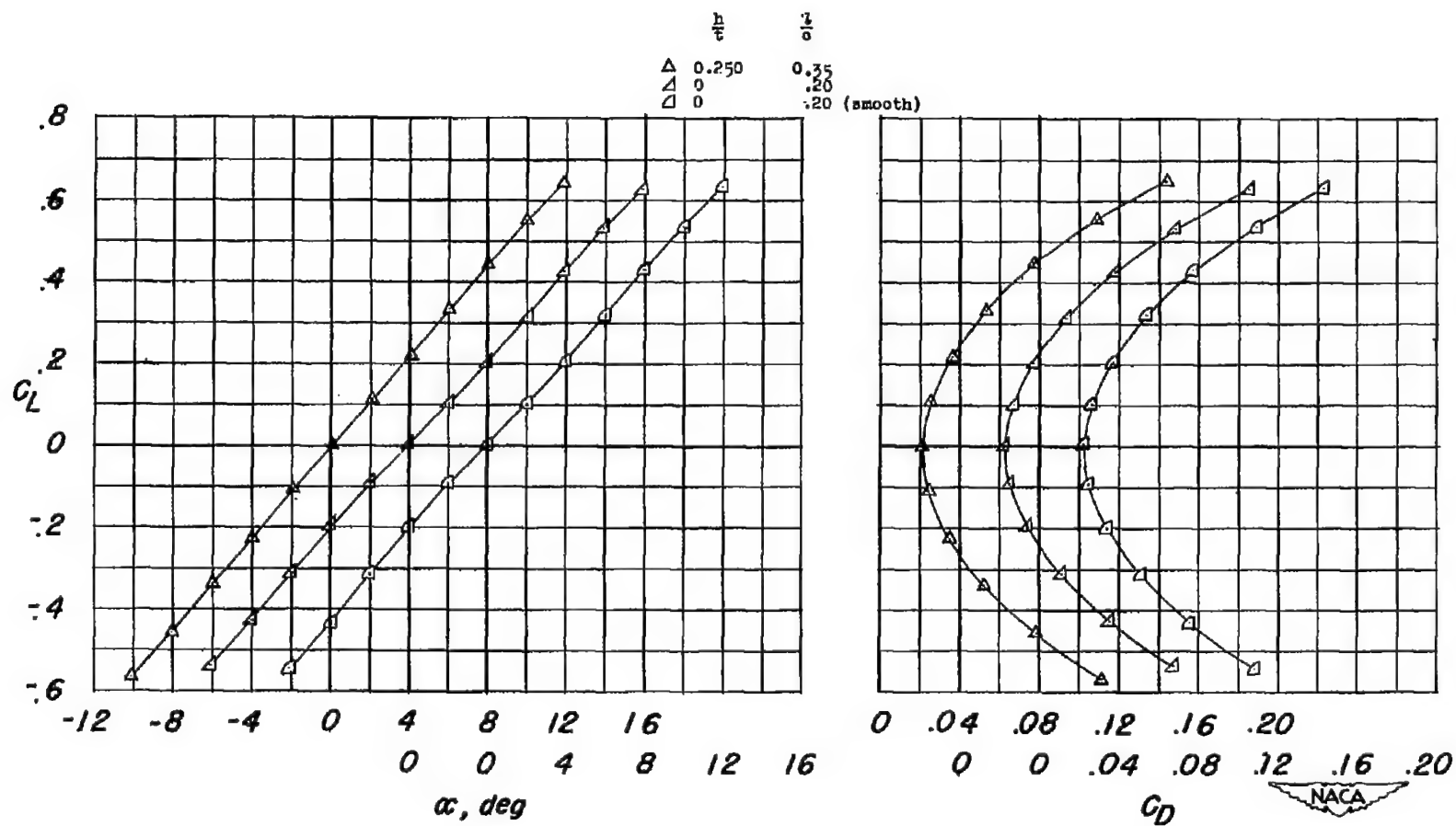
Figure 11.- Wing-plus-interference lift and drag characteristics of 45° sweptback wings at a Mach number of 1.41.





(b)  $\frac{t}{c} = 0.060$ .

Figure 11.- Continued.



(b) Concluded.

Figure 11.- Continued.

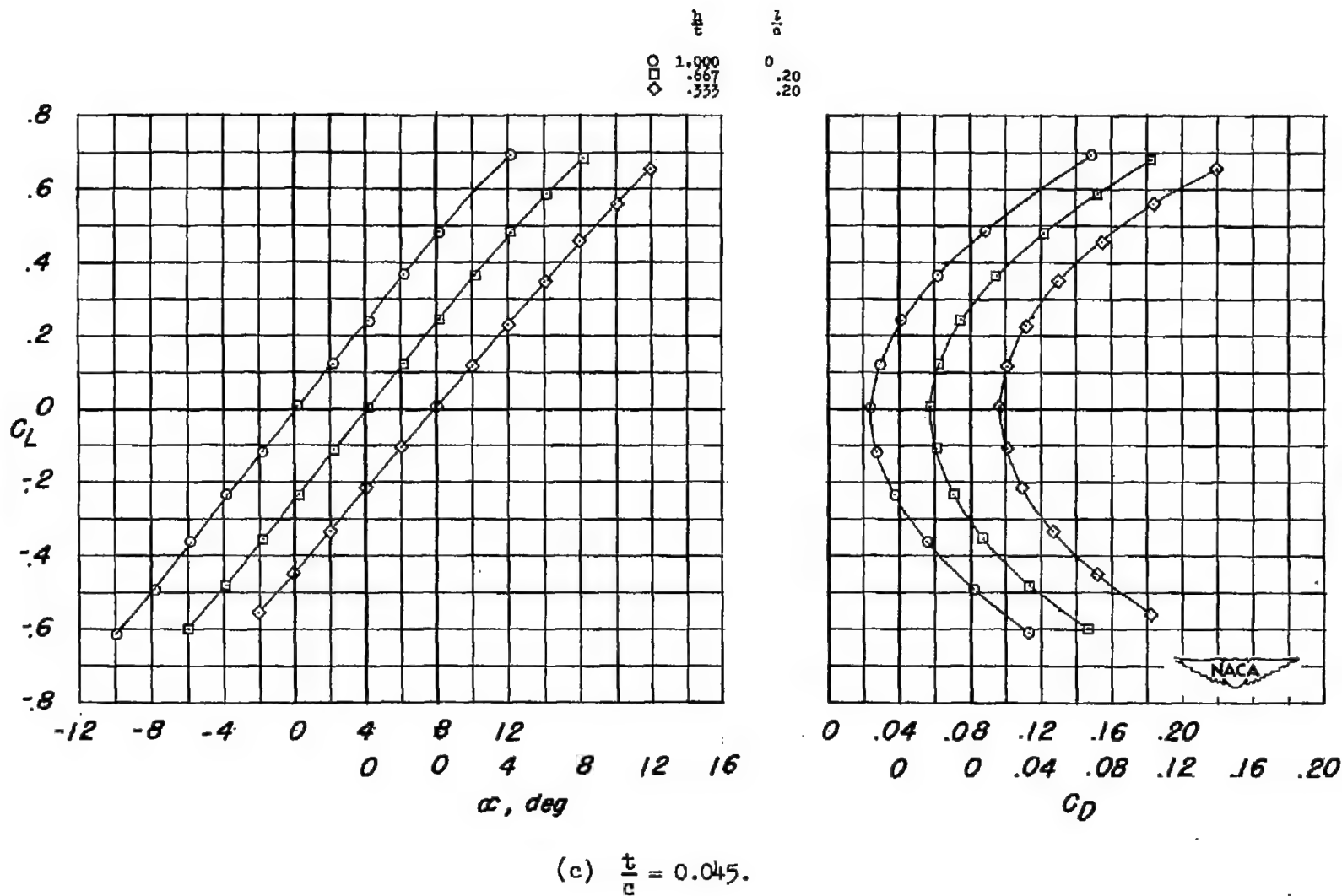
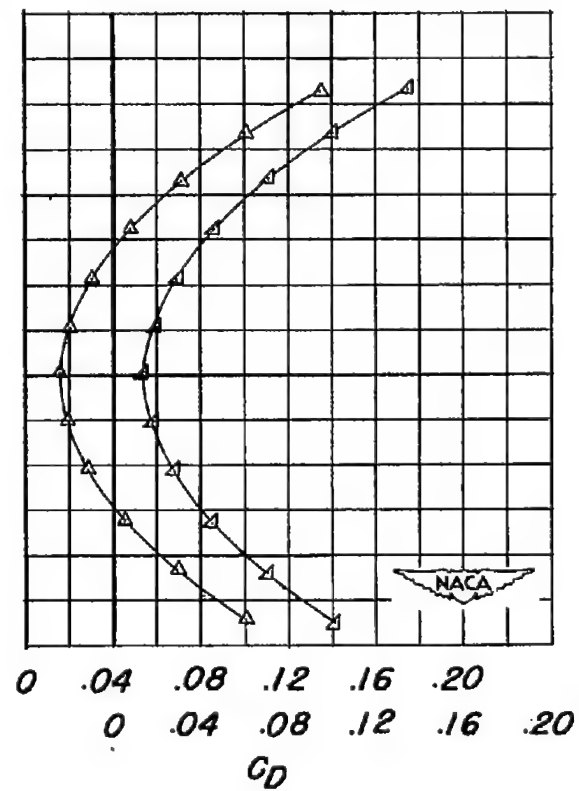
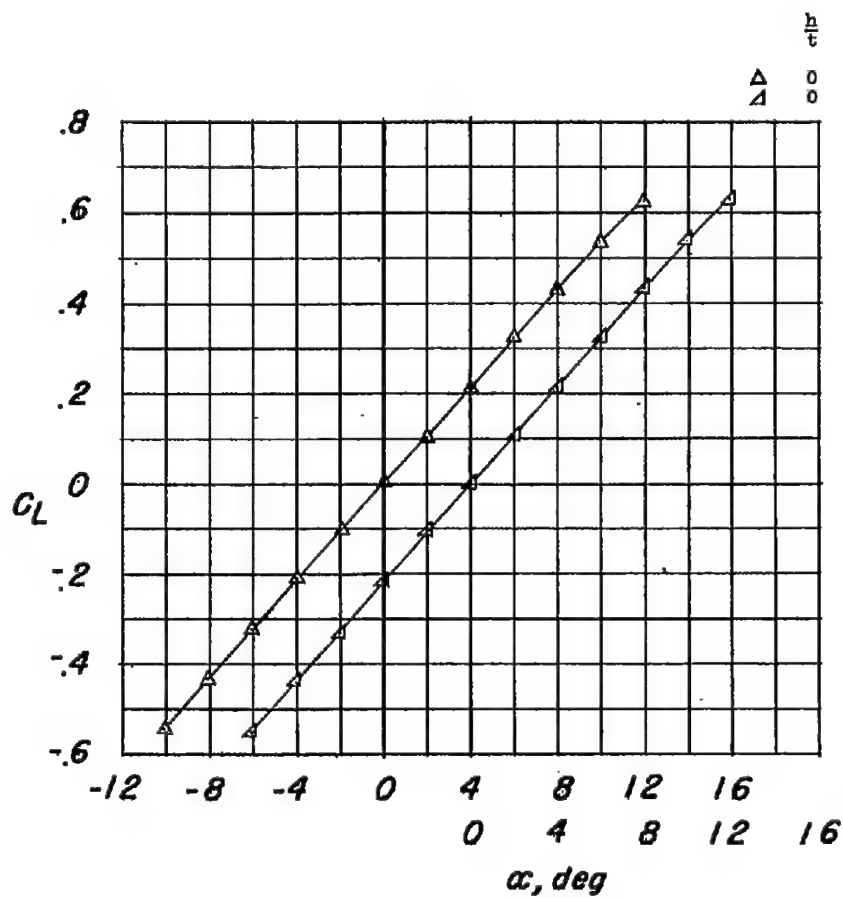
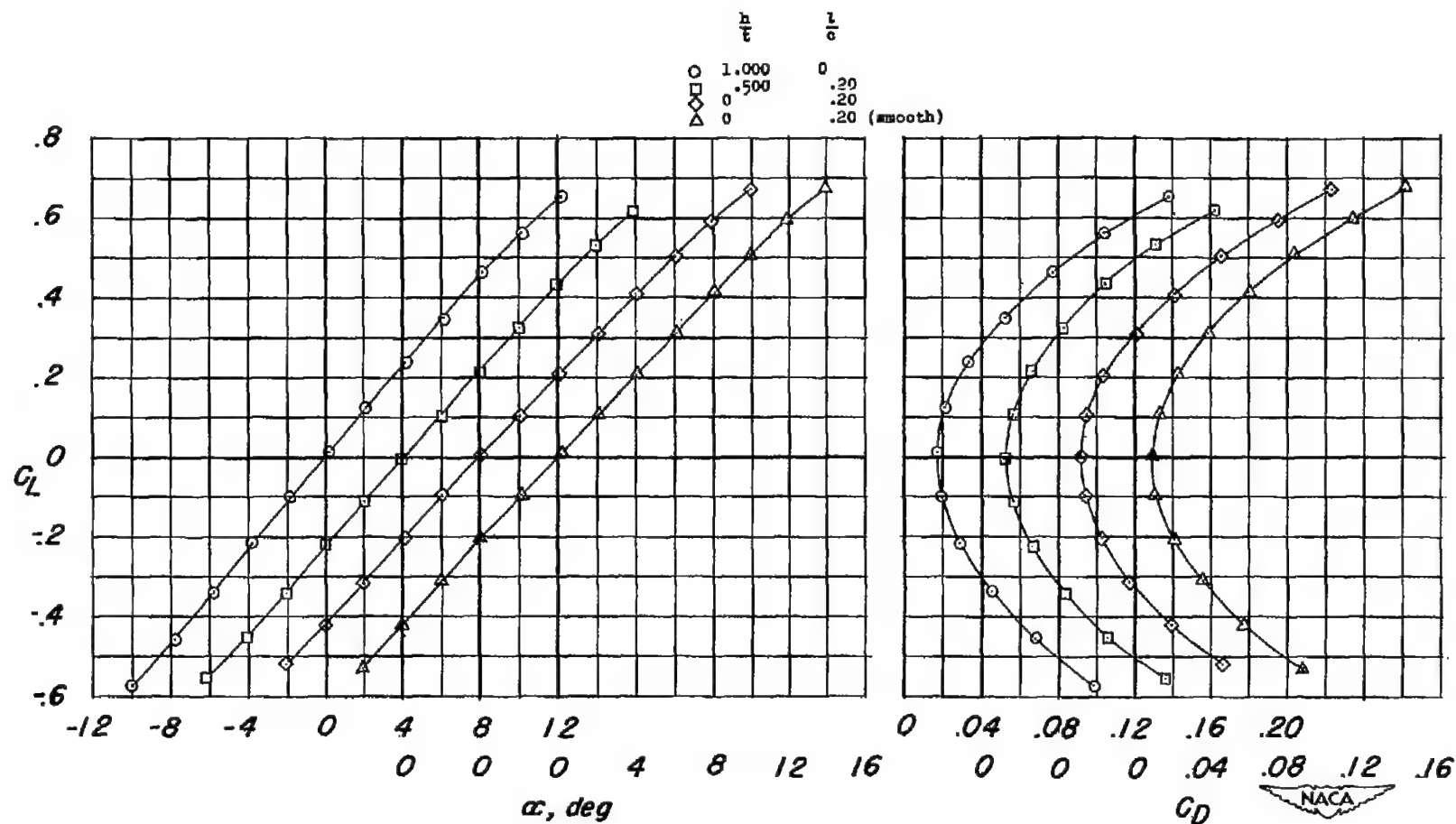


Figure 11.- Continued.



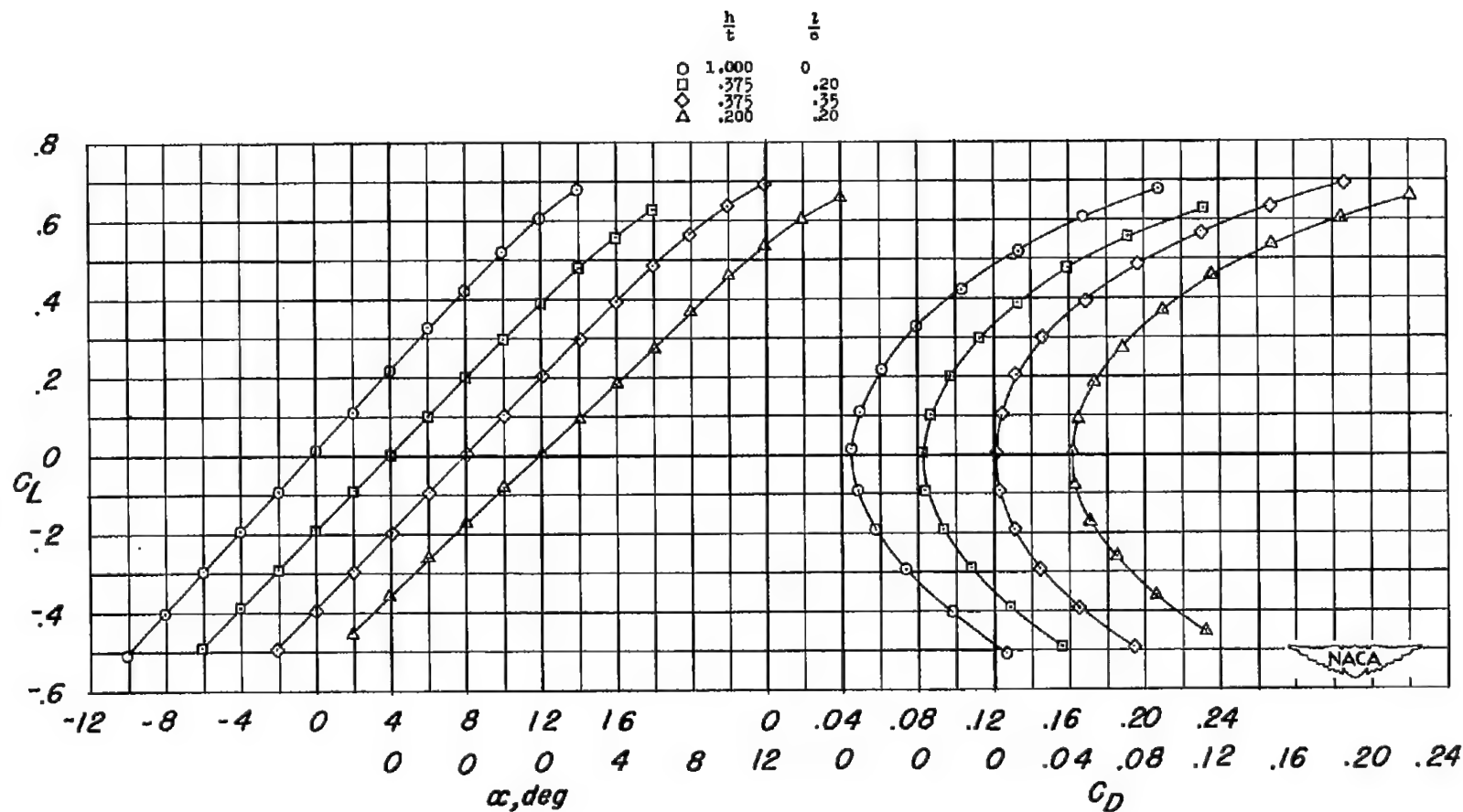
(c) Concluded.

Figure 11.- Continued.



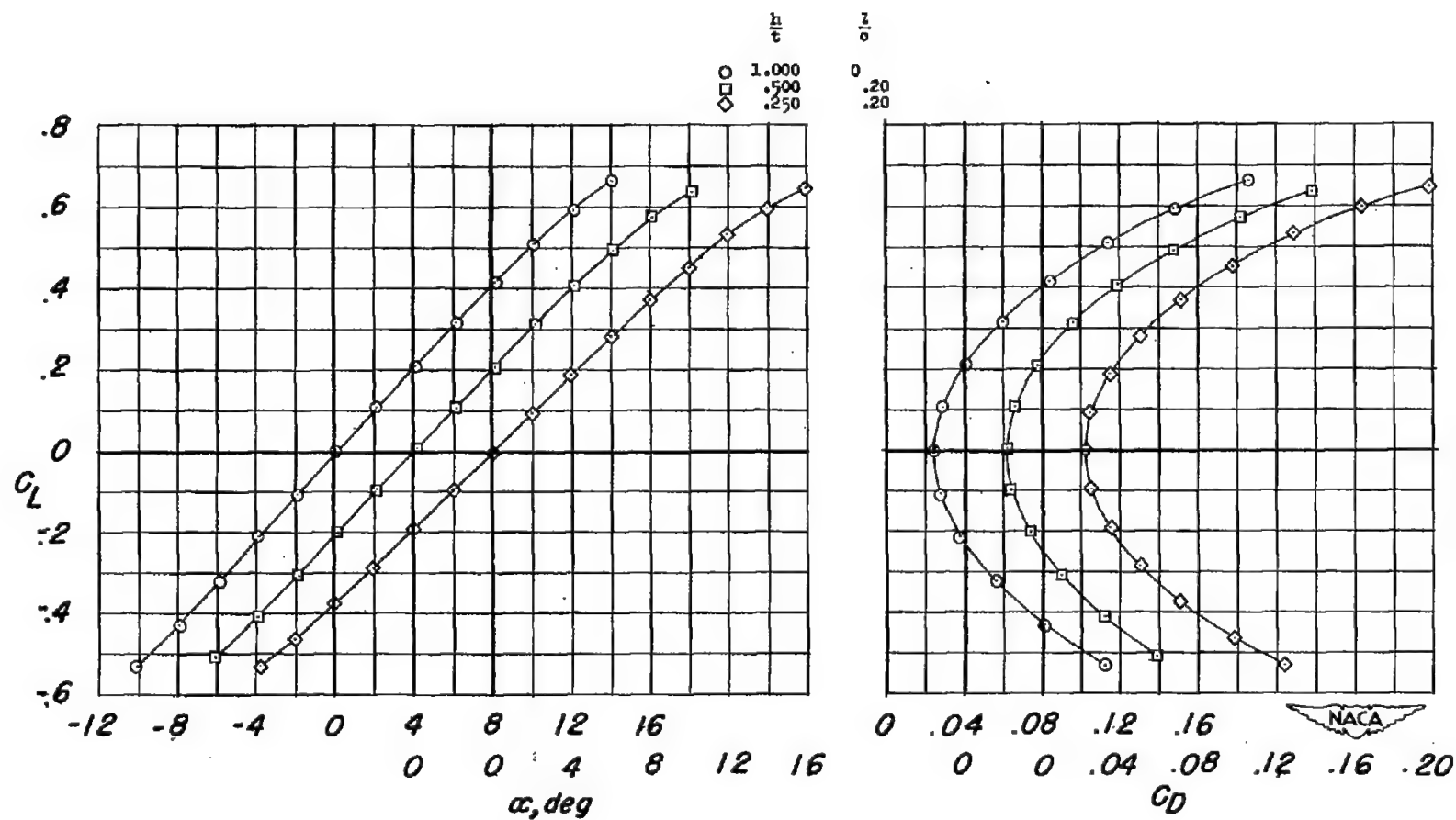
(d)  $\frac{t}{c} = 0.030$ .

Figure 11.- Concluded.



(a)  $\frac{t}{c} = 0.100$ .

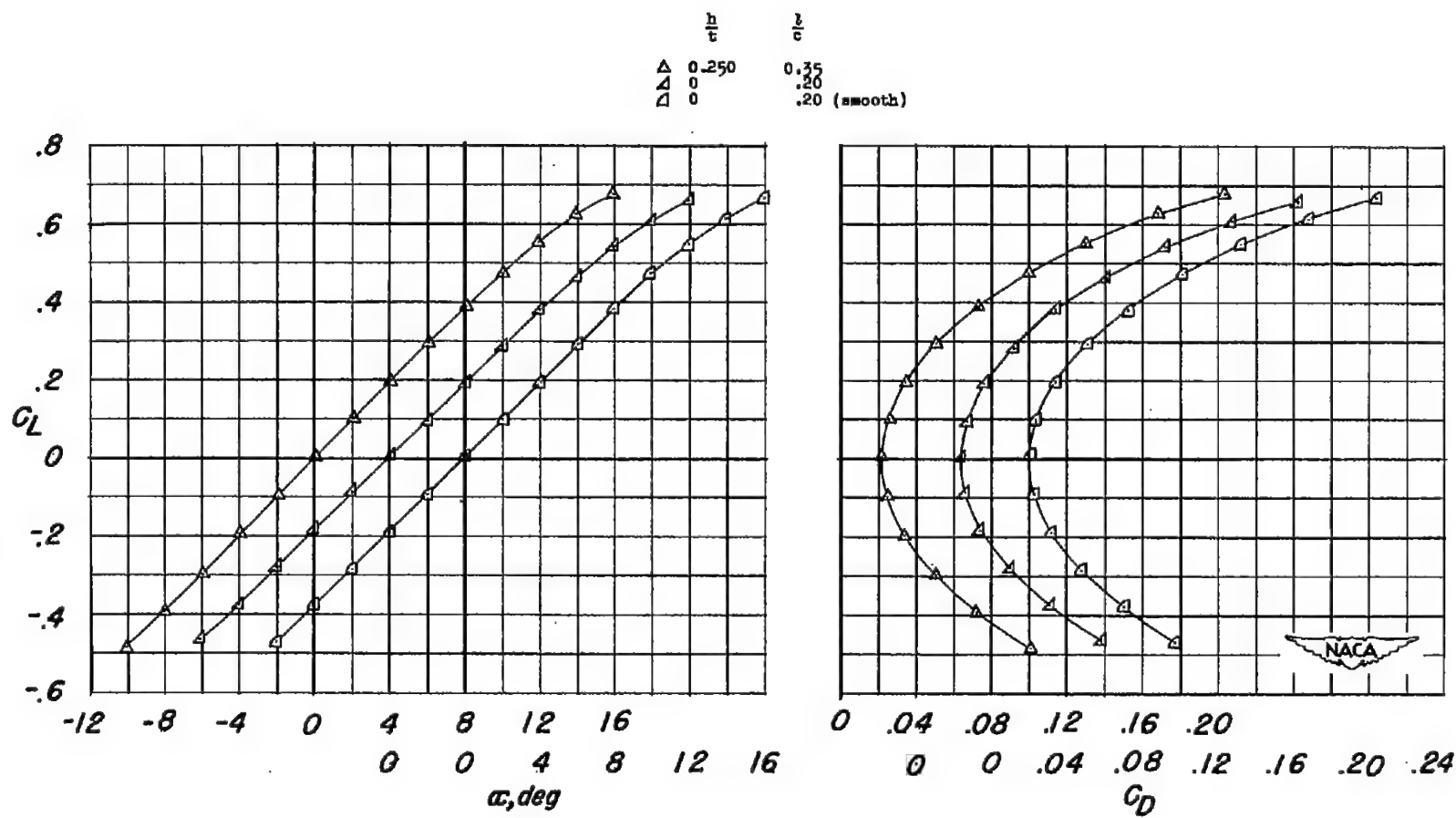
Figure 12.- Wing-plus-interference lift and drag characteristics of 45° sweptback wings at a Mach number of 1.62.



(b)  $\frac{t}{c} = 0.060$ .

Figure 12.- Continued.

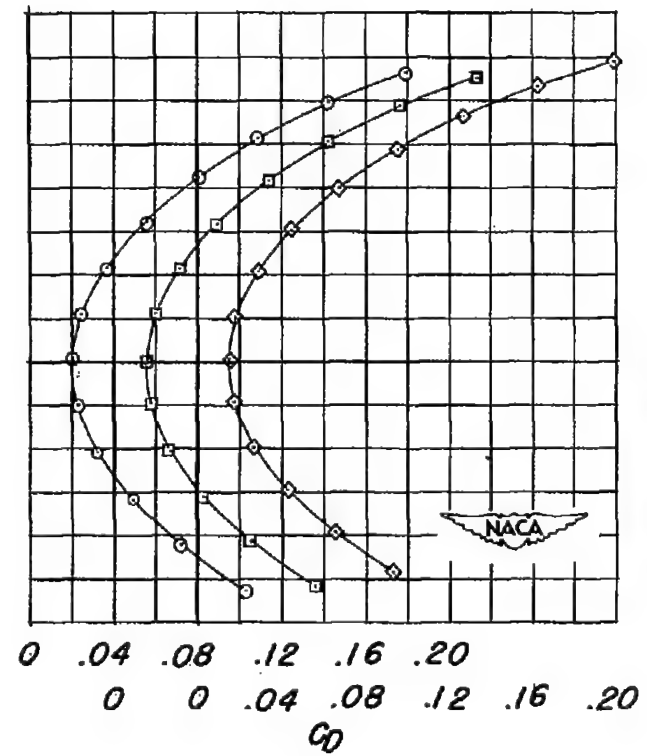
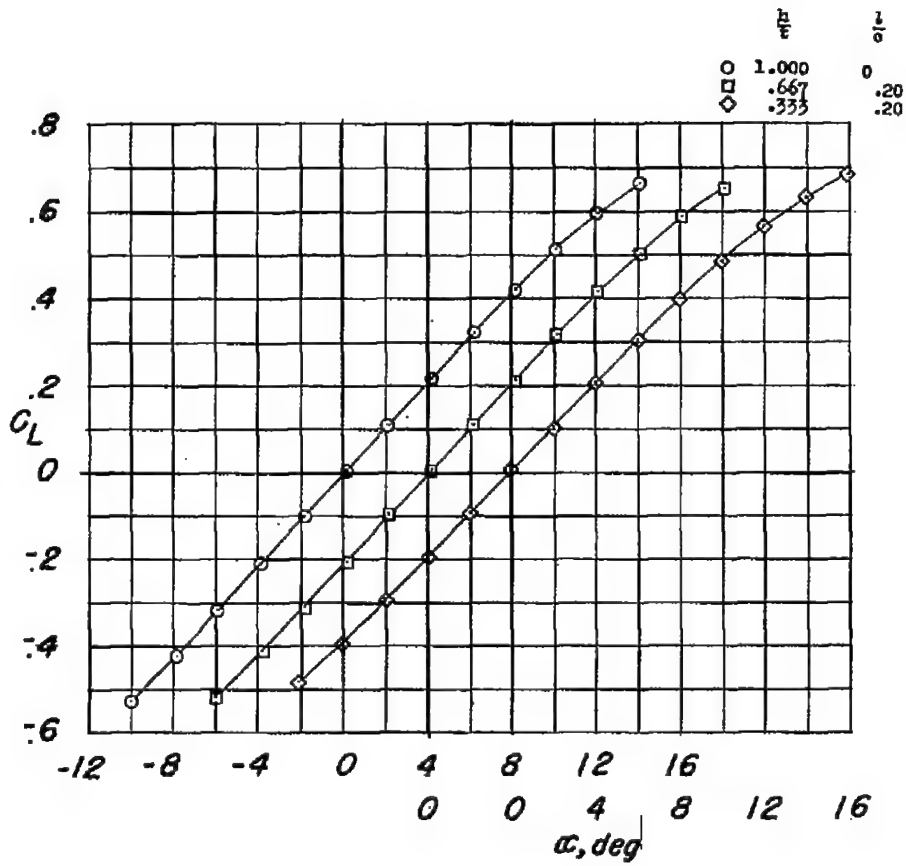
CONFIDENTIAL



(b) Concluded.

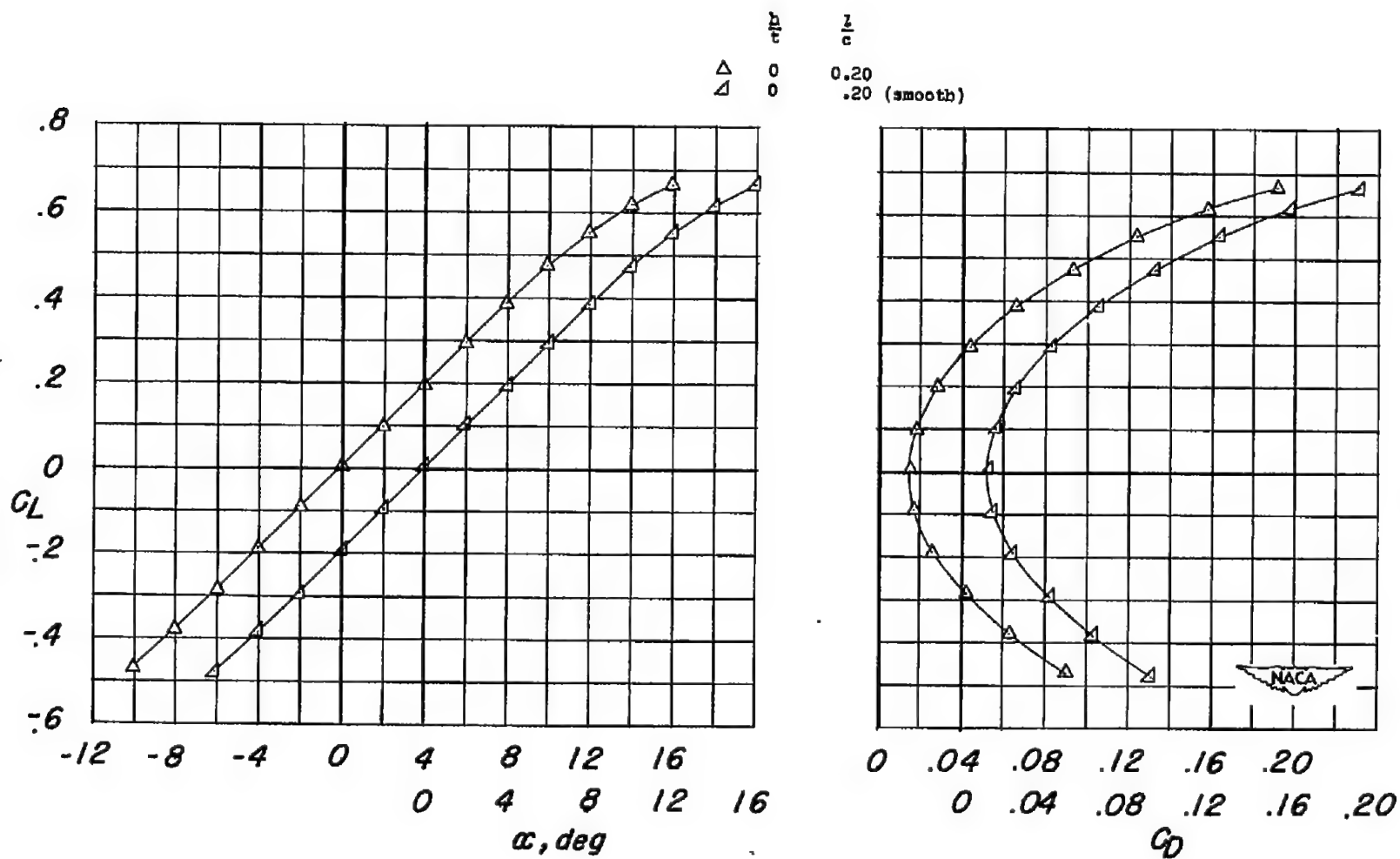
Figure 12.- Continued.





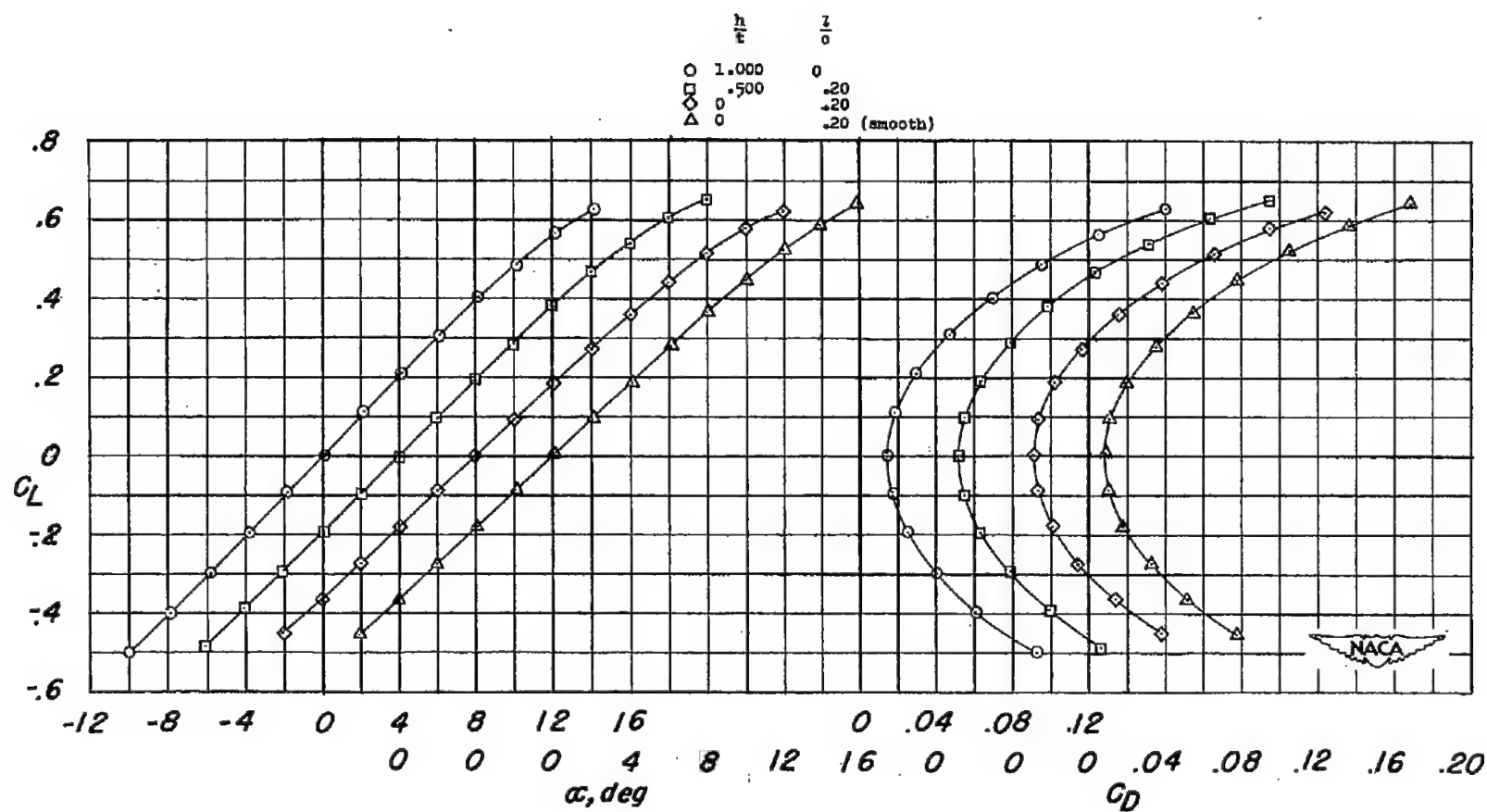
(c)  $\frac{t}{c} = 0.045$ .

Figure 12.- Continued.



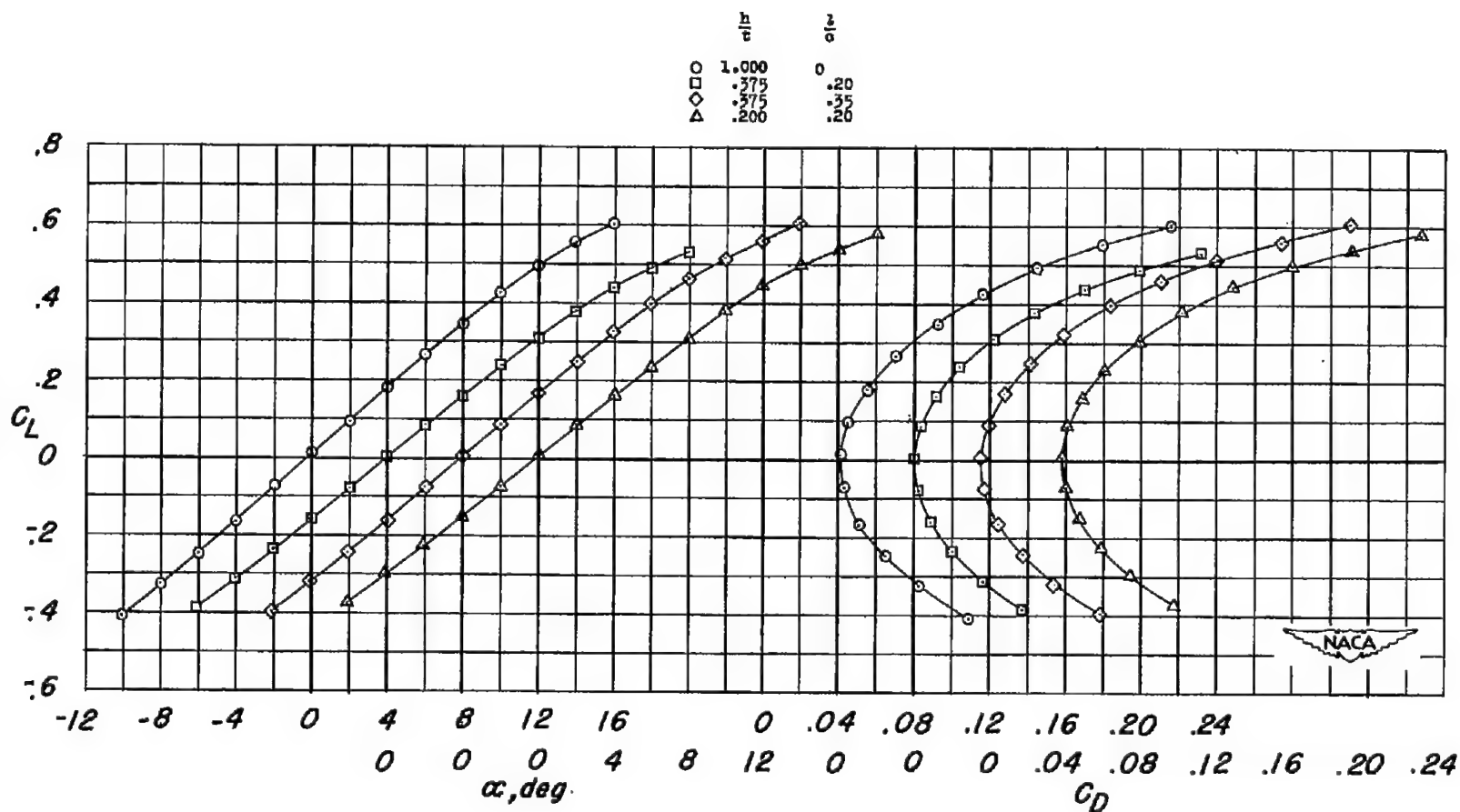
(c) Concluded.

Figure 12.- Continued.



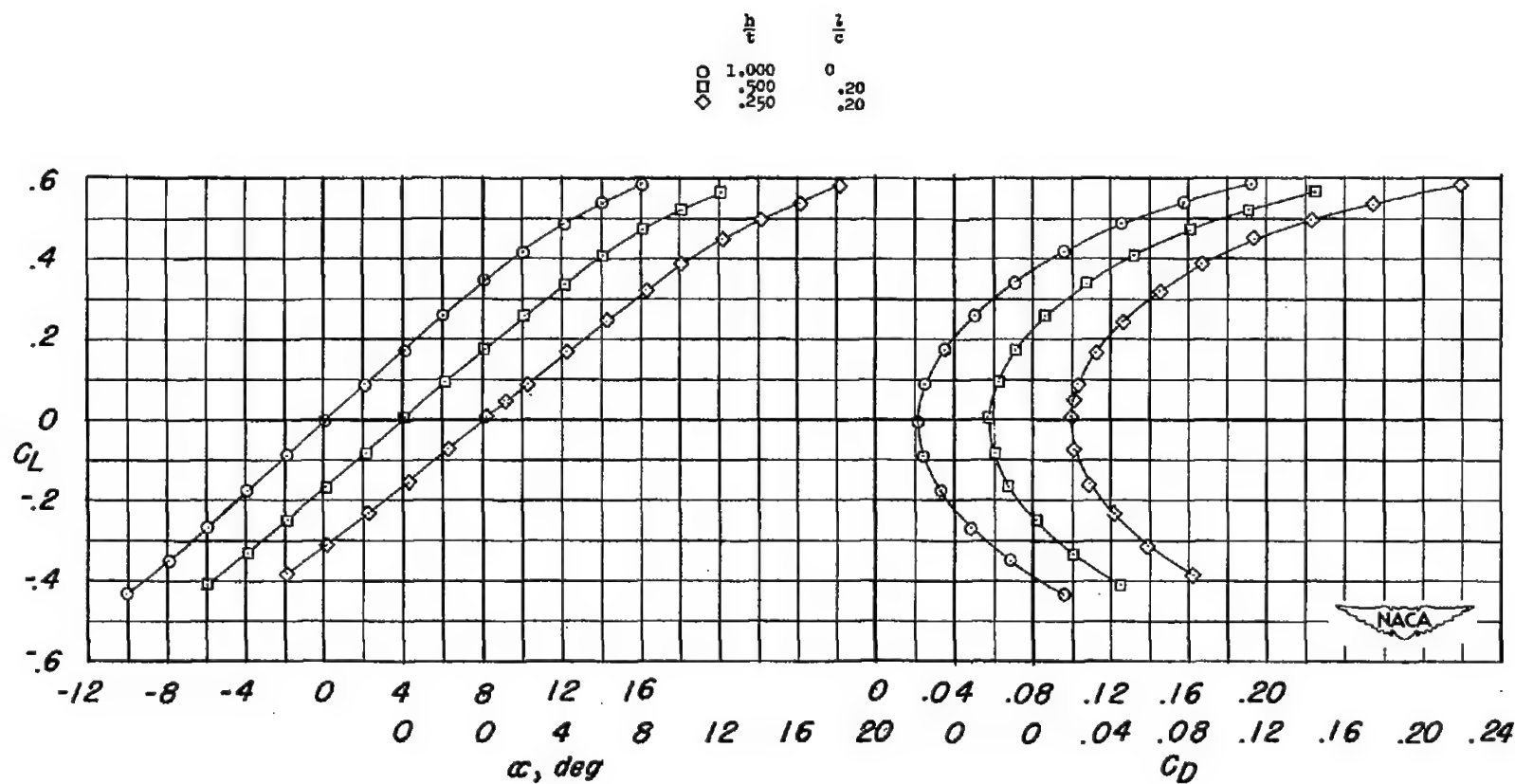
(d)  $\frac{t}{c} = 0.030$ .

Figure 12.- Concluded.



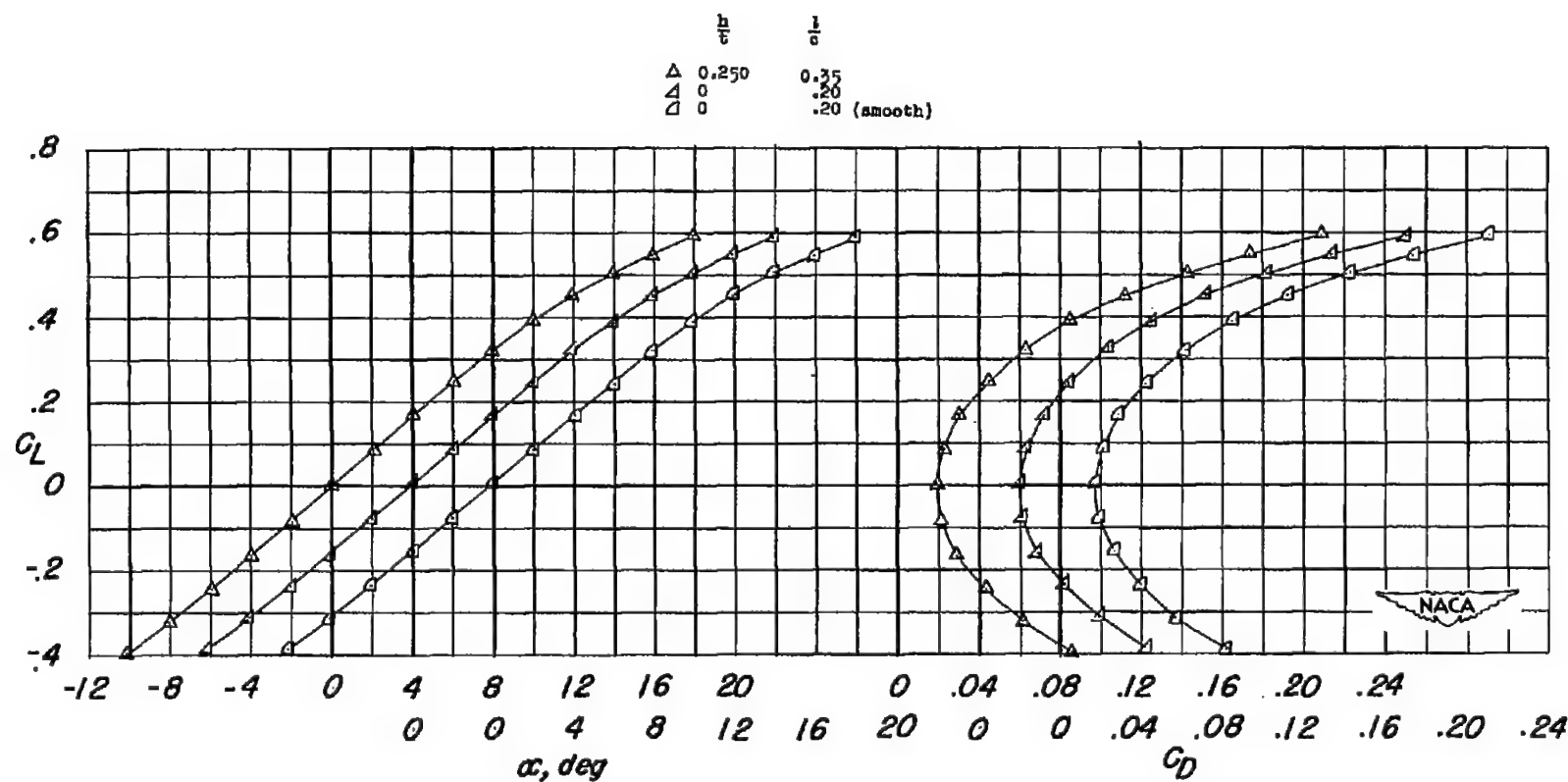
(a)  $\frac{t}{c} = 0.100$ .

Figure 13.- Wing-plus-interference lift and drag characteristics of 45° sweptback wings at a Mach number of 1.96.



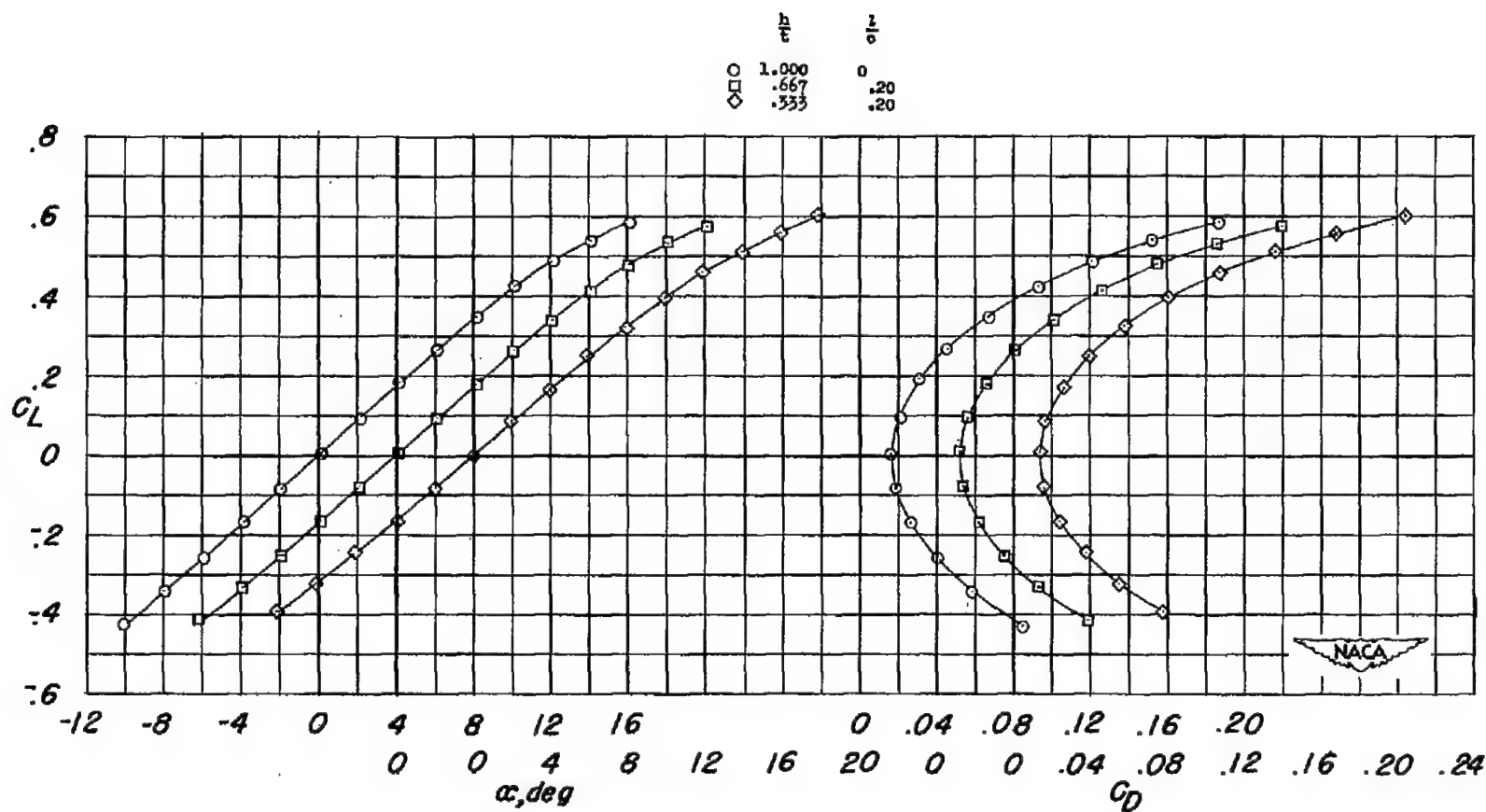
(b)  $\frac{t}{c} = 0.060$ .

Figure 13.- Continued.



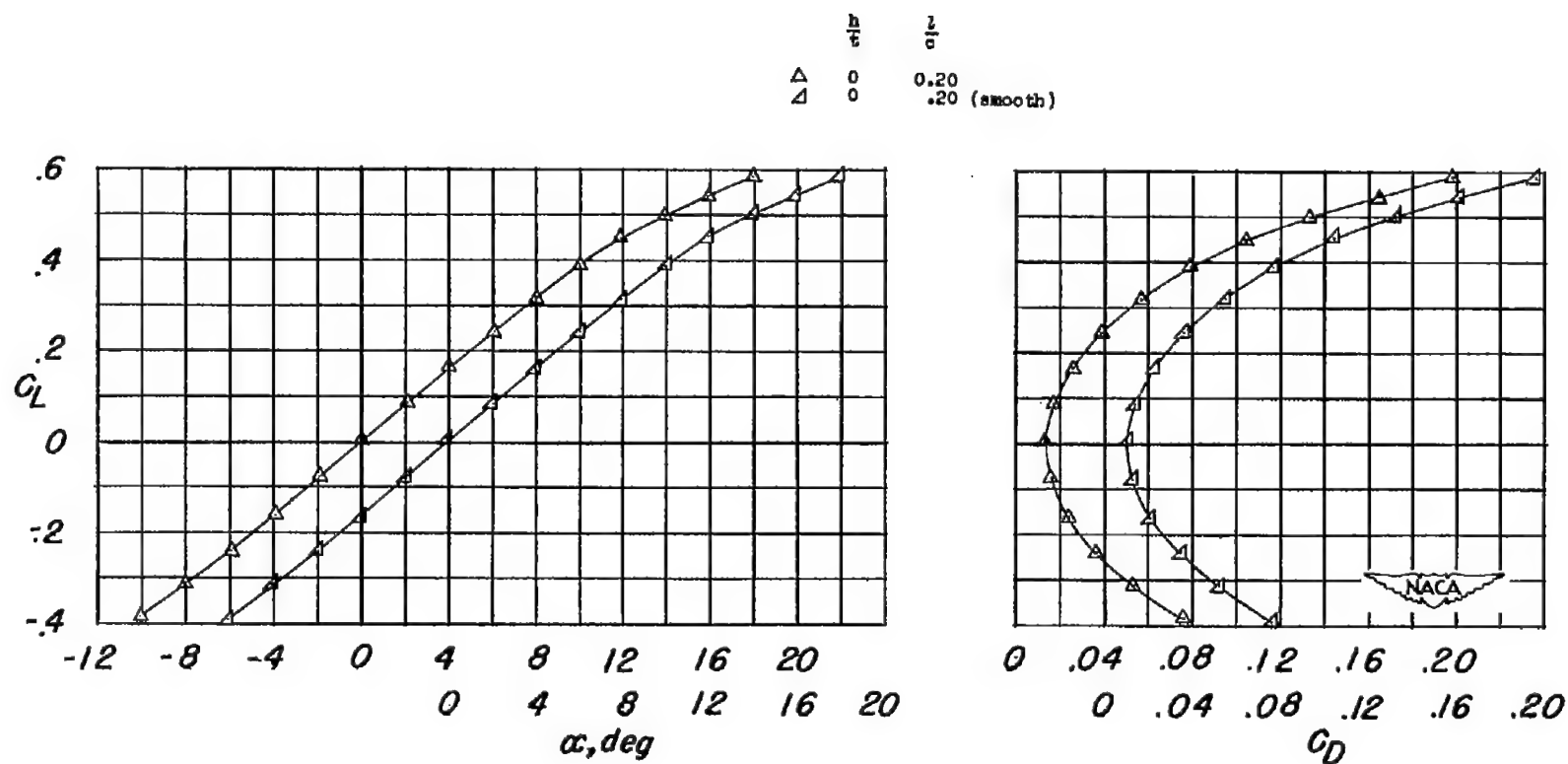
(b) Concluded.

Figure 13.- Continued.



(c)  $\frac{t}{c} = 0.045$ .

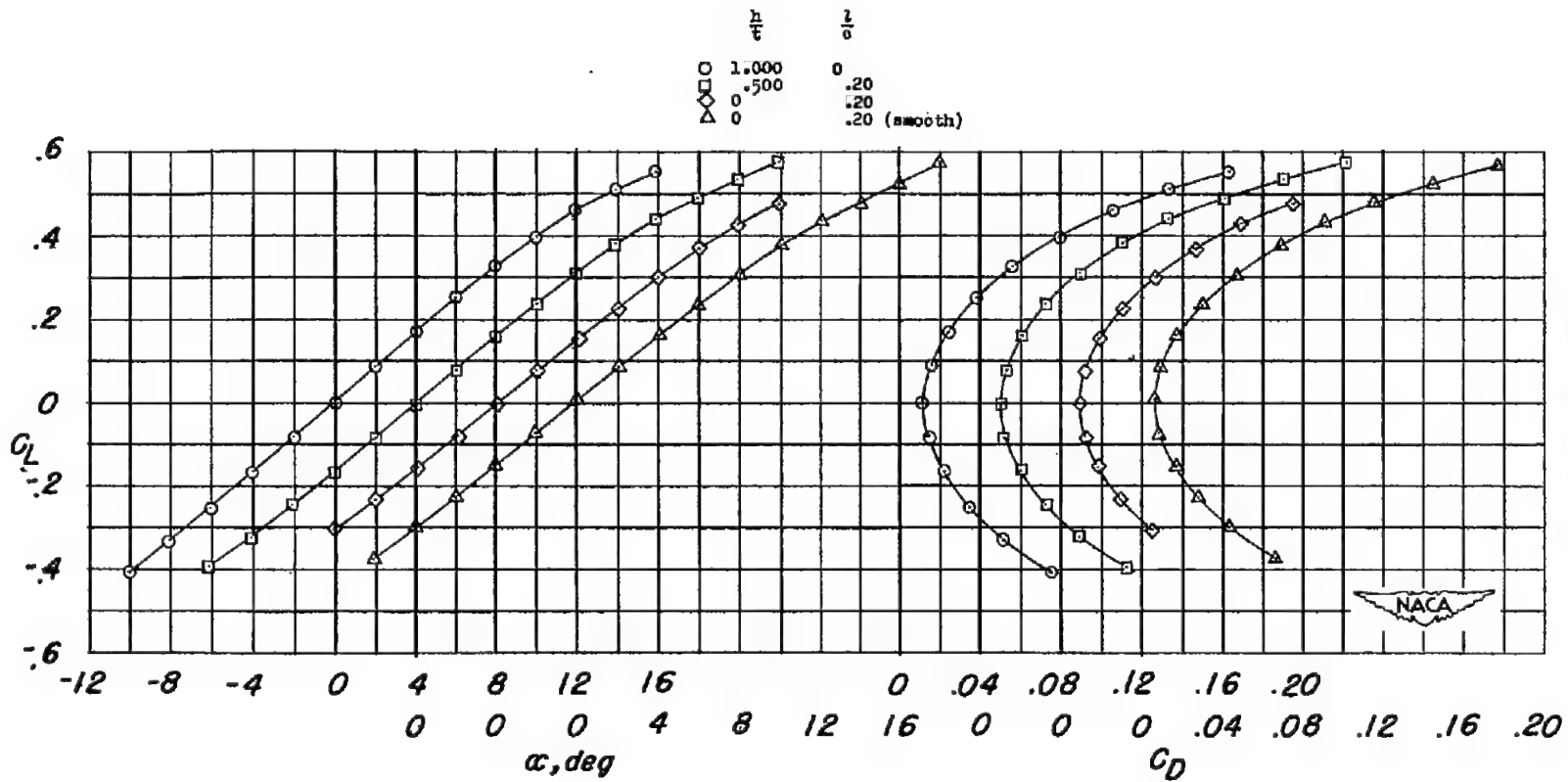
Figure 13.- Continued.



(c) Concluded.

Figure 13.- Continued.





(d)  $\frac{t}{c} = 0.030$ .

Figure 13.- Concluded.

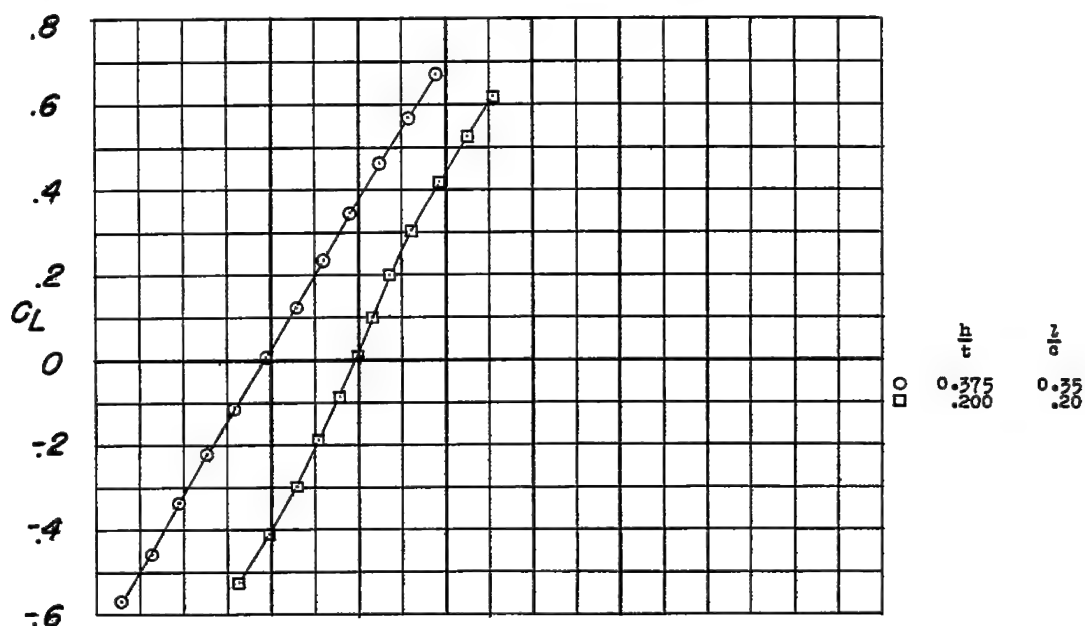
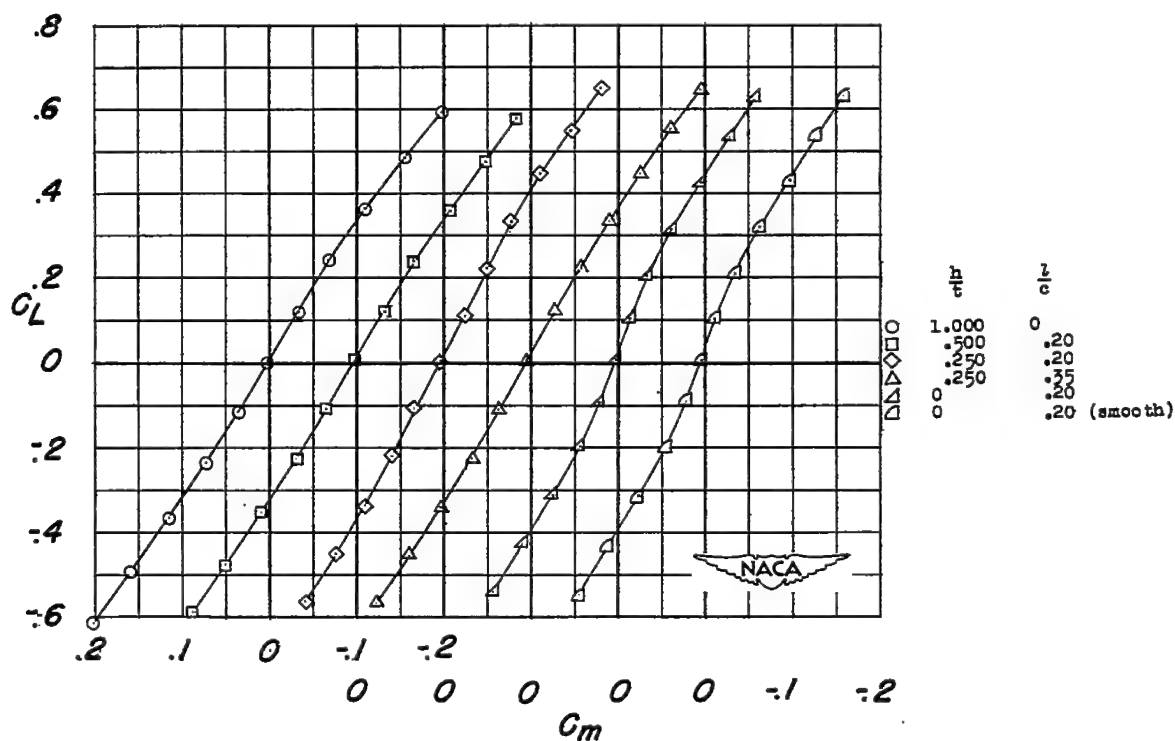
(a)  $\frac{t}{c} = 0.100$ .(b)  $\frac{t}{c} = 0.060$ .

Figure 14.- Wing-plus-interference pitching-moment characteristics of 45° sweptback wings at a Mach number of 1.41.

CONFIDENTIAL

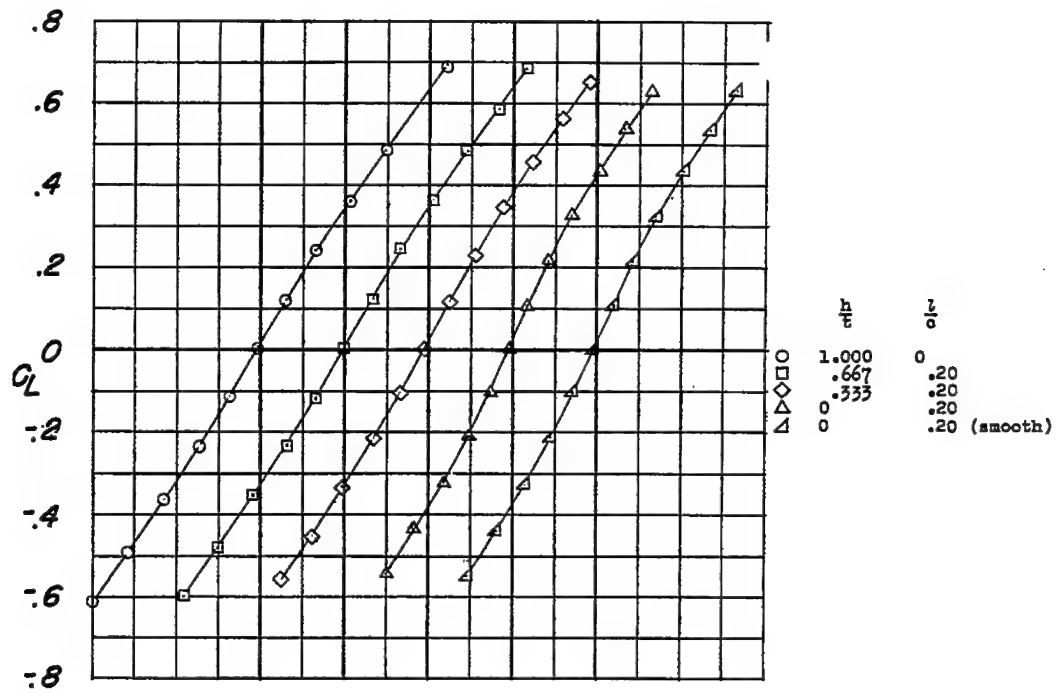
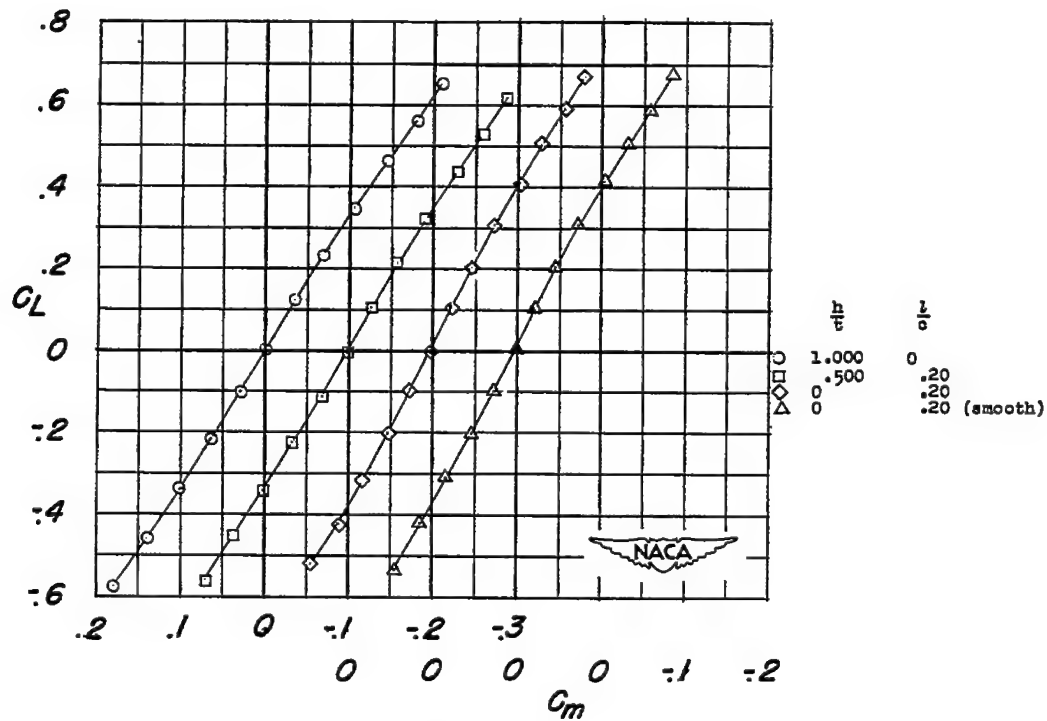
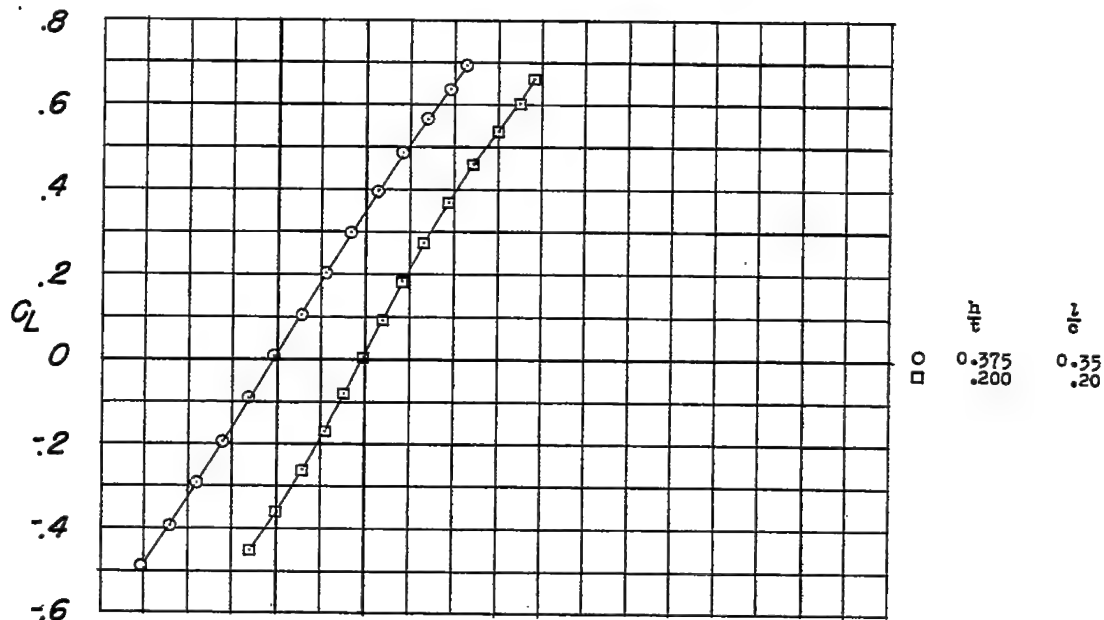
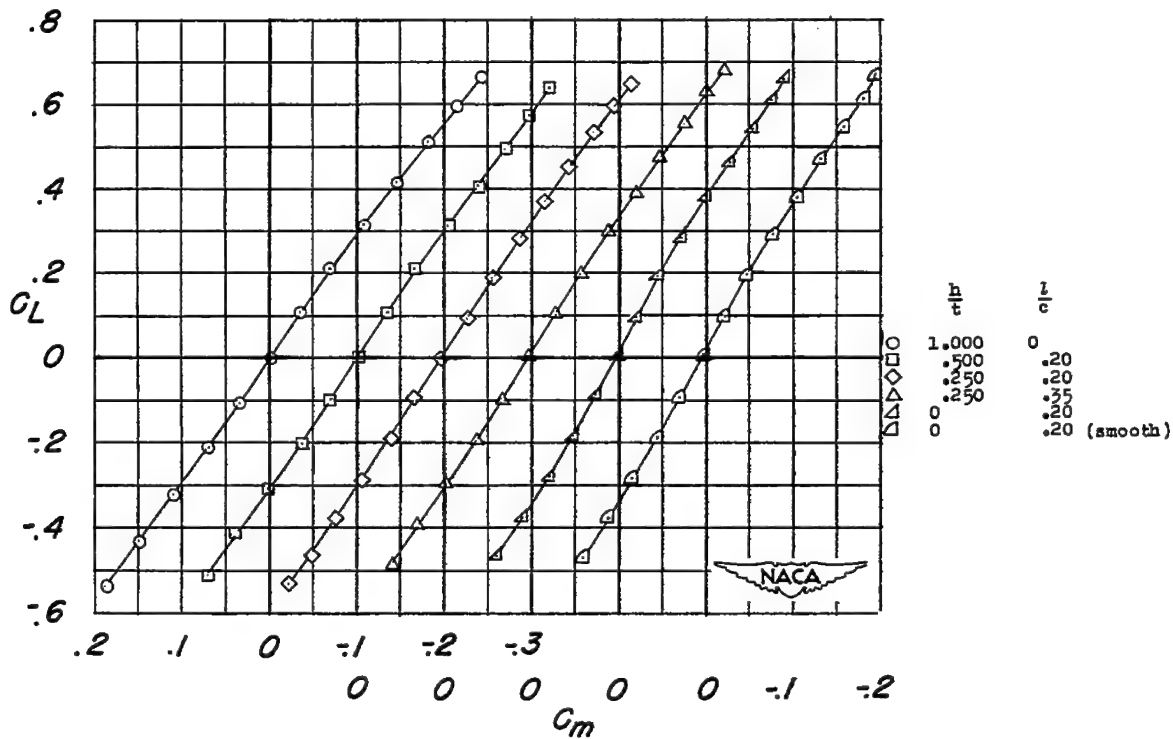
(c)  $\frac{t}{c} = 0.045$ .(d)  $\frac{t}{c} = 0.030$ .

Figure 14.- Concluded.

CONFIDENTIAL

(a)  $\frac{t}{c} = 0.100$ .(b)  $\frac{t}{c} = 0.060$ .Figure 15.- Wing-plus-interference pitching-moment characteristics of  $45^\circ$  sweptback wings at a Mach number of 1.62.

CONFIDENTIAL

NACA RM L53D13

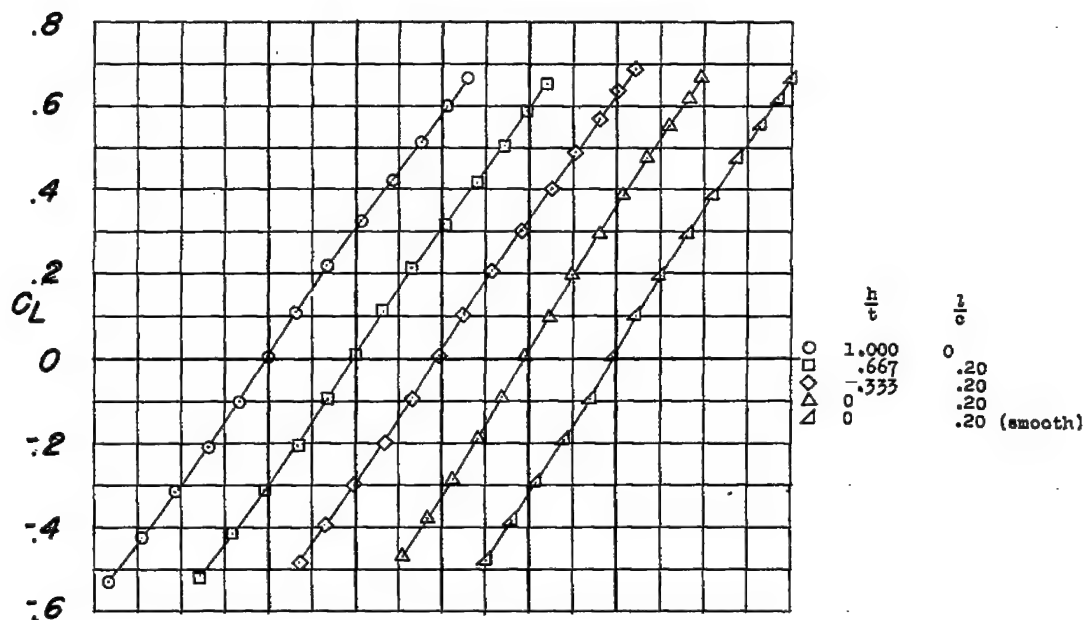
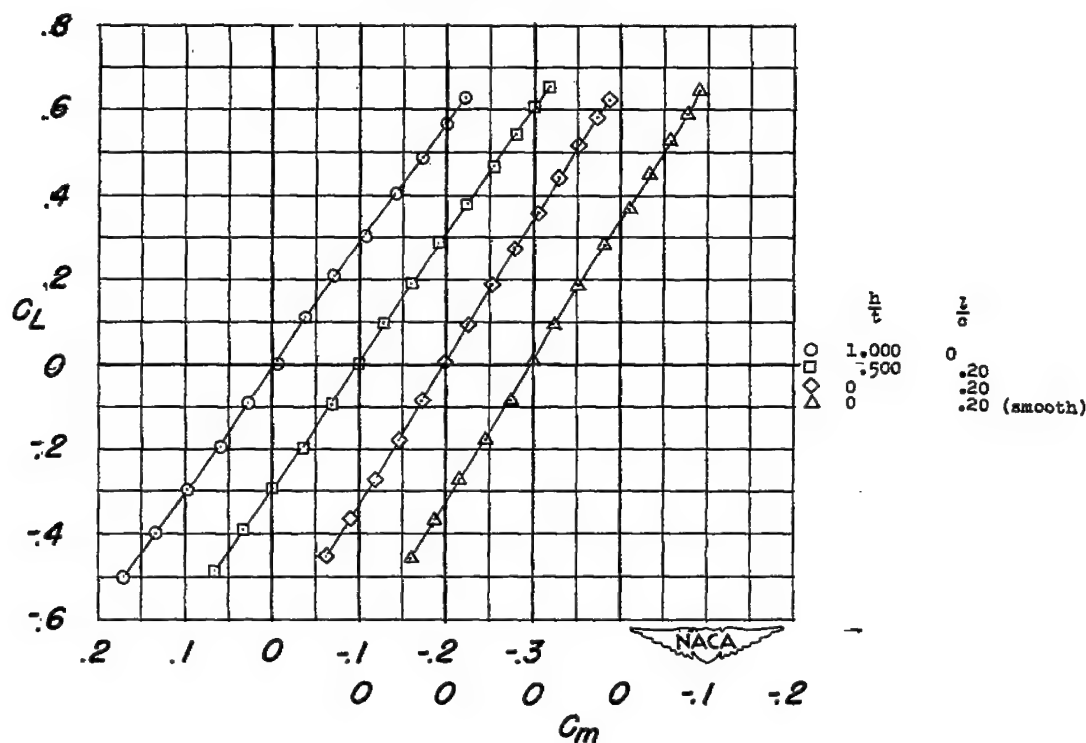
(c)  $\frac{t}{c} = 0.045$ .(d)  $\frac{t}{c} = 0.030$ .

Figure 15.- Concluded.

CONFIDENTIAL

CONFIDENTIAL

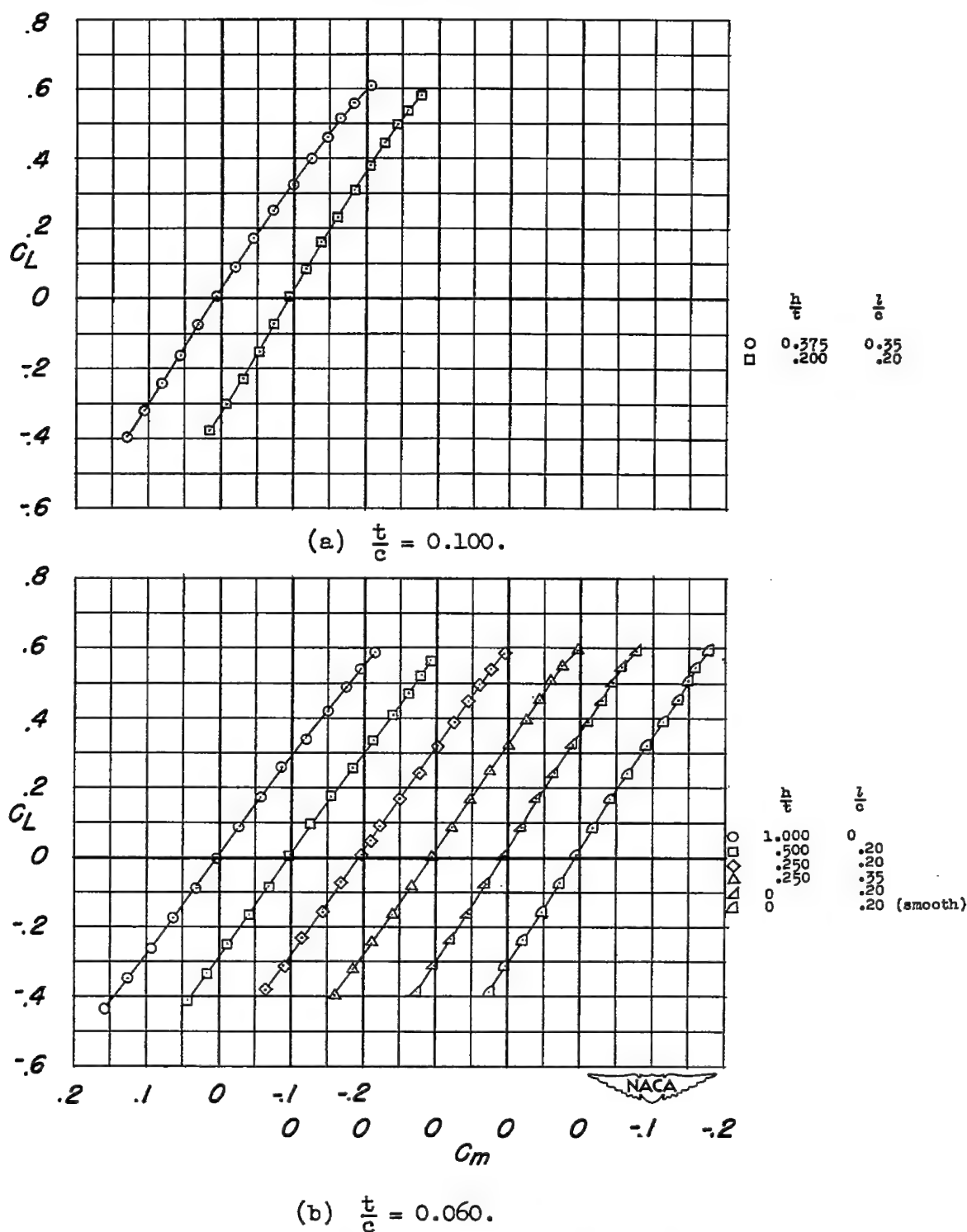


Figure 16.- Wing-plus-interference pitching-moment characteristics of 45° sweptback wings at a Mach number of 1.96.

CONFIDENTIAL

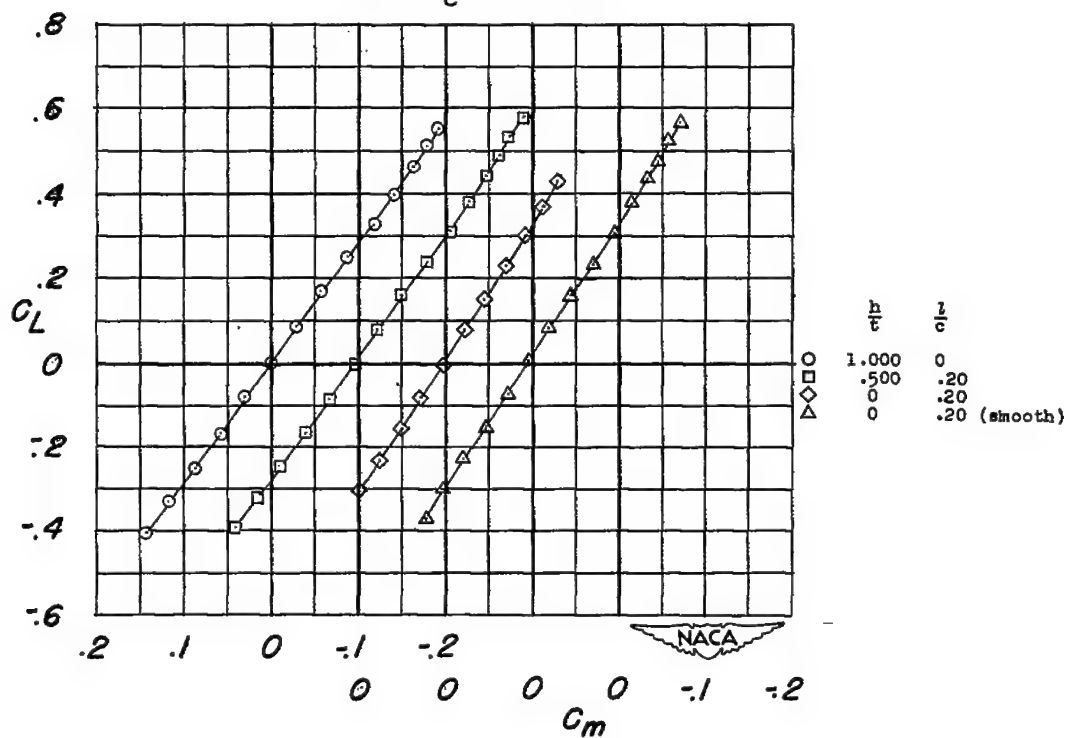
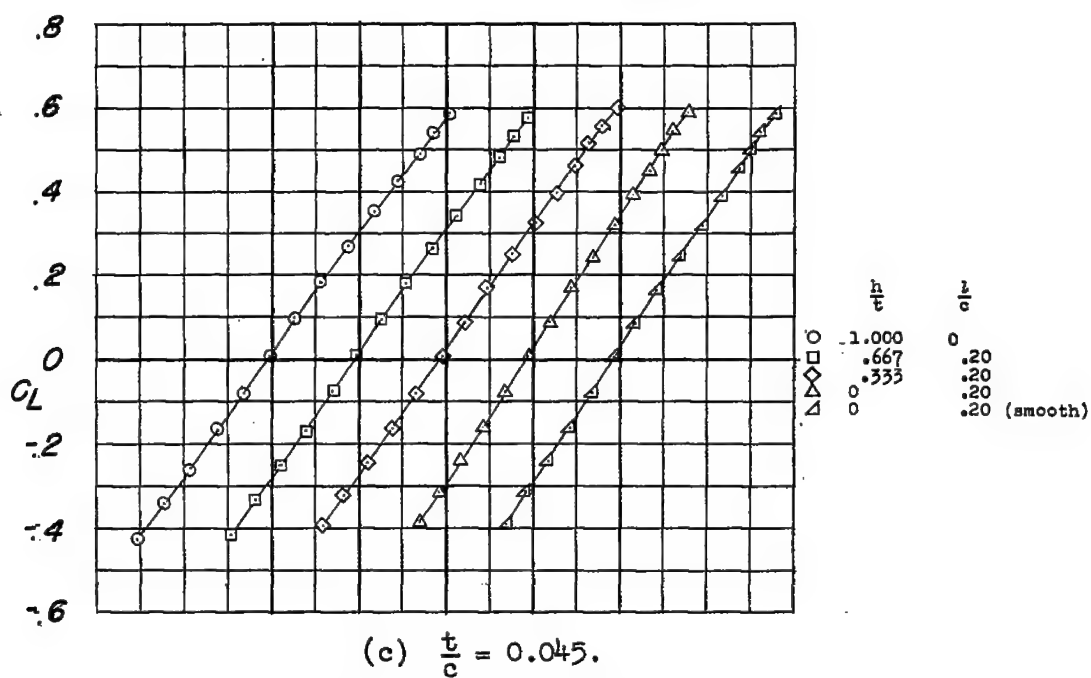
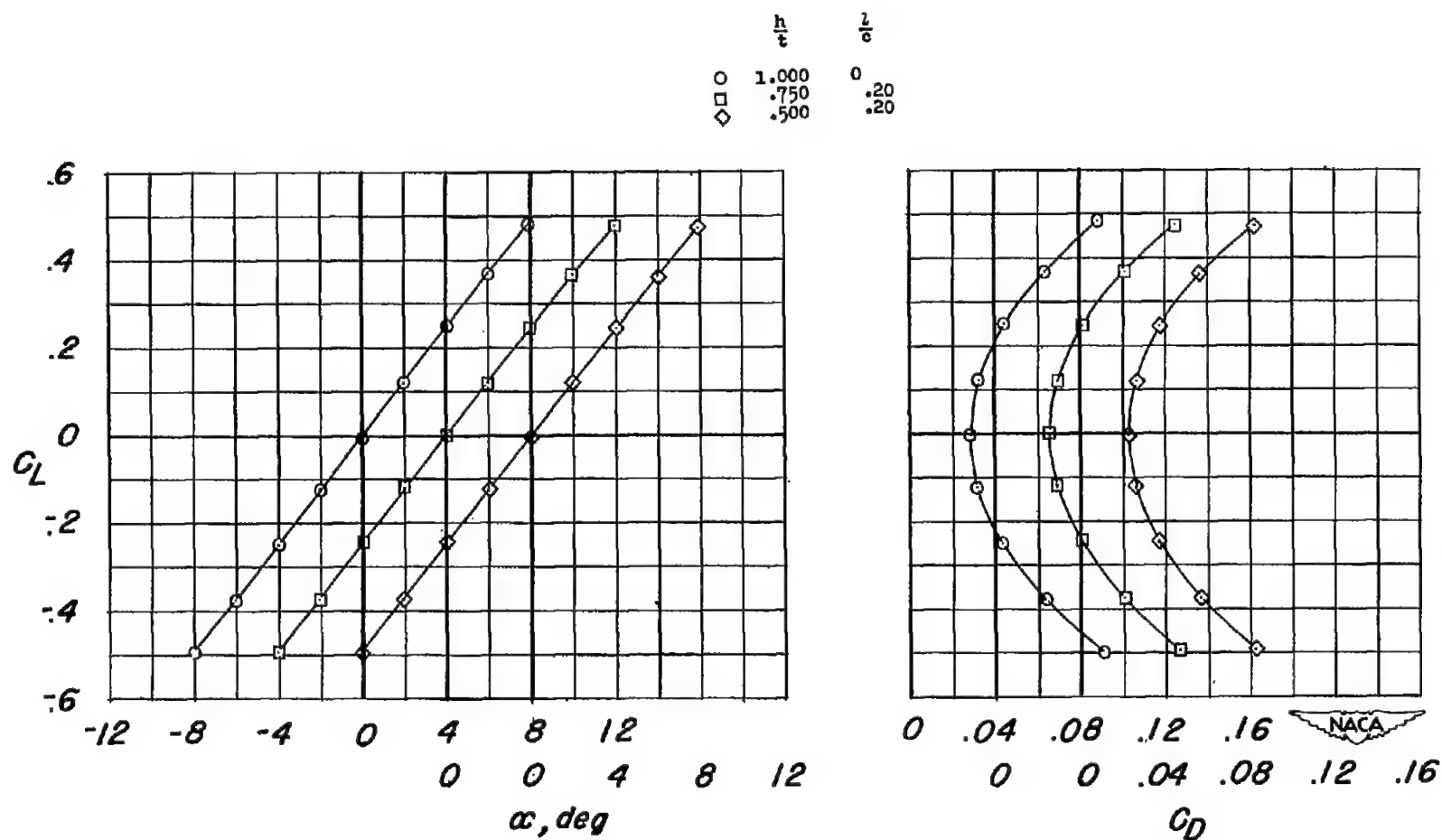


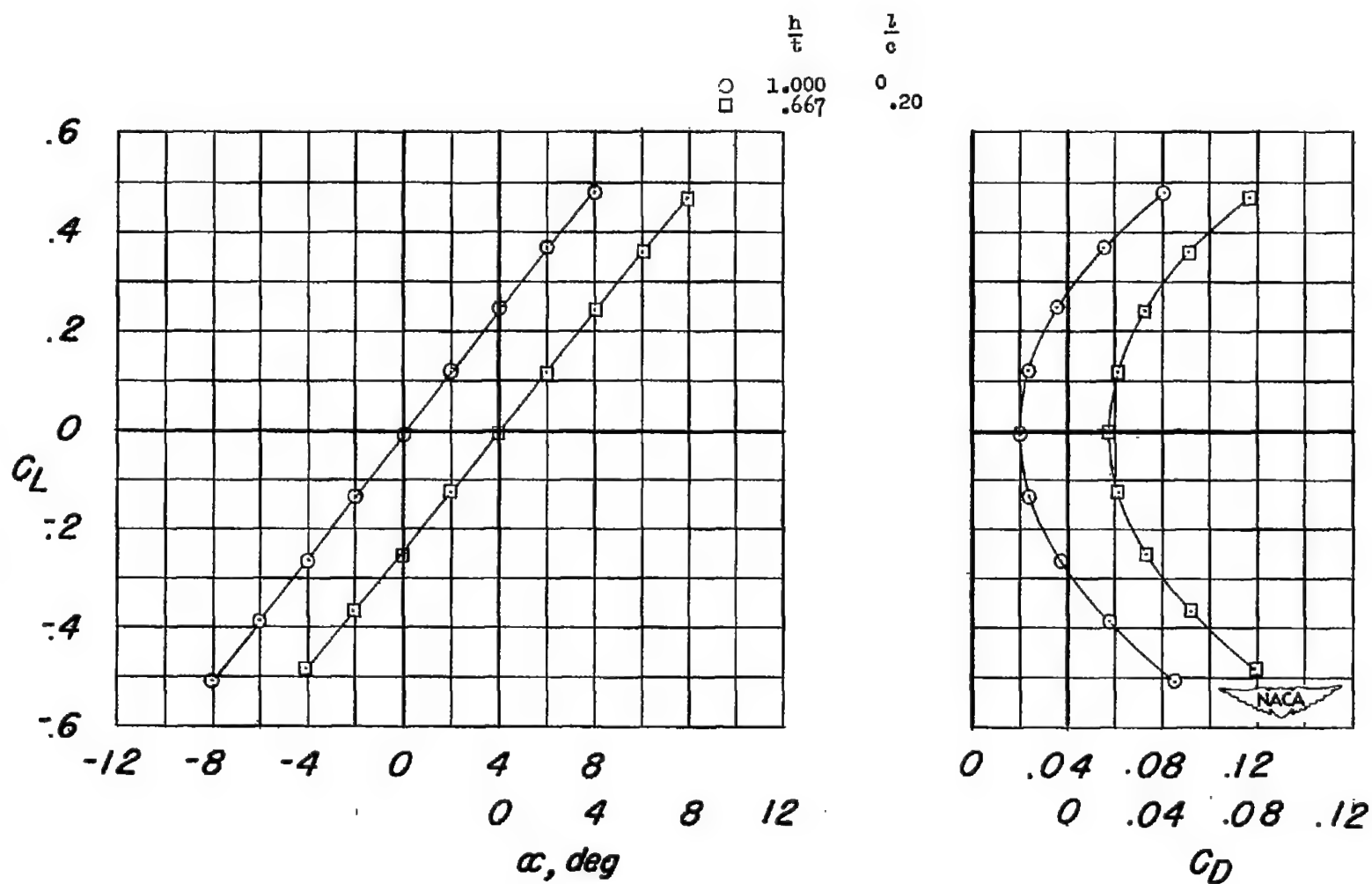
Figure 16.- Concluded.



(a)  $\frac{t}{c} = 0.060$ .

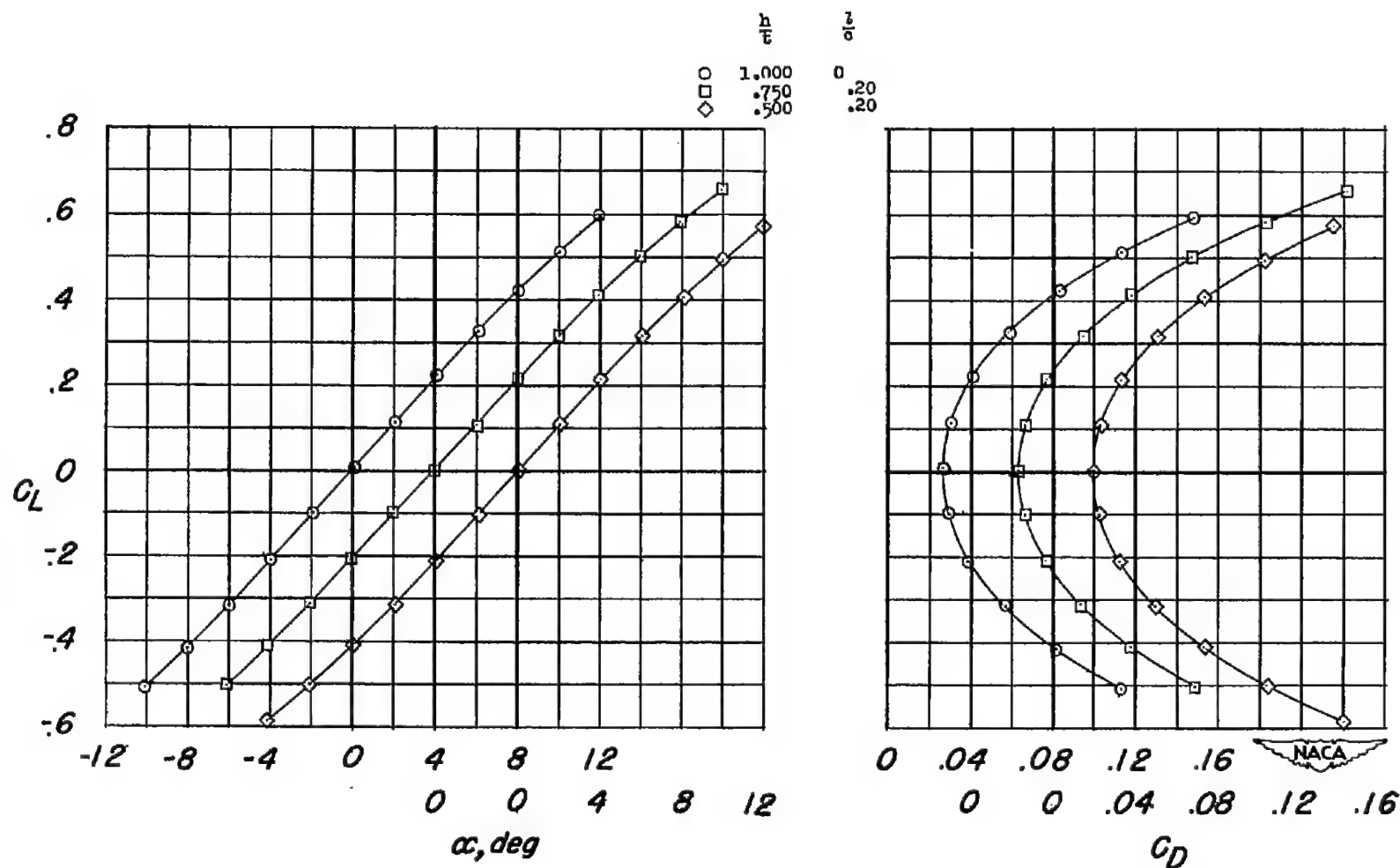
Figure 17.- Wing-plus-interference lift and drag characteristics of  $45^\circ$  delta wings at a Mach number of 1.41.





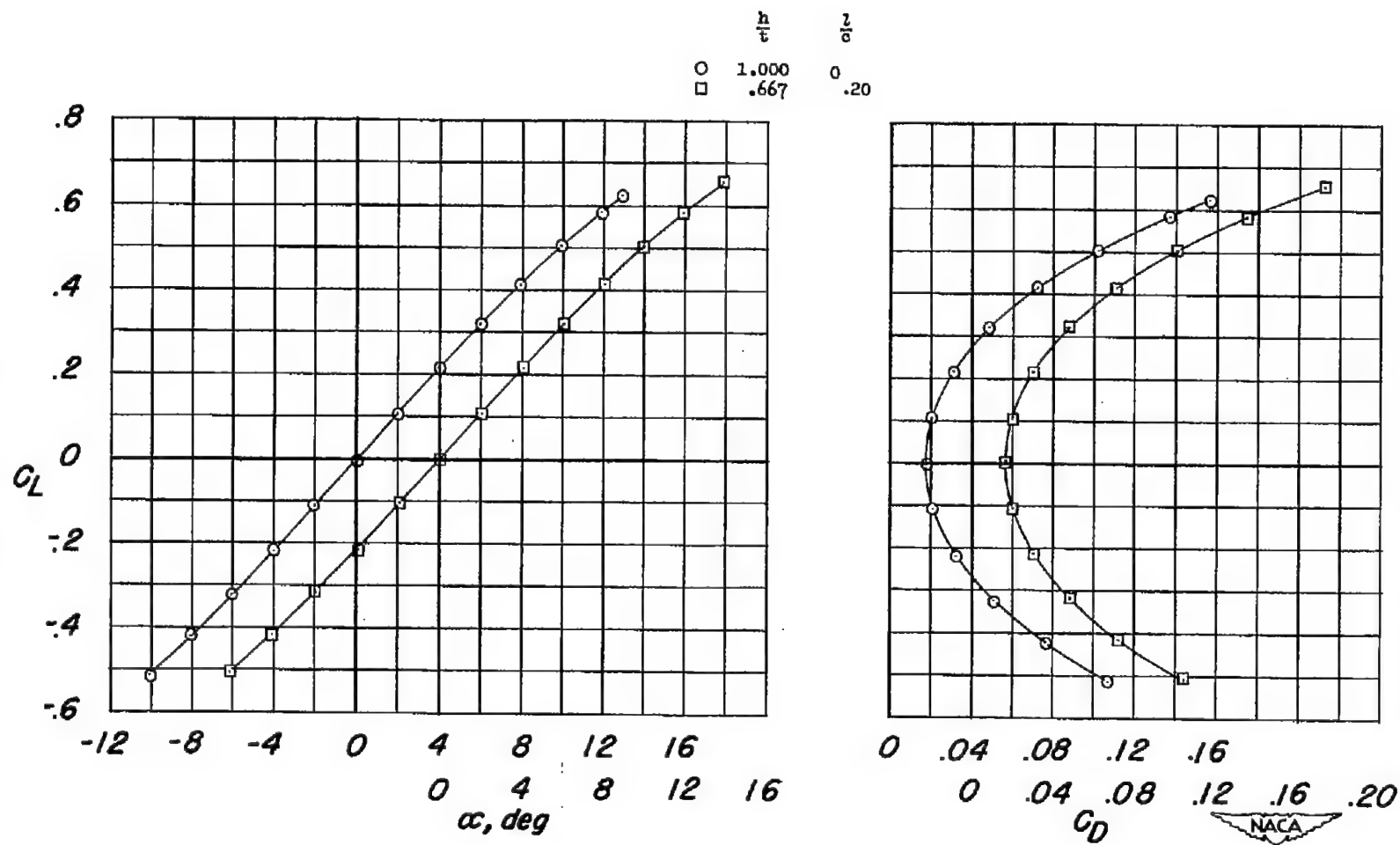
(b)  $\frac{t}{c} = 0.045$ .

Figure 17.- Concluded.



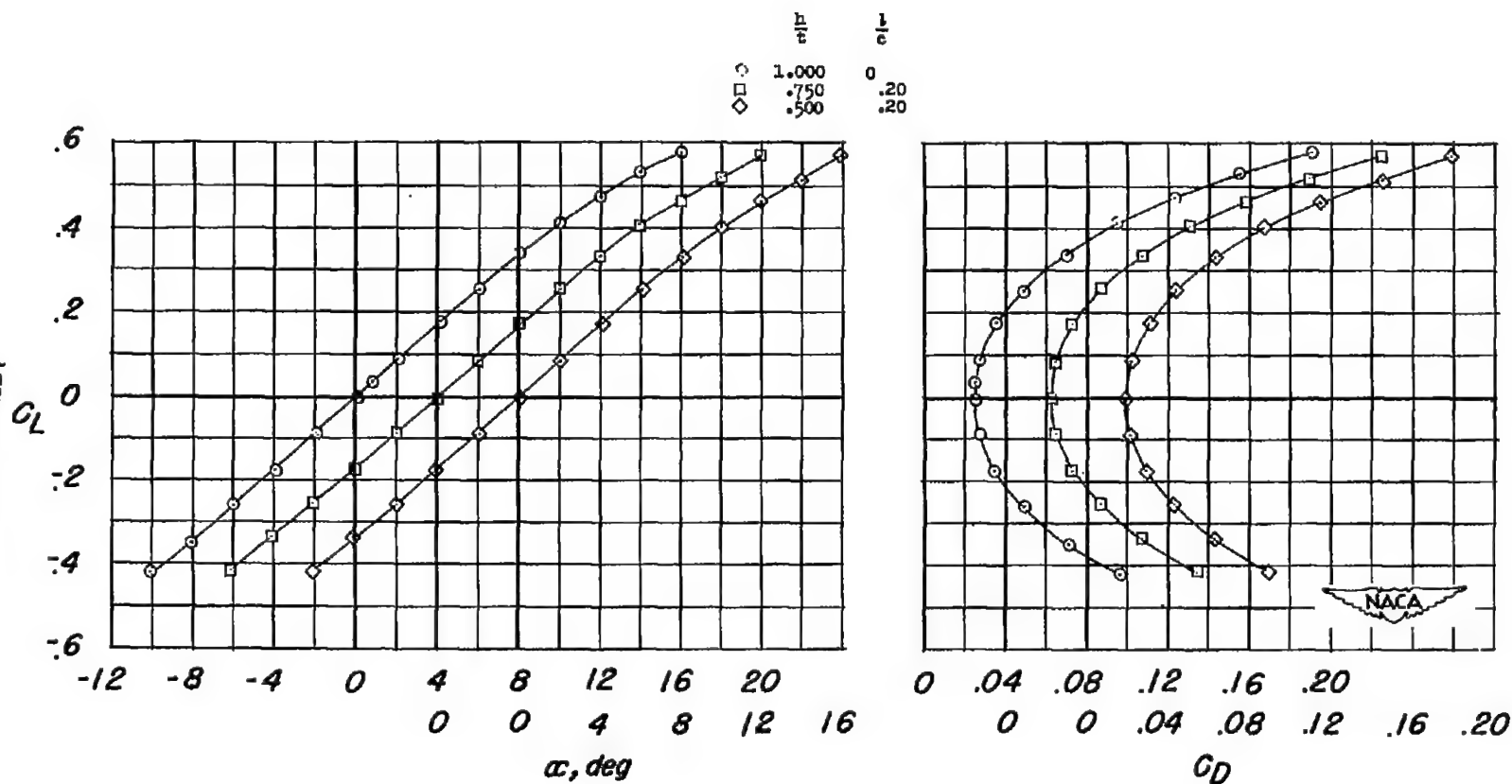
(a)  $\frac{t}{c} = 0.060$ .

Figure 18.- Wing-plus-interference lift and drag characteristics of  $45^\circ$  delta wings at a Mach number of 1.62.



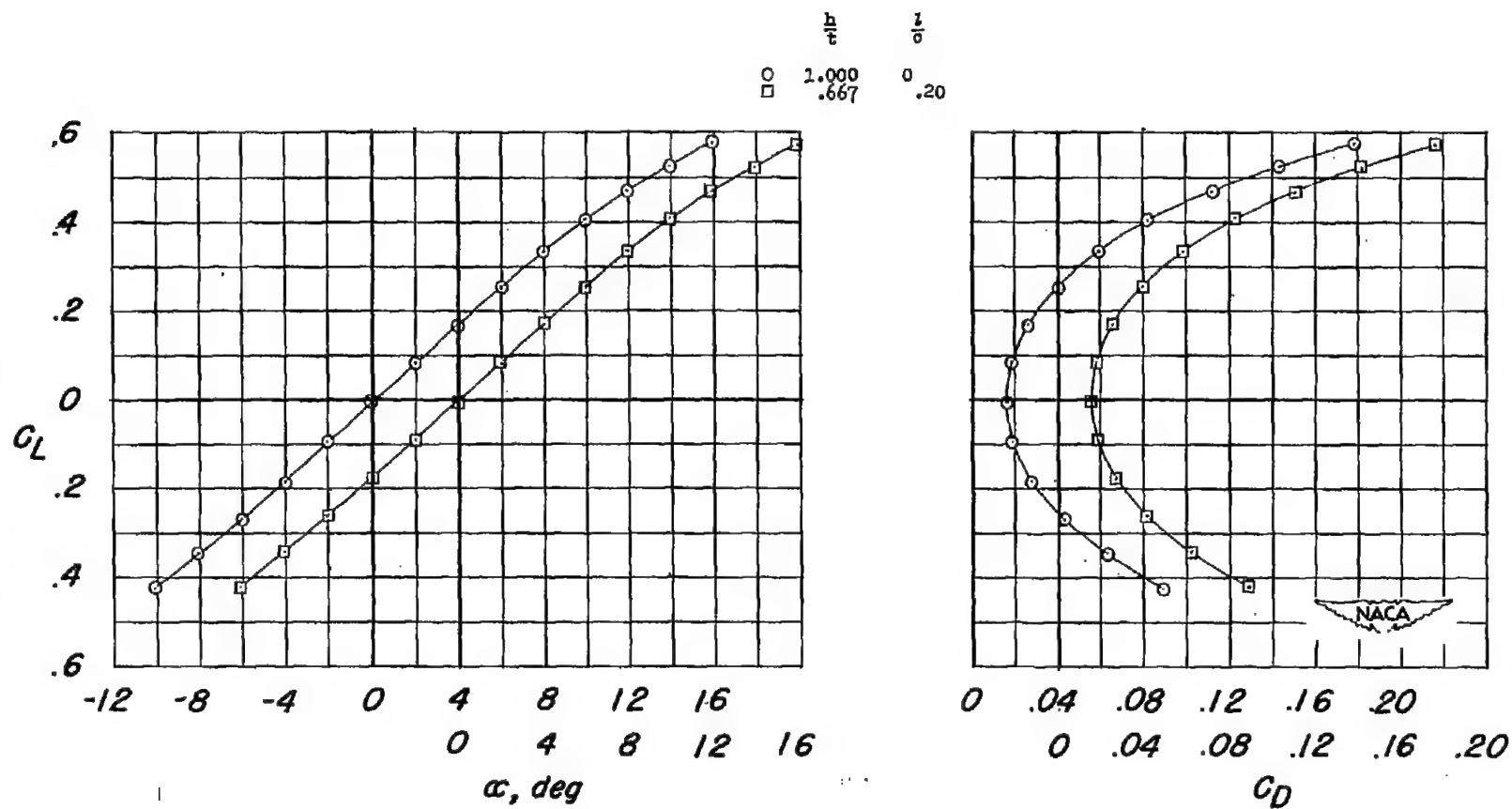
(b)  $\frac{t}{c} = 0.045$ .

Figure 18.- Concluded.



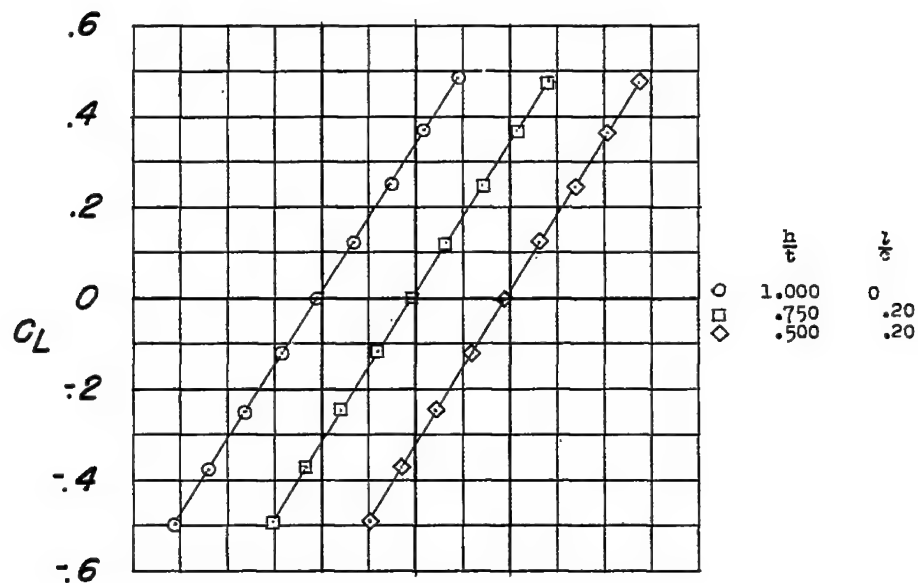
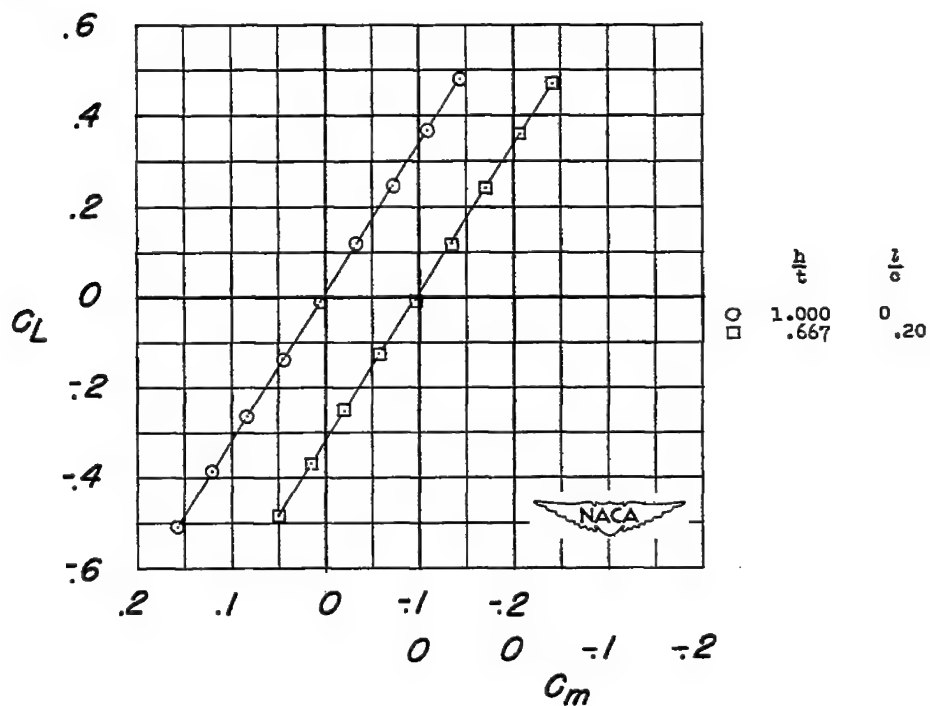
(a)  $\frac{t}{c} = 0.060$ .

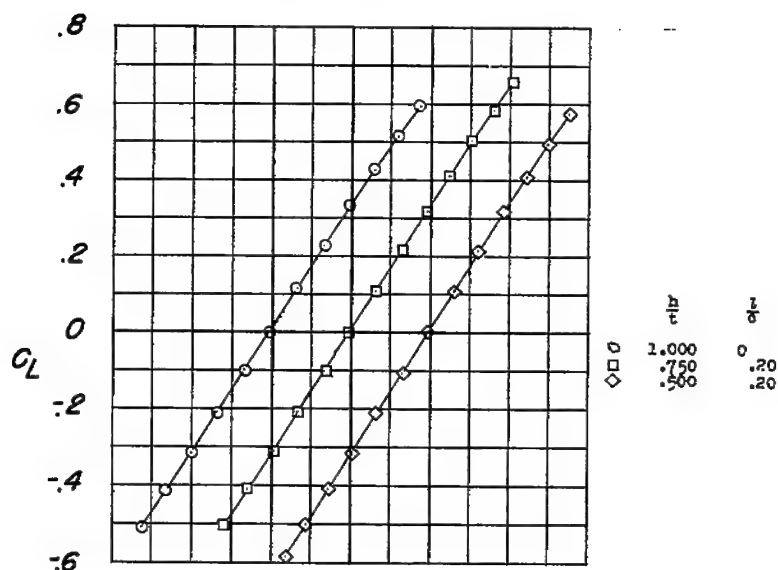
Figure 19.- Wing-plus-interference lift and drag characteristics of  $45^\circ$  delta wings at a Mach number of 1.96.



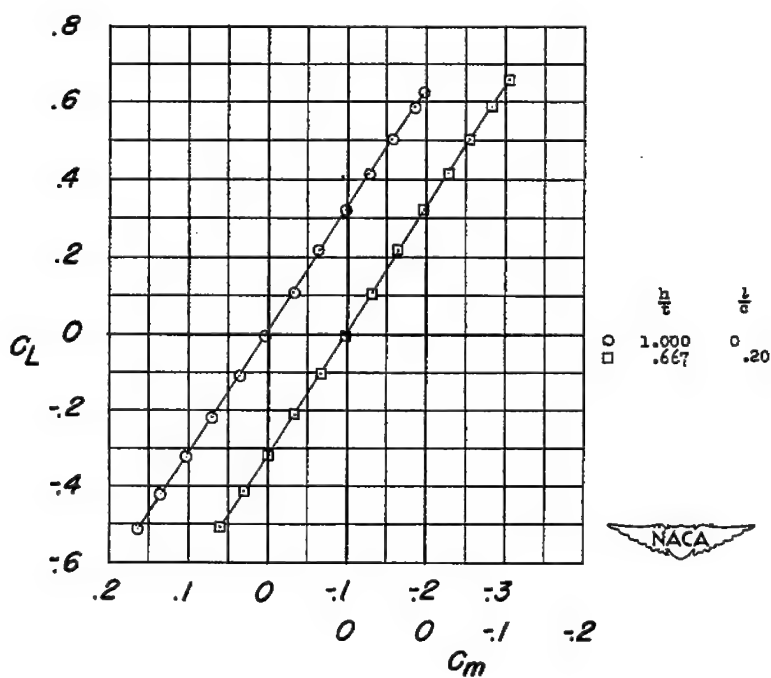
(b)  $\frac{t}{c} = 0.045$ .

Figure 19.- Concluded.

(a)  $\frac{t}{c} = 0.060$ .(b)  $\frac{t}{c} = 0.045$ .Figure 20.-- Wing-plus-interference pitching-moment characteristics of  $45^\circ$  delta wings at a Mach number of 1.41.

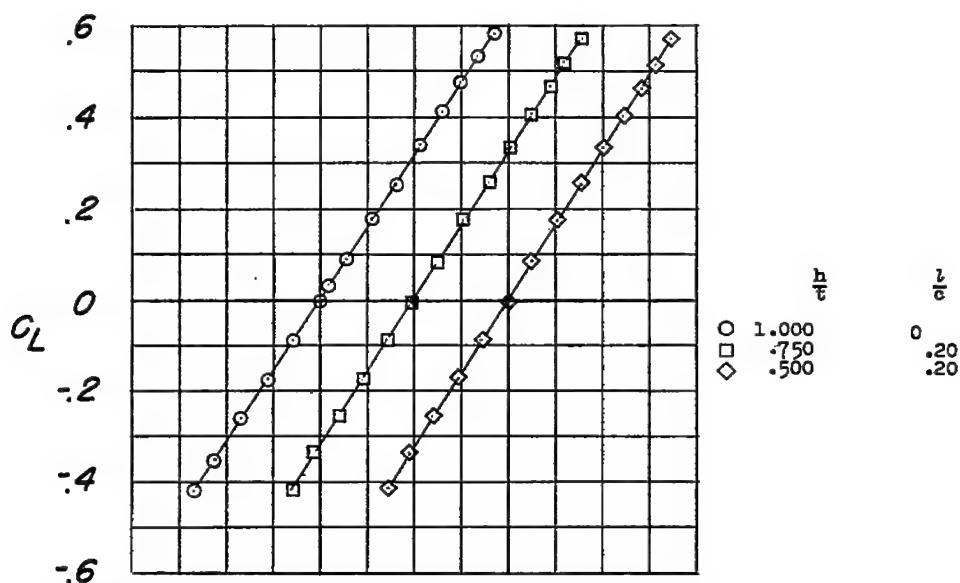
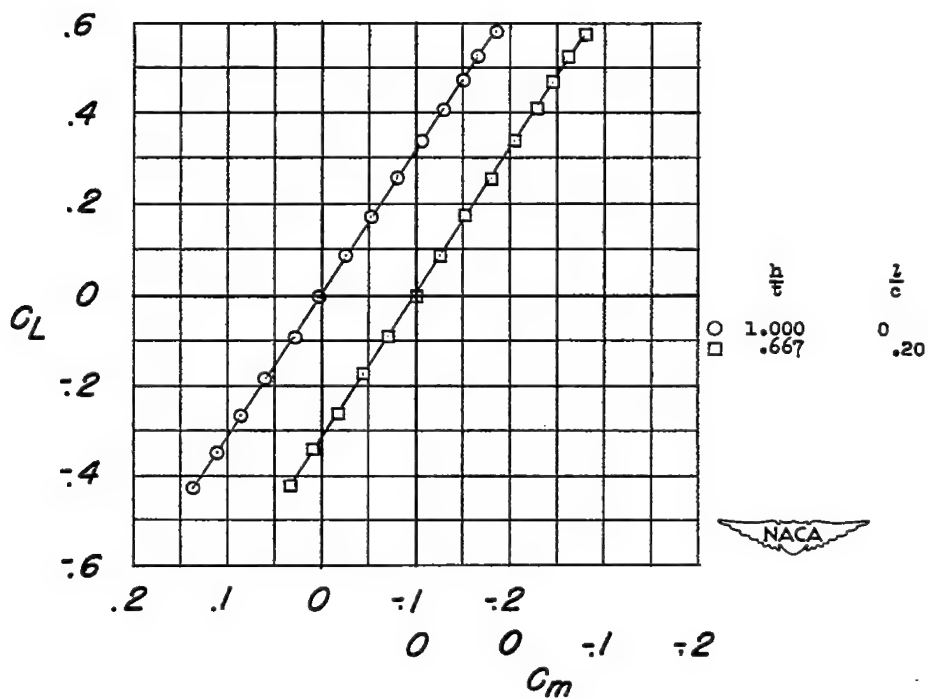


(a)  $\frac{t}{c} = 0.060$ .



(b)  $\frac{t}{c} = 0.045$ .

Figure 21.- Wing-plus-interference pitching-moment characteristics of  $45^\circ$  delta wings at a Mach number of 1.62.

(a)  $\frac{t}{c} = 0.060$ .(b)  $\frac{t}{c} = 0.045$ .Figure 22.- Wing-plus-interference pitching-moment characteristics of  $45^\circ$  delta wings at a Mach number of 1.96.



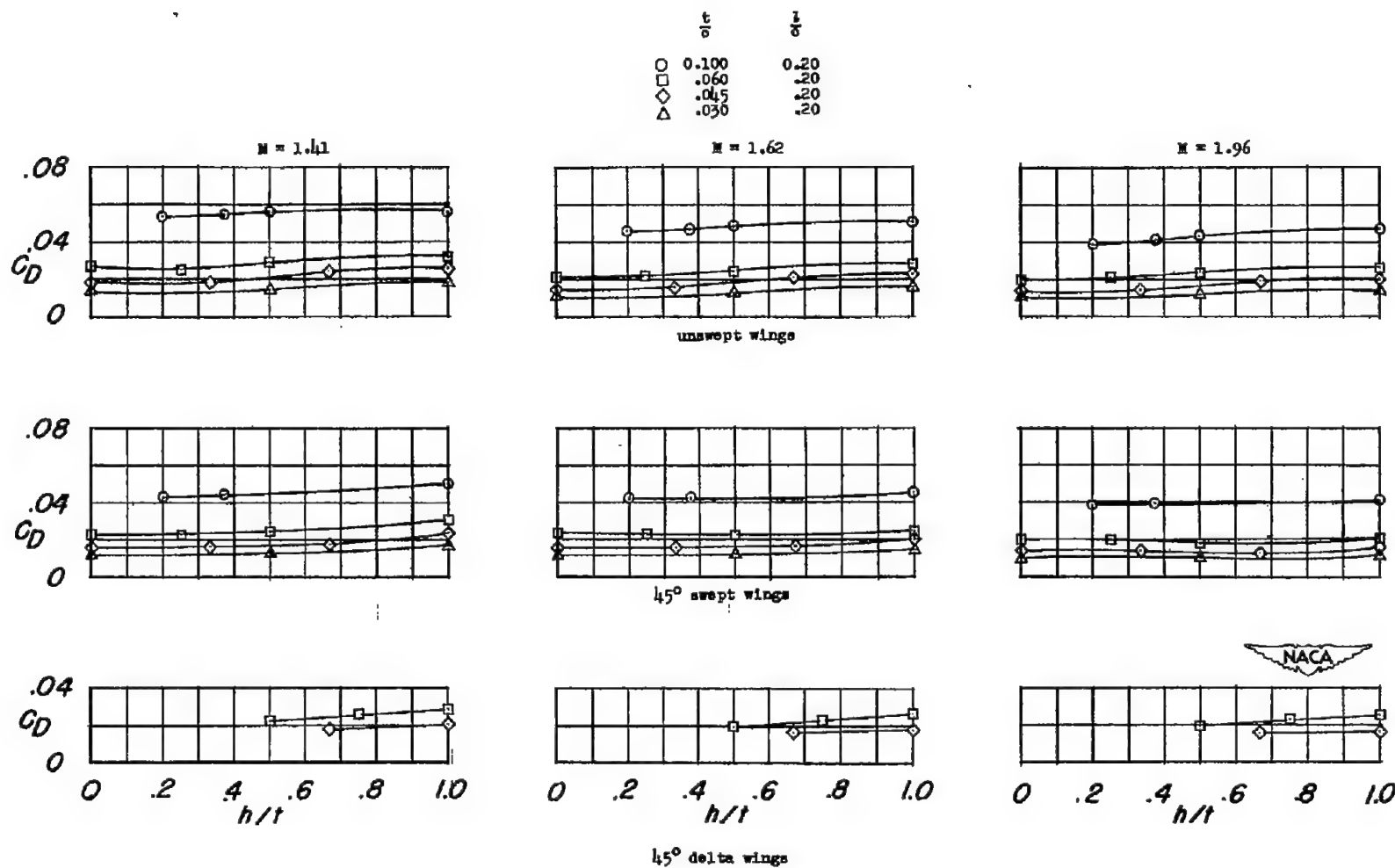


Figure 23.- Summary variations with trailing-edge thickness of wing-plus-interference zero-lift drag for unswept, 45° sweptback and 45° delta wings.

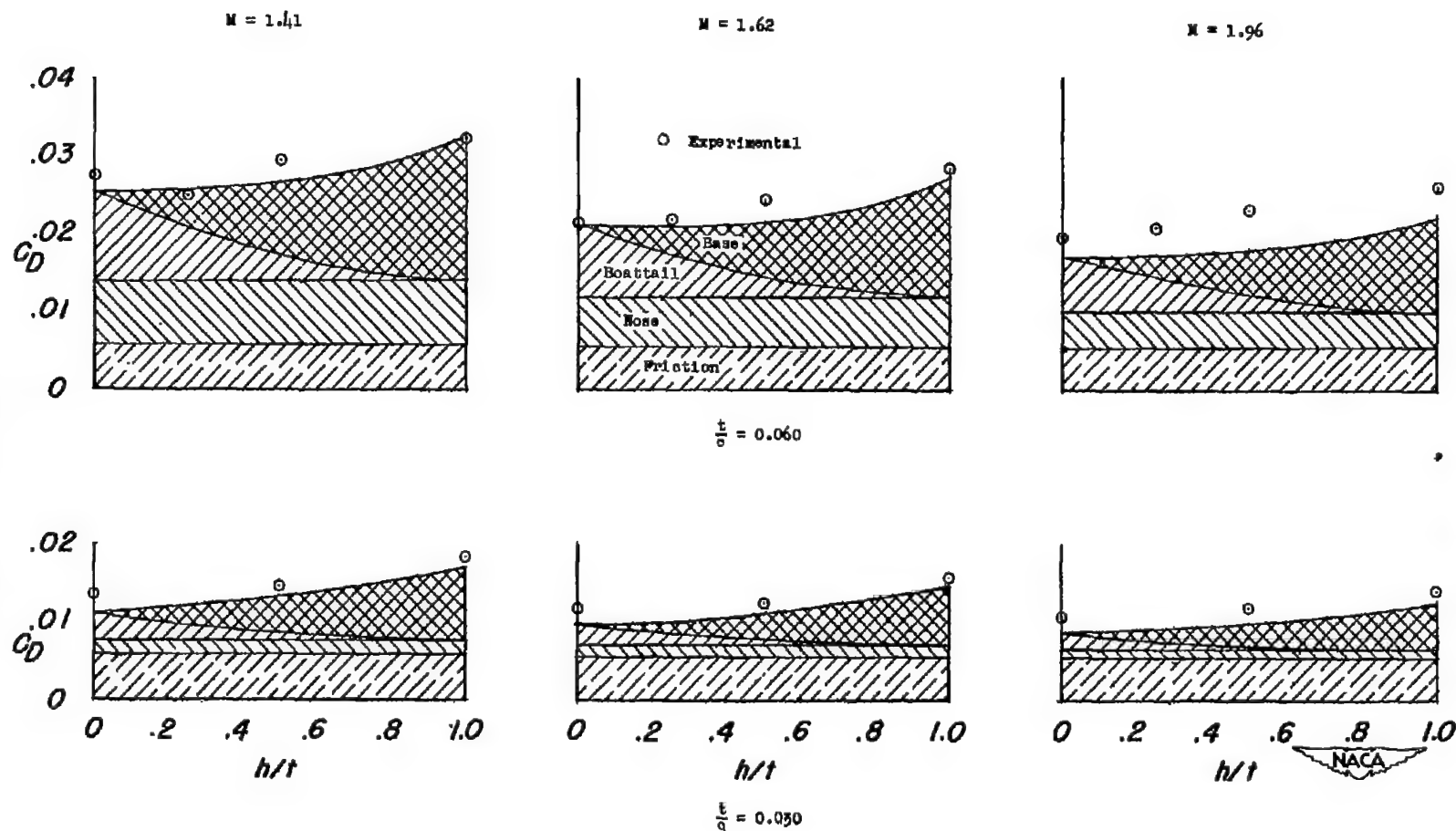


Figure 24.- Comparison at  $C_L = 0$  of experimental wing-plus-interference drags and calculated drags, and illustrations of the breakdown into components of calculated drags, for the 3.0- and 6.0-percent-thick unswept wings with  $\frac{l}{c} = 0.20$ .

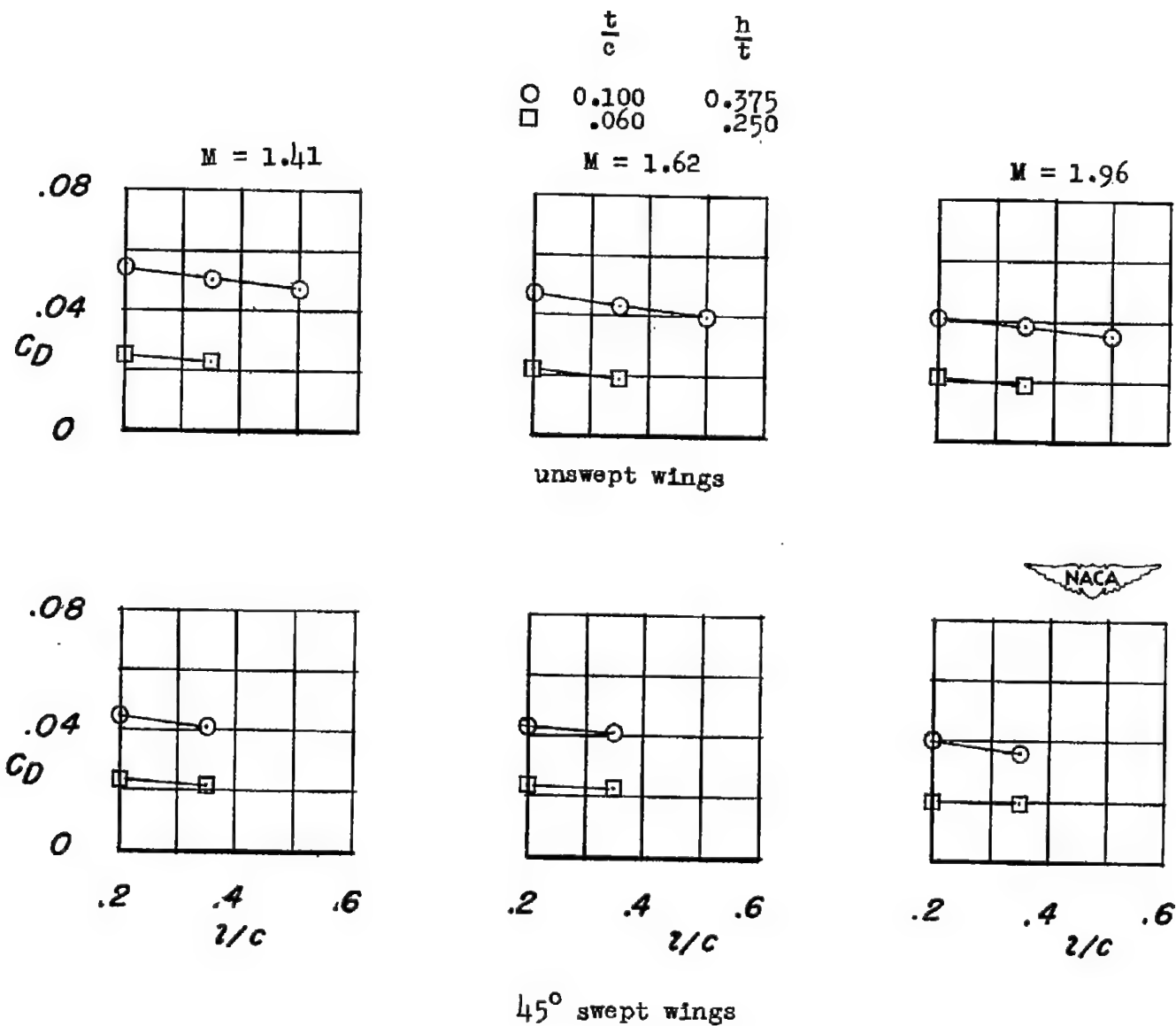


Figure 25.- Variations of wing-plus-interference zero-lift drag with length of trailing-edge bevel of untapered wings.

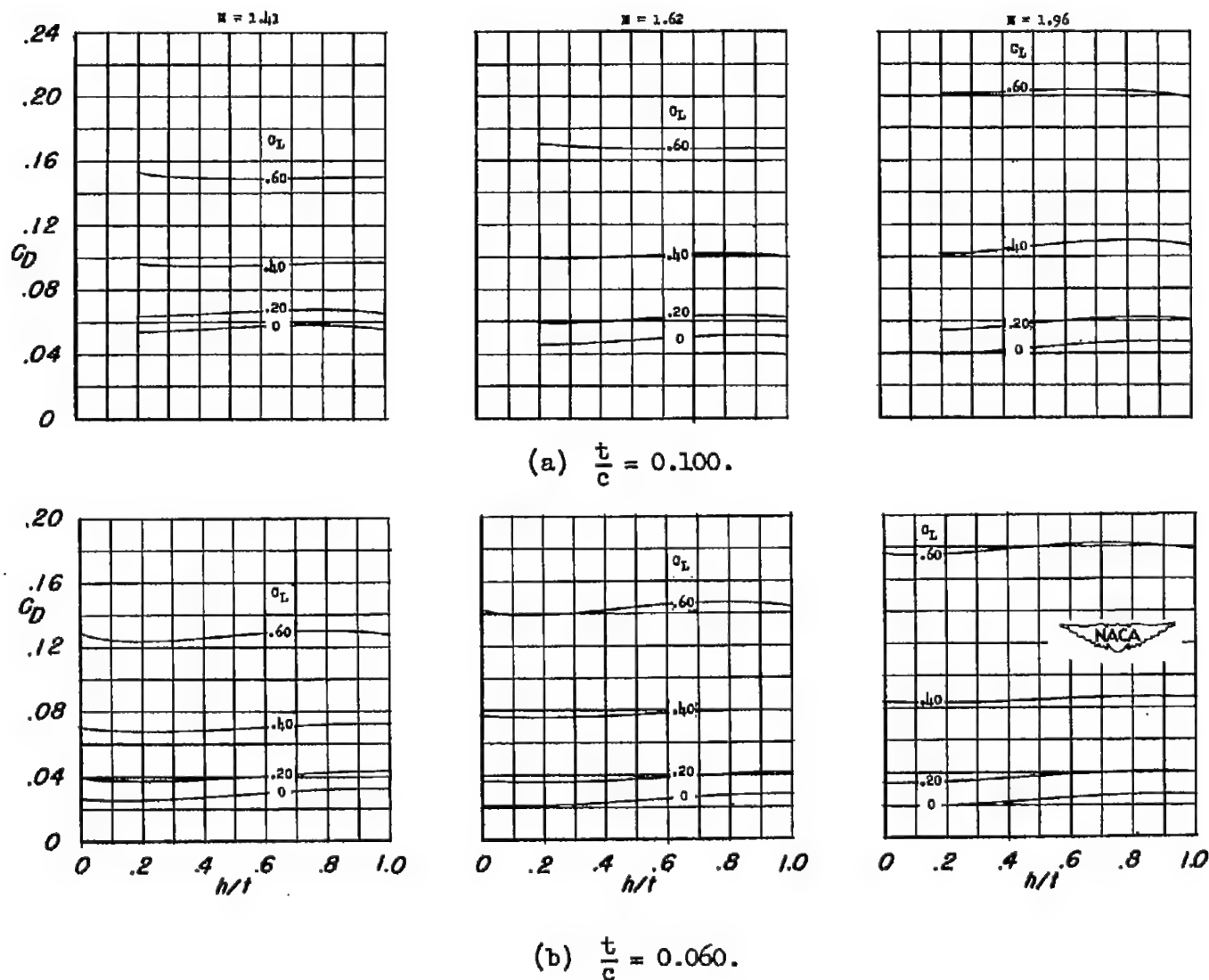
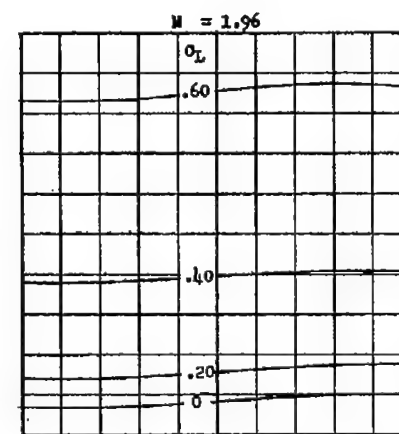
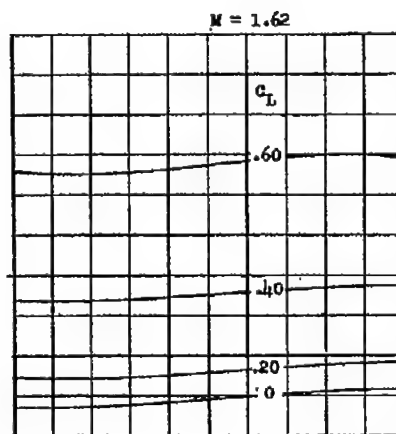
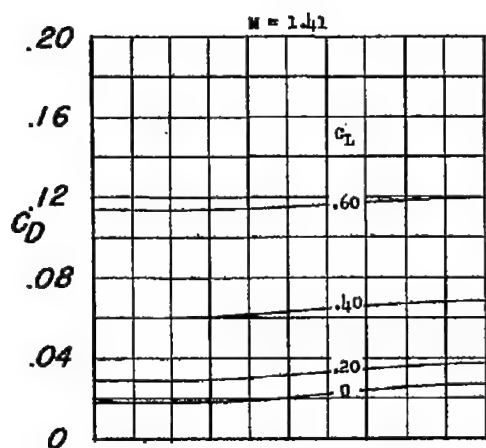
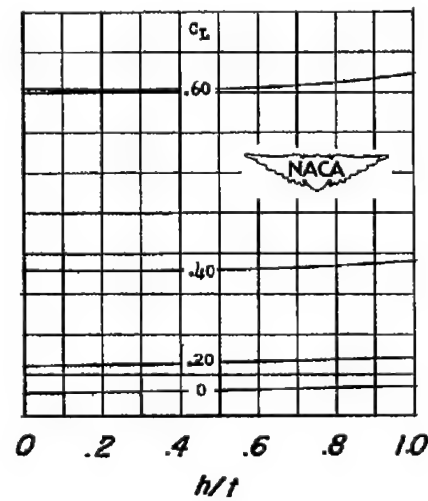
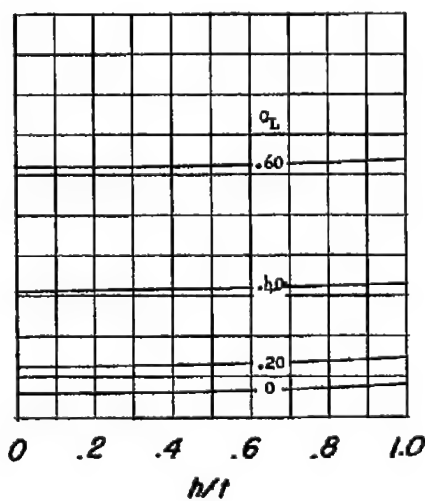
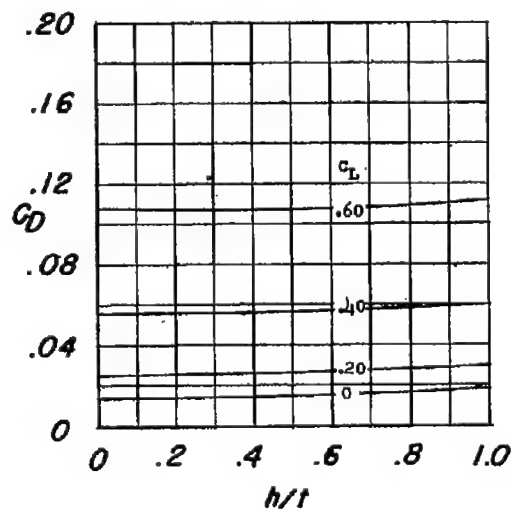


Figure 26.- Summary of wing-plus-interference drag at various lift coefficients for unswept wings having  $\frac{l}{c} = 0.20.$



(c)  $\frac{t}{c} = 0.045$ .



(d)  $\frac{t}{c} = 0.030$ .

Figure 26.- Concluded.

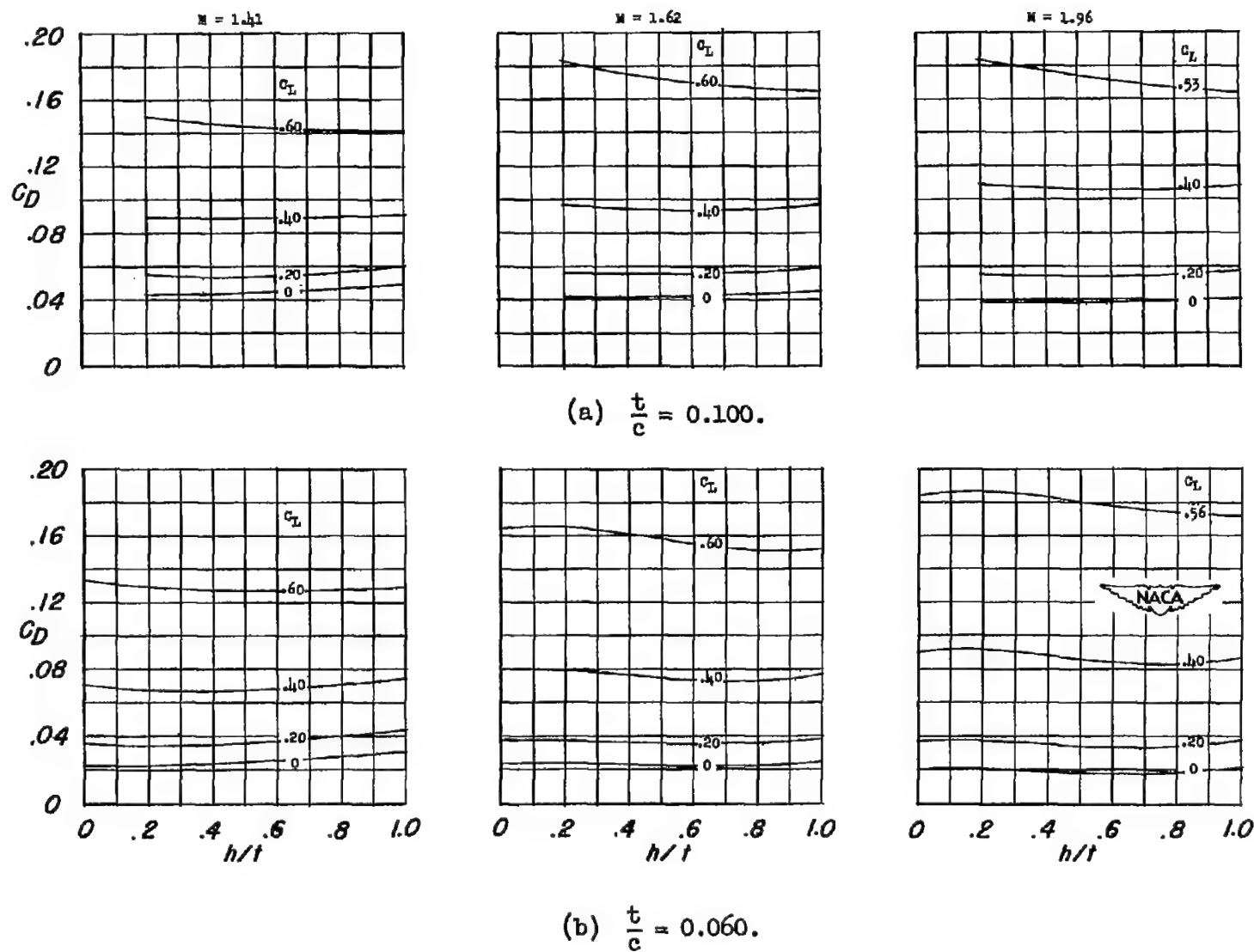
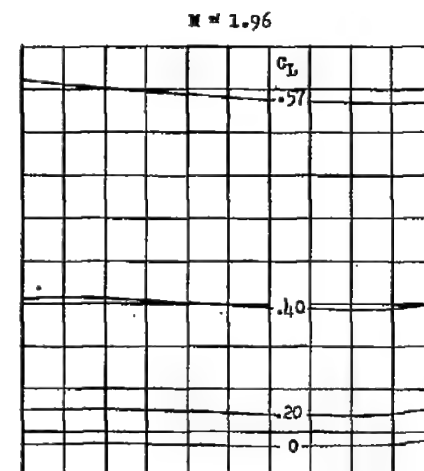
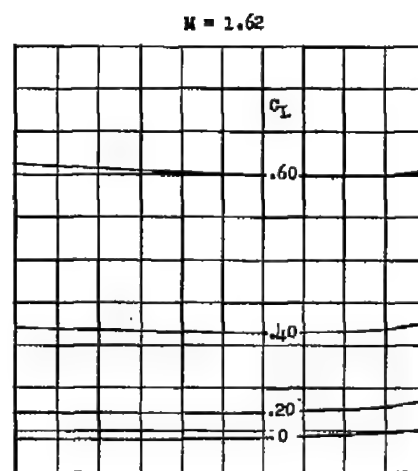
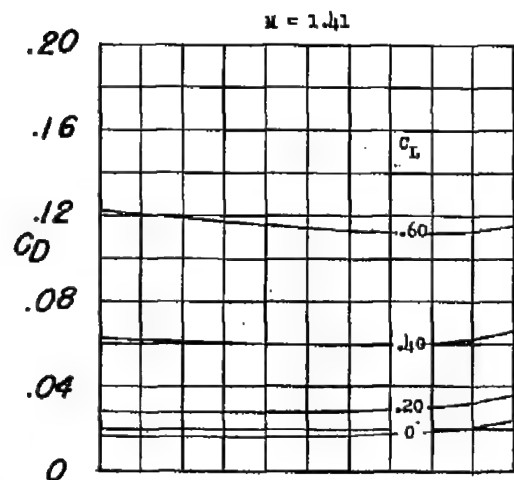
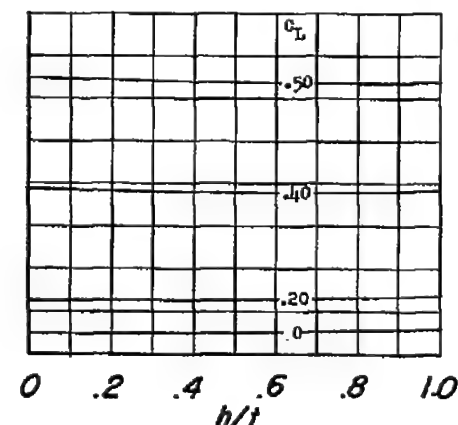
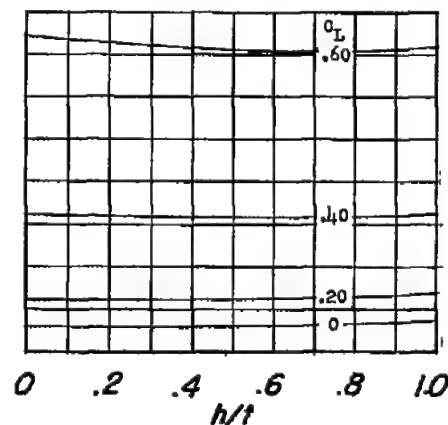
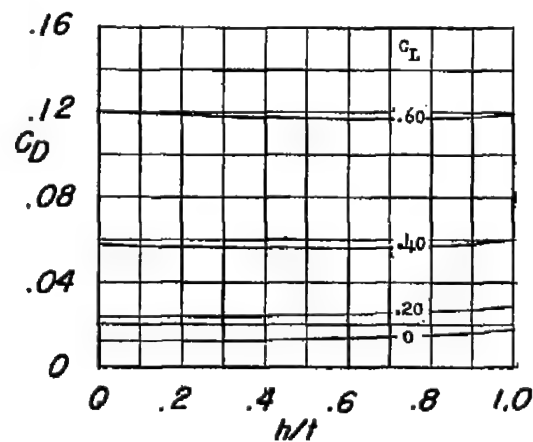


Figure 27.- Summary of wing-plus-interference drag at various lift coefficients for  $45^\circ$  sweptback wings having  $\frac{l}{c} = 0.20$ .



(c)  $\frac{t}{c} = 0.045$ .



(d)  $\frac{t}{c} = 0.030$ .

Figure 27.- Concluded.

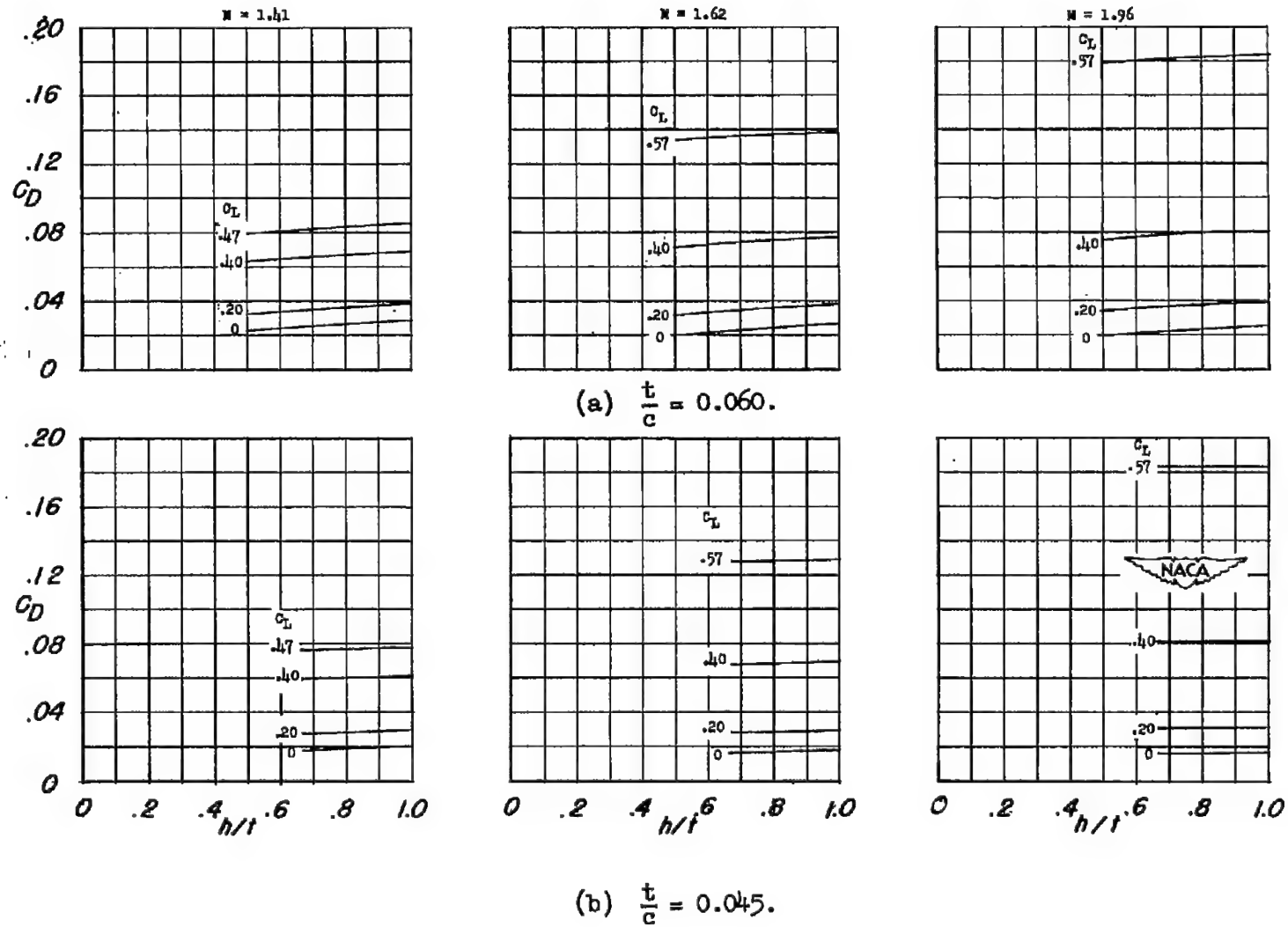


Figure 28.- Summary of wing-plus-interference drag at various lift coefficients for  $45^\circ$  delta wings having  $\frac{l}{c} = 0.20.$



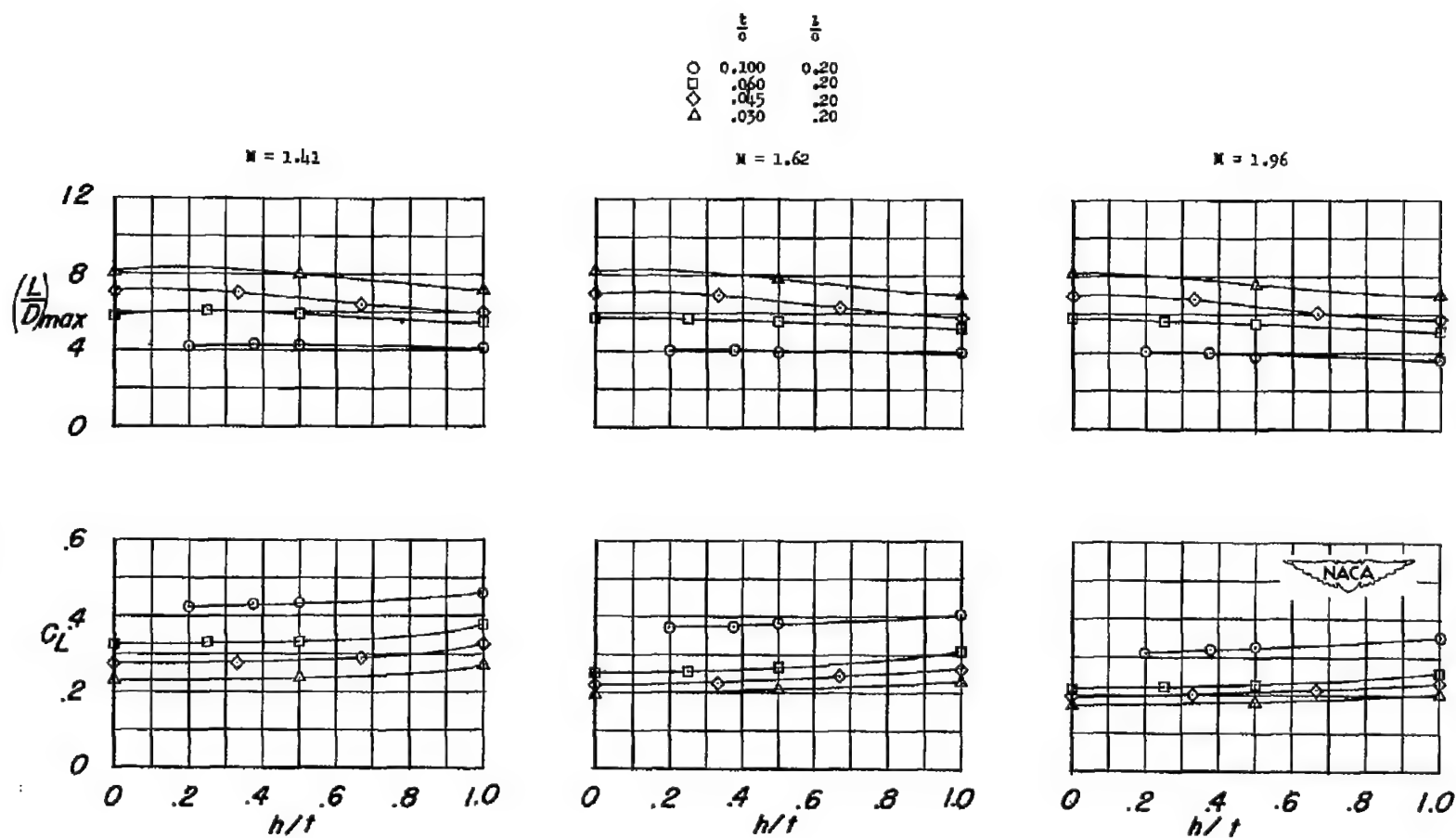


Figure 29.- Summary of maximum lift-drag ratios and lift coefficients at maximum lift-drag ratios for unswept wings.

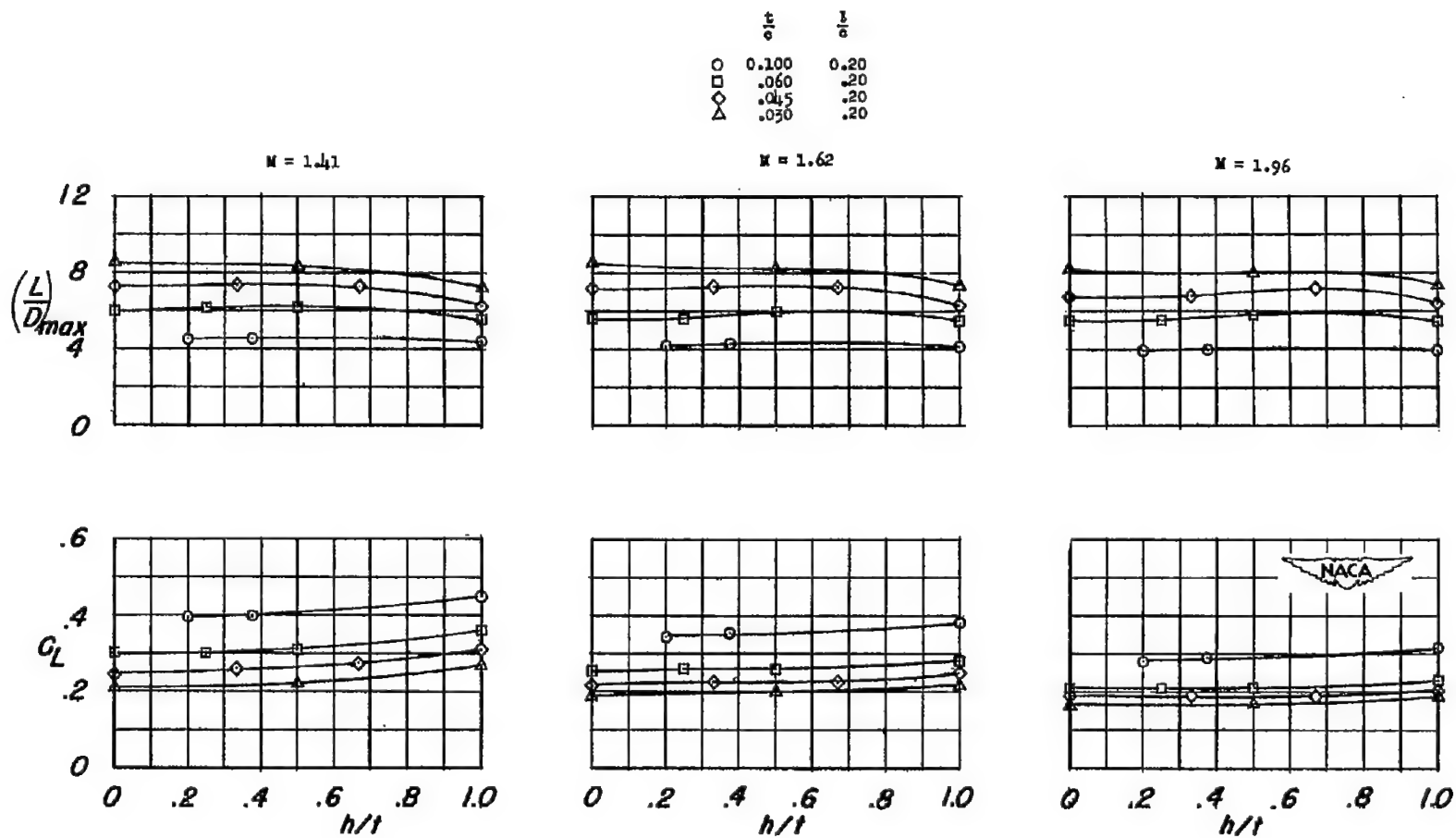


Figure 30.- Summary of maximum lift-drag ratios and lift coefficients at maximum lift-drag ratios for 45° sweptback wings.

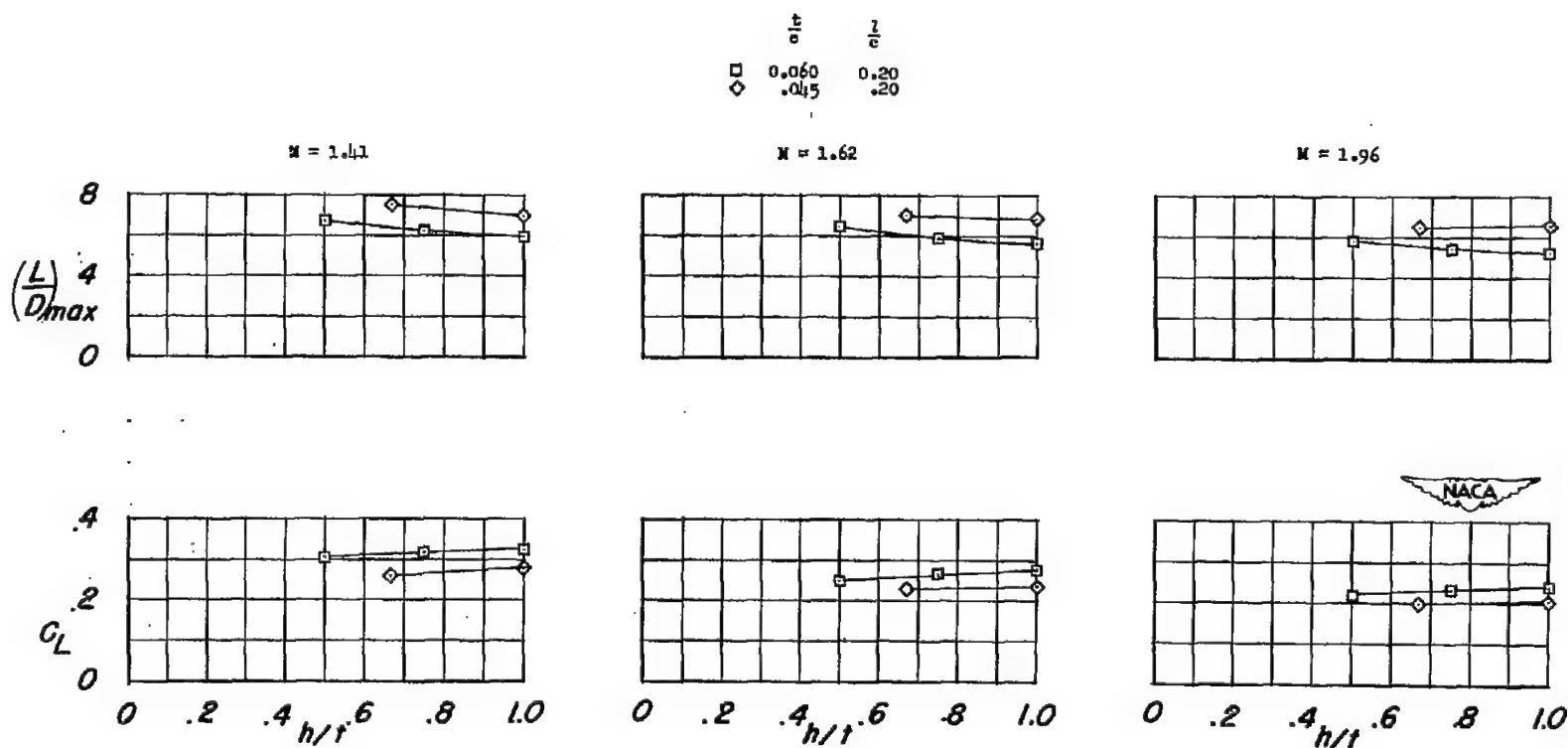


Figure 31.- Summary of maximum lift-drag ratios and lift coefficients at maximum lift-drag ratios for  $45^\circ$  delta wings.

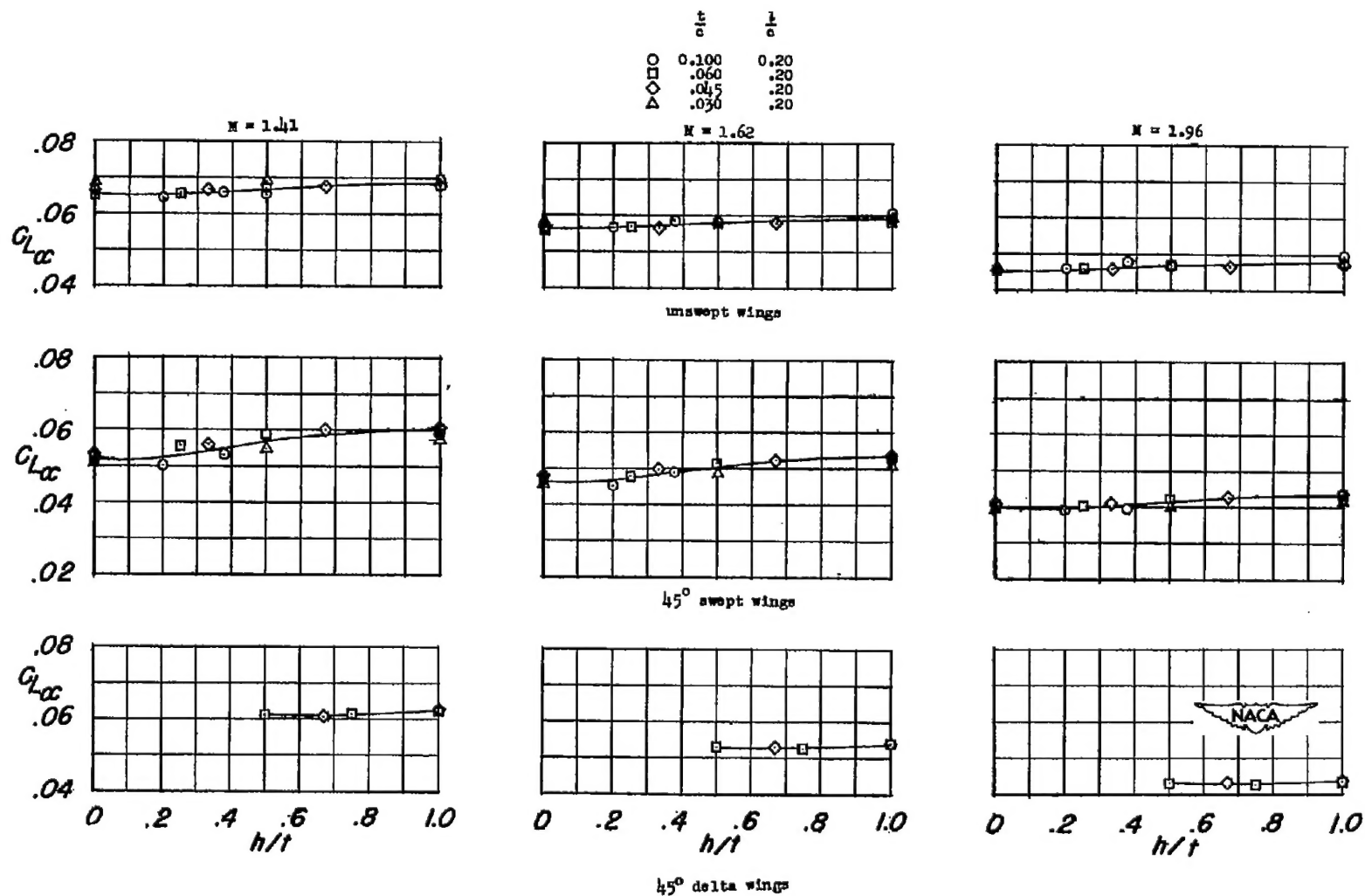


Figure 32.- Summary of variations with trailing-edge thickness of wing-plus-interference lift-curve slopes for unswept,  $45^\circ$  sweptback and  $45^\circ$  delta wings.  $C_L = 0$ .

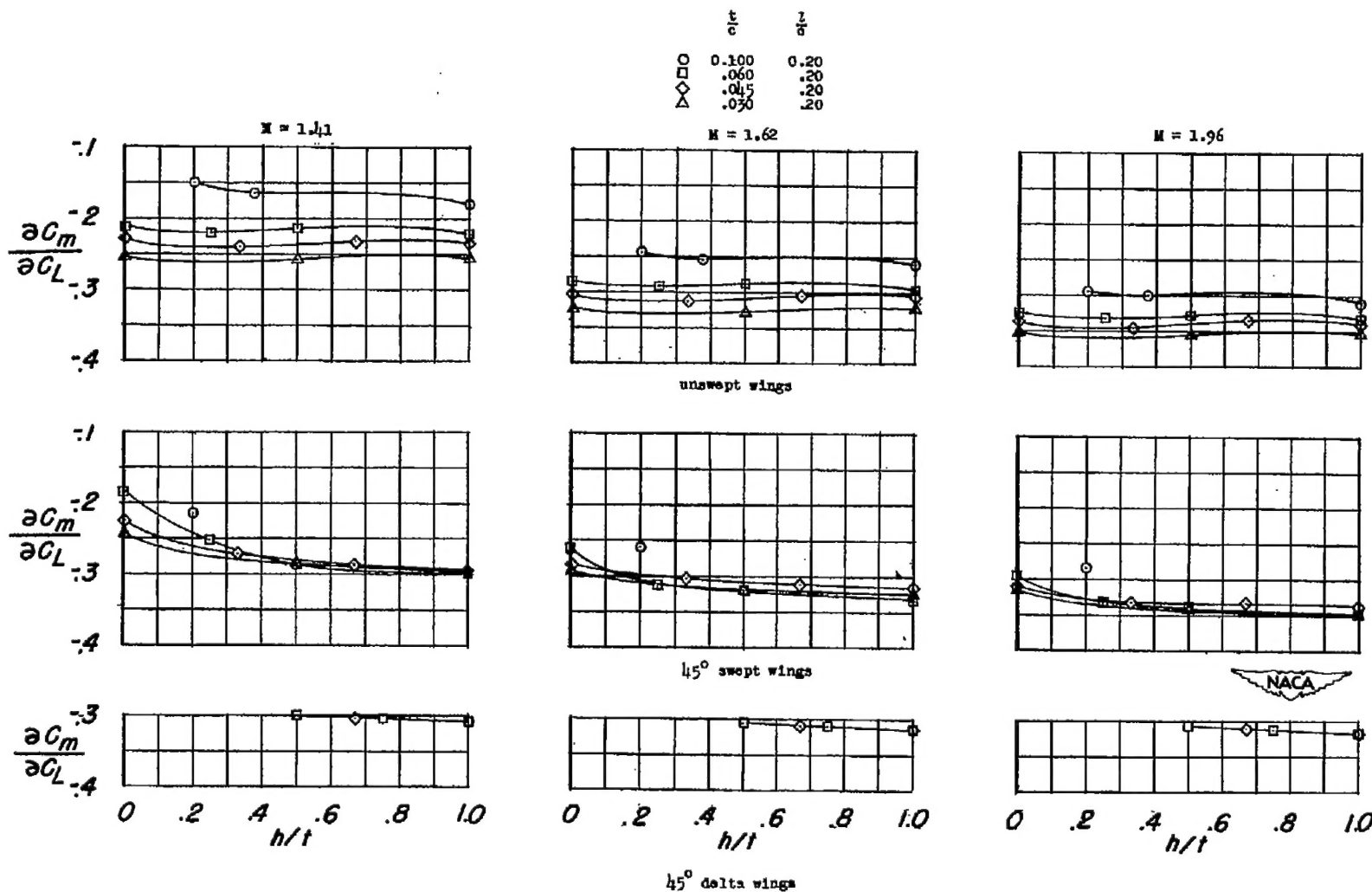
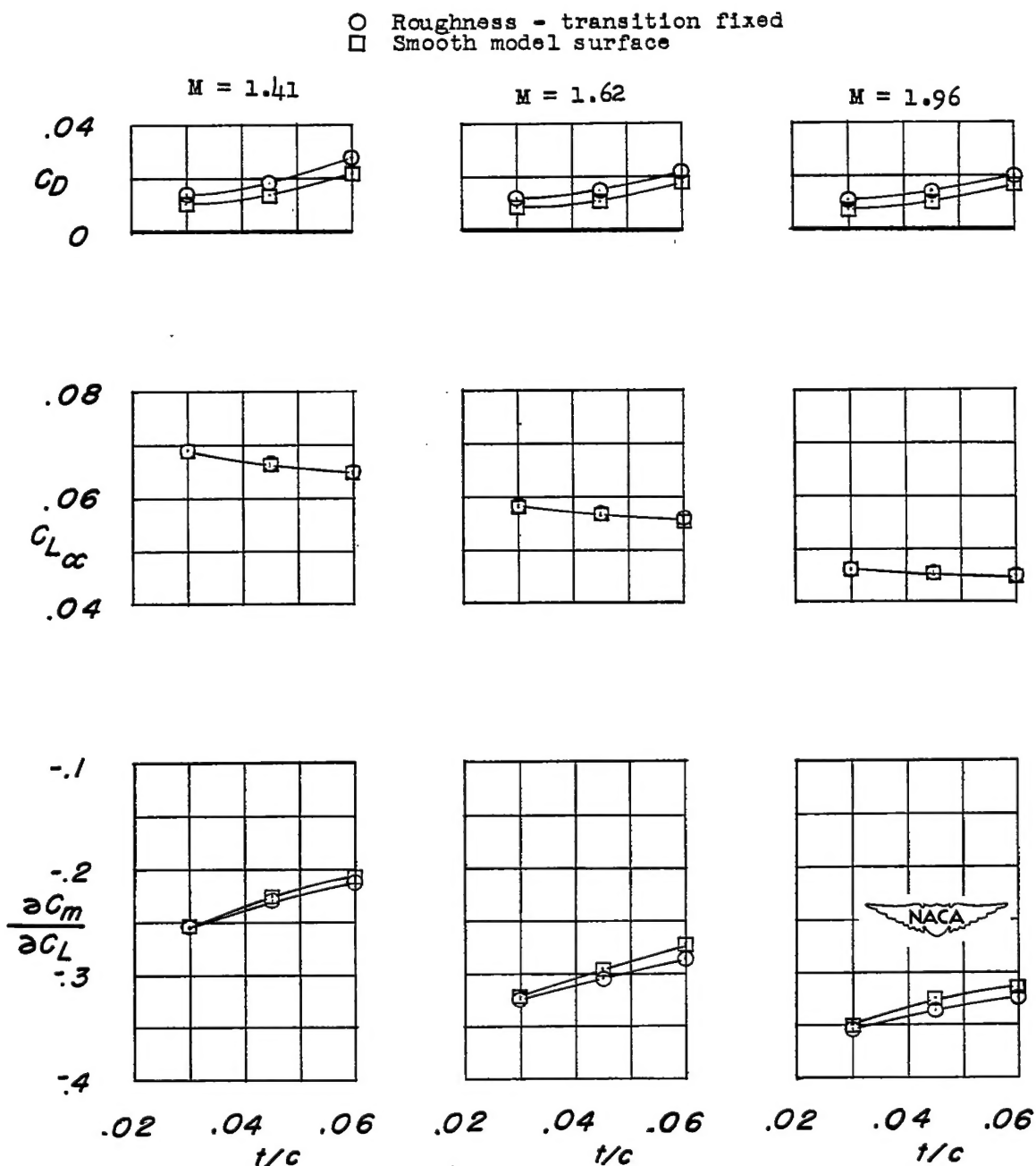


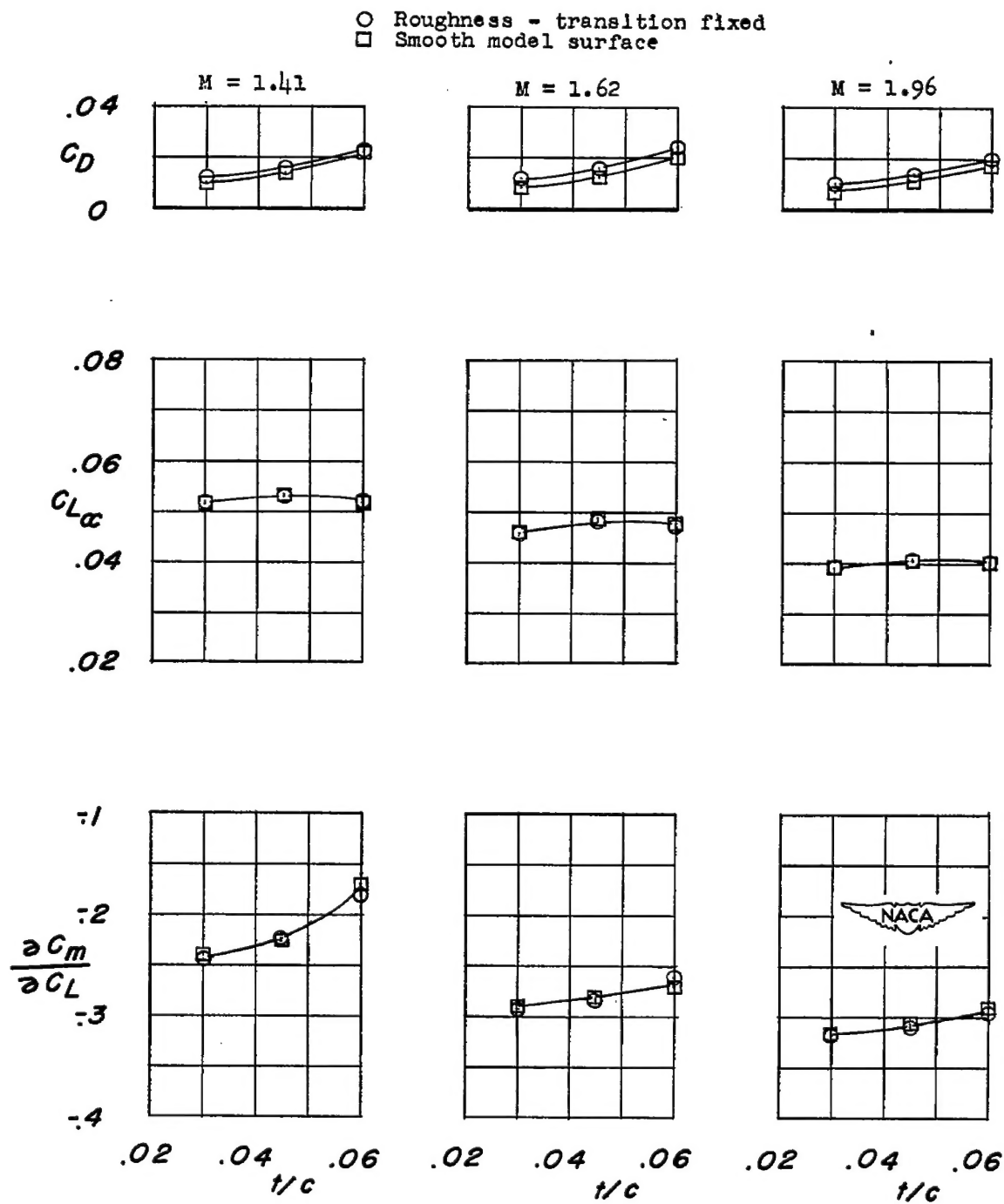
Figure 33.- Summary variations with trailing-edge thickness of wing-plus-interference pitching-moment parameter  $\partial C_m / \partial C_L$  for unswept,  $45^\circ$  swept-back and  $45^\circ$  delta wings.  $C_L = 0$ .

~~CONFIDENTIAL~~

(a) Unswept wings.

Figure 34.- Effects of fixed transition on the wing-plus-interference lift, drag, and pitching-moment characteristics of untapered sharp-trailing-edge wings.  $\frac{l}{c} = 0.20$ ;  $C_L = 0$ .

~~CONFIDENTIAL~~



(b)  $45^\circ$  sweptback wings.

Figure 34.- Concluded.